GDOT Research Project No. 12-07

Final Report

MEASUREMENTS OF DYNAMIC AND RESILIENT MODULI OF ROADWAY TEST SITES

Submitted by

Sung-Hee (Sonny) Kim, Ph.D., P.E.

Associate Professor and Director

Georgia Pavement and Traffic Research Center
Civil and Construction Engineering
Southern Polytechnic State University
1100 South Marietta Parkway
Marietta, GA 30060

Contract with

Georgia Department of Transportation

In cooperation with

U.S. Department of Transportation
Federal Highway Administration

December, 2013

ACKNOWLEDGEMENTS

The author would like to thank the support of the Georgia Department of Transportation (GDOT). The work conducted in this report was sponsored by the office of Material and Research of GDOT (Special Research Study Project 12-07). The strong support and valuable input provided by GDOT in the course of this research project is deeply appreciated. The author would like to acknowledge Steve Pahno, Binh Bui, David Jared, and Georgene Geary for their strong support during this project.

TABLE OF CONTENTS

Page

TABLE OF CONTENTS (Cont'd)

Page

LIST OF TABLES

TABLE Page

LIST OF FIGURES

FIGURE Page

LIST OF FIGURES (Cont'd)

FIGURE Page

EXECUTIVE SUMMARY

This study developed a material input library of dynamic and resilient moduli of local pavement materials for the Mechanistic Empirical Pavement Design Guide (MEPDG) implementation in Georgia. A database includes: 1) dynamic moduli of asphalt concrete mixtures prepared based on two Job Mix Formulas (Plant A and Plant B) with three different nominal maximum aggregate size (25mm base, 19mm intermediate, and 12.5 mm surface) and two asphalt cements (PG 64-22 and PG 67-22) , 2) resilient moduli of eleven different sources of Graded Aggregate Base, and 3) resilient moduli of nine different sources of subgrade.

Dynamic modulus of asphalt concrete was measured with six frequencies (25, 10, 5, 1, 0.5, 0.1 Hz) at five test temperatures (14, 40, 70, 100, 130 ^{o}F) in accordance with AASHTO T 342. The measured dynamic moduli were used to construct master curve for MEPDG Level 1 input value in asphalt concrete layer.

For graded aggregate base and subgrade layers, the material coefficients k_1, k_2, and k_3 were calculated from the measured resilient moduli at fifteen different stress states in accordance with AASHTO T 307. A developed database can be used as an input for flexible pavement design with a high level of reliability. Further, the propensity of recycled aggregate systems to hold moisture was investigated in this study to estimate moisture damage in the pavement structure because this type of damage manifests itself through the decay of resilient modulus and consequently results in loss of performance upon freezing and thawing cycles.

An Artificial Neural Network (ANN) model was developed to estimate granular material resilient modulus. The stress state and physical properties on resilient behavior of granular materials were successfully correlated with an ANN model developed in this report. The results demonstrated that the stress state and physical properties of granular materials significantly influenced the resilient modulus, which in turn has a substantial effect on the pavement response predictions that impact pavement design.

1.0 INTRODUCTION

To perform the structural analyses of existing flexible pavements using Mechanistic-Empirical Pavement Design Guide (MEPDG) or Pavement ME, the accurate measurements of dynamic modulus (E*) for asphalt materials and resilient moduli (M_R) for unbound materials are essential. E* is a direct input of Pavement ME software and it explains the viscoelastic behavior of Hot Mix Asphalt (HMA), which is the function of the loading frequency and temperature. The resilient behavior is the nature of granular material behavior and thus, M_R is one of the most important material properties, that is directly related to the structural performance of flexible pavement. The accurate measurements of dynamic and resilient moduli are required to correctly analyze the existing pavement and to properly design new pavement with highest level of reliability. In this study, the Georgia Pavement and Traffic Research Center (GPTRC) at Southern Polytechnic Applied Research Corporation (SPARC) developed the material input library to assist the GDOT for successful implementation of MEPDG in the State.

2.0 OBJECTIVES

The purpose of this study is to develop materials input library of E* and M_R for Pavement ME. To achieve the objectives of this study, measurements of E* for HMA and M_R for granular materials were conducted using the materials commonly used in Georgia. Results from this study provide pavement design professionals with appropriate structural analysis and design tools of the existing and new roadway in Georgia.

3.0 MECHANISTIC EMPIRICAL PAVEMENT DESIGN GUIDE (MEPDG)

The State-of-the-practice pavement design guides of conventional flexible pavement rely on empirical approaches developed through the long-term performance observation of specific pavement structures. These structures were constructed at one general location with limited number of types of pavement material and one climatic condition. Therefore, use of empirical models should be limited to the conditions on which they are based and cannot usually account for changes in loading and environmental conditions. To overcome the limitations induced from the use of empirical approaches there has been a movement towards the use of Mechanistic-Empirical Pavement Design Guide (MEPDG).

The first mechanistic design curves for flexible pavements, based on elastic layered theory, were developed in the early 1960s. Due to the lack of computational resources, each design curve had to be laboriously calculated by hand and thus, they could only be developed for a limited range of idealized pavement systems. The advent of innovative computational resources made it possible to calculate the load-induced pavement responses in multi-layered pavement systems. This advent has made it much more feasible to employ mechanistic analysis procedures in pavement design. Since 1986, the AASHTO Joint Task Force on Pavements (JTFP) has supported and prompted the development of Mechanistic-Empirical procedures for pavement thickness design. The National Cooperative Highway Research Project (NCHRP) 1-26 (1990 and 1992) was the first sponsored research project for developing mechanistic empirical pavement design procedures. NCHRP 1-26 researchers proposed working versions of mechanistic empirical design processes and procedures that relate pavement response variables, such as stresses (σ), strains (ε) and deflections (Δ) due to the surface wheel loads. Since 1997, NCHRP 1-37 (Development of the 2002 Guide for the Design of New and Rehabilitated Pavement Structures) was initiated with the objective of developing mechanistic pavement analysis and design procedures suitable for use in future versions of the AASHTO guide. The general concepts of a mechanistic-empirical design procedure are illustrated in Fig. 1.

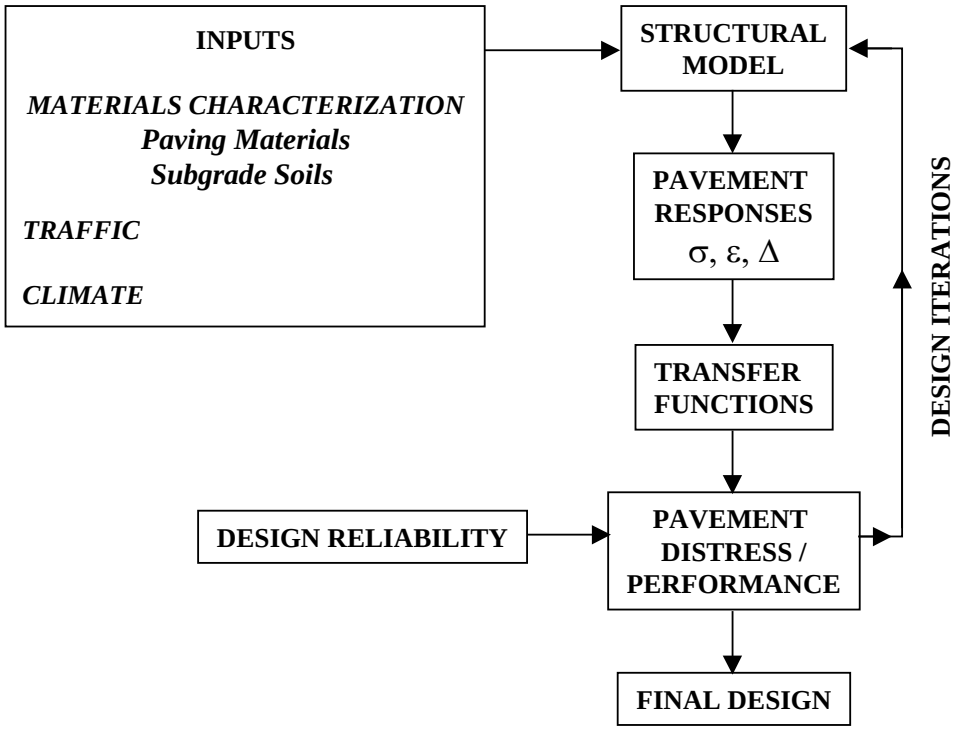

Fig. 3.1 Components of Mechanistic-Empirical Pavement Design (Kim, 2004)

The two major components are: (1) a pavement structural model to calculate as accurately as possible the critical pavement responses (σ, ε, Δ) and (2) transfer functions to translate those responses into measures of pavement performance. The design process entails iteratively adjusting the pavement structure until the desired level of performance and reliability are achieved.

The state-of-the-art in flexible pavement design approach is manifested in MEPDG and there are comprehensive well-established theories to embark on a different approach to pavement design. This is the *mechanistic design* approach that the pavement structure is modeled based on principles of engineering mechanics, mathematical system, and important engineering parameters, such as normal stresses and strains and shear stresses and strains are calculated under simulated traffic loading. These parameters are then related to performance through empirical correlations developed in practice. Thus, this approach is not entirely *mechanistic*, but *mechanistic-empirical*. The main advantage of the MEPDG is 1) the ability to predict future performance of new materials and new types of loadings, 2) better characterization of material properties and 3) capability to estimate existing pavement structural response through the experiments, nondestructive testing, and backcalculation

methods. A prerequisite for the successful mechanistic pavement design approach is that the material behavior is properly understood. The pavement materials are characterized by strength, and resilient properties that can be obtained directly from laboratory tests or backcalculated from nondestructive tests conducted in situ.

The main input parameters for the MEPDG are divided by five categories, which are project information, design information, traffic data, climatic data, and materials data. The MEPDG provides three levels of reliability: 1) Level 1 needs input from actual laboratory test for a site or project specific for the highest level of reliability; 2) Level 2 estimates the material input through correlations or region specific values that have been measured; and 3) Level 3 obtains from the local material database. Level 1 input is desirable for heavy traffic pavement design since it provides the highest level of reliability for pavement design. Level 2 provides an intermediate level of reliability while Level 3 provides the lowest level of reliability that could be used for the relatively less significant level of pavement design. This study deals with the development of Level 1 and Level 2 material input library for locally available materials in Georgia for successful implementation of MEPDG into new and overlay pavement design.

3.1 MEPDG Implementation Efforts for HMA layer

Many state agencies made an efforts to develop HMA E* input library for commonly used HMA mixtures in their States. Based on the developed material input library, several researchers attempted to evaluate the Witczak model or Hirsch for its ability to predict reasonable E*. The following table summarizes the efforts made by the previous researchers for the E* database development.

Table 3.1 MEPDG Implementation Activities for HMA Materials by State Agencies

Reference	State Agency	MEPDG Implementation Activities
Marasteanu et al. (2003)	MnROAD	Laboratory testings on four different HMA mixtures obtained from the MnROAD site to determine MEPDG Level 1 were conducted. It was observed that the Witczak model provided higher estimates of E*at high temperature than the measured values.

Birgisson et al. (2004)	Florida DOT	E* material library was developed and a new method to evaluate the relationships between the E*and the performance of mixtures in rutting and fracture.
Kim et al. (2005)	North Carolina DOT	E*material input library was developed for commonly used HMA mixtures. It was observed that the precision of the Witczak model compared better at lower temperatures than higher temperatures.
Cross et al. (2007)	Oklahoma DOT	A procedure to predict dynamic modulus was developed based on a material input database.
Carpenter (2007)	Illinois DOT	E* database was developed for twenty mixtures at 7 and 4% air voids.
Tashman and Elangovan (2007)	Washington DOT	A dynamic modulus database for typical Superpave mixes widely used in the State was developed using the mixtures prepared by seven job mix formula (JMF) selected for this study.
Witczak (2008)	Arizona DOT	A comprehensive HMA material characterization was conducted using eleven typical ADOT mixtures using five different aggregate types, and dynamic modulus and thermal fracture database were developed.
Bennert (2009)	New Jersey DOT	A catalog of E*inputs for plant-produced and laboratory-compacted samples of various HMA mixtures was developed.
Romanoschi et al. (2009)	Kansas DOT	A material inputs library for HMA mixtures were developed with 7 and 4% air voids. The study concludes that both the Witczak and Hirsch models underestimated dynamic modulus compared to the measure values.
Bonaquist (2010)	Wisconsin DOT	A database containing dynamic modulus master curve and flow numbers was developed for MEPDG implementation.
Im et al., (2010)	Nebraska Department of Roads (NDOR)	A database of E*and creep compliance was developed. It was observed that some discrepancies between measured and predicted E*.
Apeagyei and Diefenderfer (2011)	Virginia Tech Transportation Institute (VTRC)	Resilient modulus tests were conducted to find correlations with the E*. Witczak model predictions were found to compare reasonably with measure binder properties.
Schwartz and Li (2011)	The Maryland State Highway Agency (MDSHA)	Material inputs database of asphalt binder properties and E* was developed.
Bayomy et al. (2012)	Idaho Transportation Department (IDT)	A materials input library for HMA was developed at all MEPDG hierarchical levels for HMA mixtures and binders typically used in Idaho.

3.2 MEPDG Implementation Efforts for Granular Materials

A development of M_R database library for granular Materials was attempted by several state agencies and prediction models were developed for the reasonably estimation of M_R for local materials in the States. The several key activities made by State agencies to develop a material input library are summarized as follows:

Table 3.2 MEPDG Implementation Activities for Granular Materials by State Agencies

Reference	**State Agency**	**Development for MEPDG Implementation**
George (2003)	Mississippi DOT	Prediction models were developed to estimate resilient modulus of unbound materials based on soil index properties.
Ping et al. (2003)	Florida DOT	A database of resilient modulus for local soils was developed.
Kim and Siddiki (2006)	Indiana DOT	Extensive testings were conducted to measure the resilient and permanent deformation behavior of 19 different soils in the State.
Titi et al (2006)	Wisconsin DOT	A study to develop statistical model was conducted to estimate k-values for subgrade and aggregate base materials.
Hopkins et al. (2007)	Kentucky Transportation Cabinet	A prediction model to estimate resilient modulus of typical GAB in the State.
Richardson et al. (2007)	Missouri DOT	A material input library of resilient modulus was developed for granular base materials and subgrade soils.
Ceylan et al. (2009)	Iowa DOT	A resilient modulus material library was developed for unbound materials.
Hossain (2008), Hossain (2010)	Virginia Tech Transportation Institute (VTRC)	A material library of resilient modulus values for Virginia's subgrade soils and unbound aggregate base was developed.

As shown in Tables 3.1 and 3.2, an initial approach for MEPDG implementation by state agencies was to establish a layer input library using their local pavement materials and mixtures for local calibration.

4.0 PAVEMENT MATERIAL CHARACTERIZATIONS

4.1 Hot Mix Asphalt

4.1.1 Background

E* is an input value for flexible pavement design in MEPDG. E* is defined as the absolute value of the complex modulus that can be obtained by dividing the peak stress (σ_O) by the peak strain (ε_O) as follows:

$$|E^*| = \frac{\sigma_O}{\varepsilon_O} \quad (1)$$

Albeit the dynamic modulus is the absolute value of the complex modulus, it is denoted by E* instead of $|E^*|$ in this report. Currently, E* is measured in five test temperatures (14, 40, 70, 100, 130 ^{o}F) with six frequencies (25, 10, 5, 1, 0.5, 0.1 Hz) in accordance with AASHTO T 342. The measured E* at various test temperatures and loading frequencies are then used to construct master curve based on the principle of time-temperature superposition at a reference temperature of 70^{o}F. Fig. 4.1 shows an example how the measured E* can be shifted to develop master curve.

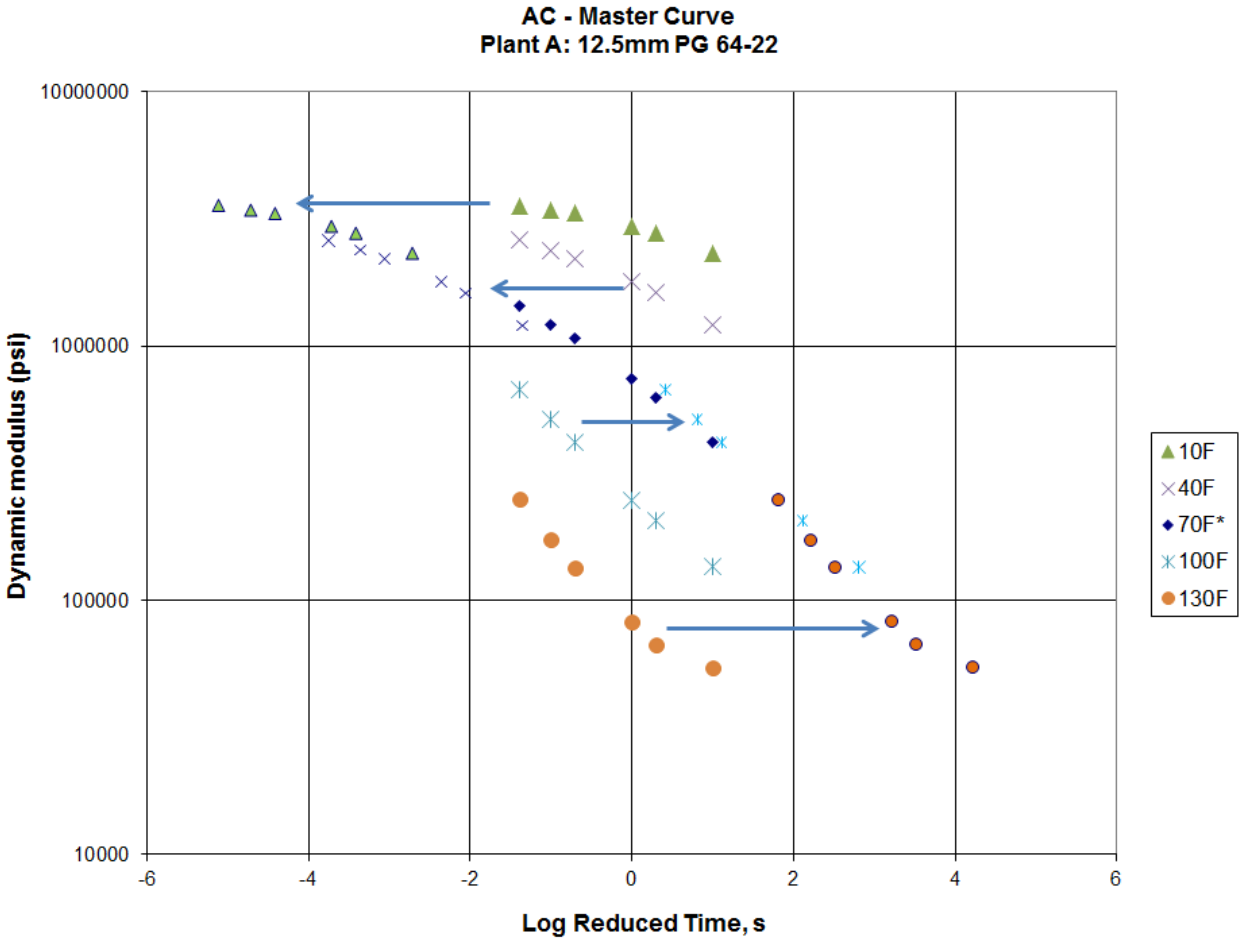

Fig. 4.1 Master Curve Construction

In MEPDG, the master curve is mathematically modeled based on a sigmoidal function as shown in Eq. (2).

$$\log(E^*) = \delta + \frac{\propto}{1+e^{\beta+\gamma(\log t_r)}} \quad (2)$$

Where,

t_r = reduced time of loading at reference temperature

δ = minimum value of E*

$\delta + \alpha$ = maximum value of E*

β, γ = parameters describing the shape of the sigmoidal function

The MEPDG also recommends use of the predictive equation if dynamic modulus is not available. For this case, the relationship between binder viscosity and temperature should be determined before shifting the mixing data. This relationship can be found by linear regression in Eq. (3) after log-log transformation of the viscosity data and log transformation of the temperature data.

$$\log\log\eta = A + VTS\log T_R \quad (3)$$

This can be done by converting the binder stiffness data to viscosity using the equation (4).

$$\eta = \frac{G^*}{10}\left(\frac{1}{sin\delta}\right)^{4.8628} \quad (4)$$

Where,

η = asphalt viscosity, cP

G* = asphalt complex shear modulus, Pa

δ = asphalt phase angle, degree

A, VTS = regression parameters

T_R = temperature, ^{o}Rankine

The measurements of binder stiffness from the Dynamic Shear Rheometer test (DSR) are not in the scope of this project. When the binder stiffness data is available, the prediction model can be compared with the measured E* values.

4.1.2 Materials and Laboratory Test

To achieve a high level of reliability for flexible pavement design, E* Level 1 input library has been developed with the selected sources of materials prepared based on Job Mix Formulas (JMF) provided from the plants of two GDOT Highway Contractors, Plant A and Plant B. Three different Nominal Maximum Aggregate Size (NMAS) was used in this study, which are 25mm base, 19mm intermediate, and 12.5mm surface NMAS mixtures from two

Georgia sources (North and South), with two asphalt cements (PG67 -22 and PG64 -22), and approximately 25% RAP. A total of 36 dynamic modulus tests was conducted and twelve (12) master curves were generated through this test matrix.

The HMA specimens were in accordance with AASHTO PP 60-09 "Preparation of Cylindrical Performance Test Specimens using Superpave Gyratory Compactor (SGC)". A SGC produced initial cylindrical specimens with a 6" (diameter) by 7" (height). The specimens were then cored and sawed to a size of 4" (diameter) x 6" (height) for dynamic modulus test. The target air void of the prepared specimens was 4% ± 0.5%. Fig. 4.2 shows the procedure to make a specimen for the dynamic modulus test.

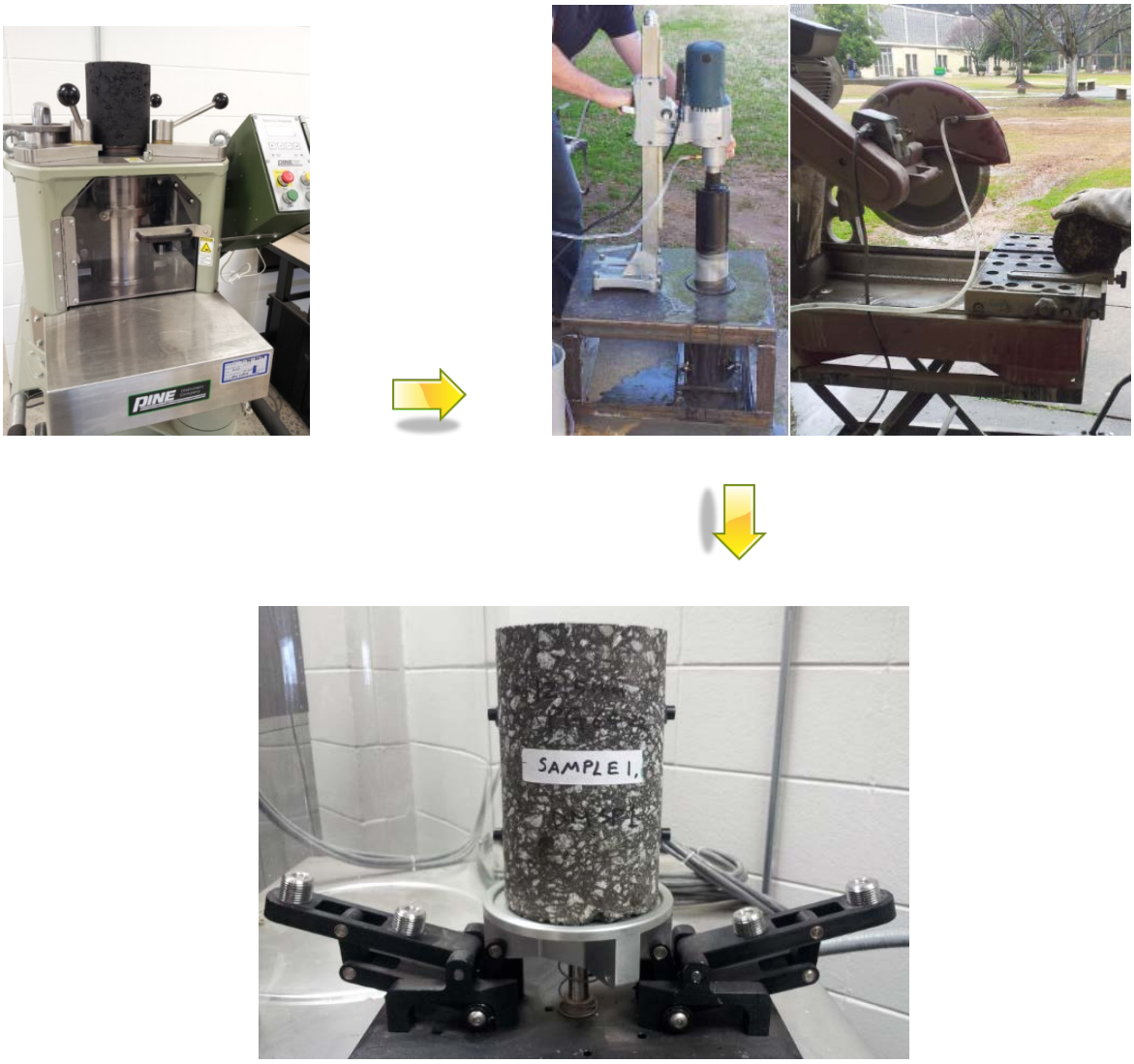

Fig. 4.2 Specimen Preparation Procedure

Table 4.2 shows the volumetric characteristics including mixture ID, air void, and asphalt mixture bulk specific gravity (Gmb) for each prepared specimens.

	Mix ID	%AV	Gmb
Plant A	12.5mm_PG64_SP1	4.28	2.44
	12.5mm_PG64_SP2	3.81	2.45
	12.5mm_PG64_SP3	4.21	2.44
	12.5mm_PG67_SP1	4.36	2.45
	12.5mm_PG67_SP2	3.93	2.46
	12.5mm_PG67_SP3	4.09	2.46
	19mm_PG64_SP1	4.06	2.48
	19mm_PG64_SP2	3.72	2.49
	19mm_PG64_SP3	3.99	2.48
	19mm_PG67_SP1	4.18	2.49
	19mm_PG67_SP2	4.17	2.49
	19mm_PG67_SP3	3.60	2.50
	25mm_PG64_SP1	4.45	2.47
	25mm_PG64_SP2	4.25	2.48
	25mm_PG64_SP3	3.91	2.49
	25mm_PG67_SP1	4.47	2.49
	25mm_PG67_SP2	3.56	2.51
	25mm_PG67_SP3	3.93	2.50
Plant B	12.5mm_PG64_SP1	4.47	2.41
	12.5mm_PG64_SP2	4.47	2.41
	12.5mm_PG64_SP3	4.40	2.41
	12.5mm_PG67_SP1	4.42	2.41
	12.5mm_PG67_SP2	4.36	2.41
	12.5mm_PG67_SP3	4.36	2.41
	19mm_PG64_SP1	4.49	2.42
	19mm_PG64_SP2	4.29	2.42
	19mm_PG64_SP3	4.10	2.43
	19mm_PG67_SP1	4.06	2.43
	19mm_PG67_SP2	4.08	2.43
	19mm_PG67_SP3	4.11	2.43
	25mm_PG64_SP1	3.73	2.45
	25mm_PG64_SP2	4.34	2.44
	25mm_PG64_SP3	4.20	2.44
	25mm_PG67_SP1	3.93	2.45
	25mm_PG67_SP2	3.58	2.46
	25mm_PG67_SP3	3.59	2.46

Table 4.2 HMA Mixture ID and Volumetric Characteristics

Fig. 4.3 shows the Interlaken UniSystem test setup for Dynamic Modulus test. Dynamic modulus test was conducted at six different frequencies under five different temperatures in

accordance with AASHTO T 342-2011. The specimens were tested from lowest to highest temperature. At each temperature, the loading from highest to lowest frequency was applied.

Fig. 4.3 Dynamic Modulus Setup

4.1.3 Test Results and Analyses

All the test results are summarized in Tables 4.2 through 4.7. As expected, E* increases as the loading frequency increases decreases as the temperature increases. From the measured three replicates, average values of E* were calculated at each loading frequency and temperatures to construct master curve. Figs. 4.4 through 4.7 show the constructed master curve for each prepared mixture.

Figs. 4.8 through 4.11 show the relationships among phase angle, temperature, and frequency. It was generally observed that phase angle decreases as loading frequency increases at temperatures of 10, 40, and 70^{o}F. A little complicated behavior of phase angle was observed

for temperatures of 100 and 130^{o}F. Similar results were also reported from other study (Flintsch et al, 2008; Im et al, 2010). The entire E* test results are reported in Appendix A.

Table 4.2 HMA Average E* Results (Plant A JMF, 12.5 mm NMAS)

Temp. (F)	PLANT A					
	12.5 mm NMAS					
	PG64-22			PG67-22		
	Specimen 1			Specimen 1		
	COAC(%)	Hz	E* (psi)	COAC(%)	Hz	E* (psi)
14	5.42	0.1	2,328,063	5.52	0.1	1,833,997
14	5.42	0.5	2,789,390	5.52	0.5	2,329,215
14	5.42	1.0	2,965,684	5.52	1.0	2,500,893
14	5.42	5.0	3,333,546	5.52	5.0	2,855,004
14	5.42	10.0	3,435,991	5.52	10.0	3,014,718
14	5.42	25.0	3,586,810	5.52	25.0	3,222,771
40	5.42	0.1	1,221,051	5.52	0.1	967,977
40	5.42	0.5	1,632,285	5.52	0.5	1,342,226
40	5.42	1.0	1,809,429	5.52	1.0	1,490,641
40	5.42	5.0	2,219,869	5.52	5.0	1,849,658
40	5.42	10.0	2,396,087	5.52	10.0	2,007,212
40	5.42	25.0	2,628,237	5.52	25.0	2,243,473
70	5.42	0.1	427,847	5.52	0.1	271,098
70	5.42	0.5	639,001	5.52	0.5	404,326
70	5.42	1.0	754,634	5.52	1.0	477,768
70	5.42	5.0	1,085,830	5.52	5.0	715,084
70	5.42	10.0	1,232,625	5.52	10.0	817,656
70	5.42	25.0	1,456,067	5.52	25.0	967,051
100	5.42	0.1	135,850	5.52	0.1	114,831
100	5.42	0.5	205,977	5.52	0.5	164,120
100	5.42	1.0	249,749	5.52	1.0	199,114
100	5.42	5.0	421,579	5.52	5.0	323,555
100	5.42	10.0	517,217	5.52	10.0	403,340
100	5.42	25.0	677,061	5.52	25.0	523,070
130	5.42	0.1	55,226	5.52	0.1	47,045
130	5.42	0.5	68,692	5.52	0.5	55,313
130	5.42	1.0	84,017	5.52	1.0	65,600
130	5.42	5.0	138,069	5.52	5.0	100,761
130	5.42	10.0	179,408	5.52	10.0	125,693
130	5.42	25.0	259,526	5.52	25.0	179,354

Table 4.3 HMA Average E* Results (Plant A JMF, 19 mm NMAS)

Temp. (F)	PLANT A					
	19 mm NMAS					
	PG64-22			PG67-22		
	Specimen 1			Specimen 1		
	COAC(%)	Hz	E* (psi)	COAC(%)	Hz	E* (psi)
14	4.62	0.1	1,715,717	4.72	0.1	2,106,102
14	4.62	0.5	2,244,767	4.72	0.5	2,868,249
14	4.62	1.0	2,434,709	4.72	1.0	3,139,518
14	4.62	5.0	2,787,932	4.72	5.0	3,599,083
14	4.62	10.0	2,949,238	4.72	10.0	3,894,405
14	4.62	25.0	3,195,463	4.72	25.0	4,280,642
40	4.62	0.1	985,705	4.72	0.1	1,149,054
40	4.62	0.5	1,361,551	4.72	0.5	1,666,910
40	4.62	1.0	1,520,561	4.72	1.0	1,867,244
40	4.62	5.0	1,795,512	4.72	5.0	2,292,181
40	4.62	10.0	2,014,849	4.72	10.0	2,526,888
40	4.62	25.0	2,230,619	4.72	25.0	2,831,866
70	4.62	0.1	294,107	4.72	0.1	417,902
70	4.62	0.5	444,239	4.72	0.5	652,965
70	4.62	1.0	529,364	4.72	1.0	781,490
70	4.62	5.0	795,477	4.72	5.0	1,133,717
70	4.62	10.0	913,939	4.72	10.0	1,298,816
70	4.62	25.0	1,095,903	4.72	25.0	1,566,827
100	4.62	0.1	100,137	4.72	0.1	133,923
100	4.62	0.5	142,394	4.72	0.5	199,977
100	4.62	1.0	170,638	4.72	1.0	248,217
100	4.62	5.0	297,171	4.72	5.0	431,771
100	4.62	10.0	368,118	4.72	10.0	536,502
100	4.62	25.0	499,888	4.72	25.0	720,388
130	4.62	0.1	46,597	4.72	0.1	53,643
130	4.62	0.5	50,242	4.72	0.5	62,686
130	4.62	1.0	60,111	4.72	1.0	76,941
130	4.62	5.0	92,748	4.72	5.0	122,006
130	4.62	10.0	112,998	4.72	10.0	156,836
130	4.62	25.0	166,190	4.72	25.0	227,892

Table 4.4 HMA Average E* Test Results (Plant A JMF, 25 mm NMAS)

Temp. (F)	PLANT A					
	25 mm NMAS					
	PG64-22			PG67-22		
	Specimen 1			Specimen 1		
	COAC(%)	Hz	E* (psi)	COAC(%)	Hz	E* (psi)
14	4.47	0.1	2,297,977	4.56	0.1	2,001,445
14	4.47	0.5	2,860,911	4.56	0.5	2,623,676
14	4.47	1.0	3,069,569	4.56	1.0	2,842,248
14	4.47	5.0	3,433,158	4.56	5.0	3,230,061
14	4.47	10.0	3,634,252	4.56	10.0	3,419,817
14	4.47	25.0	3,931,528	4.56	25.0	3,728,750
40	4.47	0.1	1,178,194	4.56	0.1	1,068,230
40	4.47	0.5	1,578,608	4.56	0.5	1,475,453
40	4.47	1.0	1,740,881	4.56	1.0	1,647,131
40	4.47	5.0	2,109,819	4.56	5.0	2,027,760
40	4.47	10.0	2,294,474	4.56	10.0	2,200,051
40	4.47	25.0	2,530,805	4.56	25.0	2,454,712
70	4.47	0.1	432,444	4.56	0.1	463,327
70	4.47	0.5	622,996	4.56	0.5	696,512
70	4.47	1.0	729,458	4.56	1.0	823,924
70	4.47	5.0	1,036,361	4.56	5.0	1,160,299
70	4.47	10.0	1,167,597	4.56	10.0	1,311,144
70	4.47	25.0	1,368,111	4.56	25.0	1,547,733
100	4.47	0.1	141,086	4.56	0.1	129,070
100	4.47	0.5	200,719	4.56	0.5	185,226
100	4.47	1.0	243,851	4.56	1.0	222,862
100	4.47	5.0	411,106	4.56	5.0	377,989
100	4.47	10.0	504,008	4.56	10.0	465,875
100	4.47	25.0	658,203	4.56	25.0	618,529
130	4.47	0.1	60,989	4.56	0.1	52,281
130	4.47	0.5	68,771	4.56	0.5	58,680
130	4.47	1.0	83,081	4.56	1.0	72,366
130	4.47	5.0	129,292	4.56	5.0	114,468
130	4.47	10.0	161,061	4.56	10.0	143,893
130	4.47	25.0	233,194	4.56	25.0	210,624

Table 4.5 HMA Average E* Test Results (Plant B JMF, 12.5 mm NMAS)

Temp. (F)	PLANT B					
	12.5 mm NMAS					
	PG64-22			PG67-22		
	Specimen 1			Specimen 1		
	COAC(%)	Hz	E* (psi)	COAC(%)	Hz	E* (psi)
14	5.45	0.1	2,411,791	5.44	0.1	1,955,000
14	5.45	0.5	3,172,272	5.44	0.5	2,462,567
14	5.45	1.0	3,424,062	5.44	1.0	2,624,622
14	5.45	5.0	3,826,041	5.44	5.0	2,981,465
14	5.45	10.0	4,103,832	5.44	10.0	3,113,580
14	5.45	25.0	4,501,528	5.44	25.0	3,300,257
40	5.45	0.1	1,240,870	5.44	0.1	1,288,101
40	5.45	0.5	1,823,837	5.44	0.5	1,733,369
40	5.45	1.0	2,059,737	5.44	1.0	1,912,368
40	5.45	5.0	2,520,279	5.44	5.0	2,301,352
40	5.45	10.0	2,784,114	5.44	10.0	2,482,687
40	5.45	25.0	3,114,133	5.44	25.0	2,705,305
70	5.45	0.1	349,656	5.44	0.1	456,507
70	5.45	0.5	567,784	5.44	0.5	683,881
70	5.45	1.0	698,413	5.44	1.0	813,170
70	5.45	5.0	1,066,219	5.44	5.0	1,170,993
70	5.45	10.0	1,244,325	5.44	10.0	1,322,310
70	5.45	25.0	1,505,021	5.44	25.0	1,544,851
100	5.45	0.1	102,323	5.44	0.1	116,193
100	5.45	0.5	152,301	5.44	0.5	172,923
100	5.45	1.0	189,263	5.44	1.0	214,716
100	5.45	5.0	350,249	5.44	5.0	372,476
100	5.45	10.0	451,531	5.44	10.0	475,295
100	5.45	25.0	629,804	5.44	25.0	641,084
130	5.45	0.1	42,101	5.44	0.1	43,746
130	5.45	0.5	44,937	5.44	0.5	50,807
130	5.45	1.0	54,938	5.44	1.0	63,247
130	5.45	5.0	87,339	5.44	5.0	103,982
130	5.45	10.0	108,805	5.44	10.0	131,024
130	5.45	25.0	170,816	5.44	25.0	202,392

Table 4.6 HMA Average E* Test Results (Plant B JMF, 19 mm NMAS)

Temp. (F)	PLANT B					
	19 mm NMAS					
	PG64-22			PG67-22		
	Specimen 1			Specimen 1		
	COAC(%)	Hz	E* (psi)	COAC(%)	Hz	E* (psi)
14	4.74	0.1	1,898,571	4.73	0.1	1,905,469
14	4.74	0.5	2,461,926	4.73	0.5	2,311,083
14	4.74	1.0	2,666,052	4.73	1.0	2,432,990
14	4.74	5.0	3,051,147	4.73	5.0	2,749,982
14	4.74	10.0	3,253,626	4.73	10.0	2,879,321
14	4.74	25.0	3,536,557	4.73	25.0	3,047,858
40	4.74	0.1	1,153,515	4.73	0.1	1,159,468
40	4.74	0.5	1,600,639	4.73	0.5	1,553,226
40	4.74	1.0	1,778,782	4.73	1.0	1,724,034
40	4.74	5.0	2,147,783	4.73	5.0	2,096,240
40	4.74	10.0	2,331,959	4.73	10.0	2,250,761
40	4.74	25.0	2,571,845	4.73	25.0	2,460,464
70	4.74	0.1	443,681	4.73	0.1	453,684
70	4.74	0.5	674,037	4.73	0.5	658,418
70	4.74	1.0	799,804	4.73	1.0	773,313
70	4.74	5.0	1,132,767	4.73	5.0	1,104,463
70	4.74	10.0	1,284,441	4.73	10.0	1,235,905
70	4.74	25.0	1,497,781	4.73	25.0	1,444,093
100	4.74	0.1	105,133	4.73	0.1	135,543
100	4.74	0.5	154,321	4.73	0.5	198,784
100	4.74	1.0	189,286	4.73	1.0	243,518
100	4.74	5.0	339,719	4.73	5.0	421,282
100	4.74	10.0	434,601	4.73	10.0	521,576
100	4.74	25.0	595,309	4.73	25.0	685,114
130	4.74	0.1	41,814	4.73	0.1	47,268
130	4.74	0.5	44,615	4.73	0.5	55,819
130	4.74	1.0	55,592	4.73	1.0	69,796
130	4.74	5.0	87,819	4.73	5.0	118,566
130	4.74	10.0	111,784	4.73	10.0	147,544
130	4.74	25.0	175,678	4.73	25.0	216,844

Table 4.7 HMA Average E* Test Results (Plant B JMF, 25 mm NMAS)

Temp. (F)	PLANT B					
	25 mm NMAS					
	PG64-22			PG67-22		
	Specimen 1			Specimen 1		
	COAC(%)	Hz	E* (psi)	COAC(%)	Hz	E* (psi)
14	4.34	0.1	2,087,539	4.33	0.1	2,518,201
14	4.34	0.5	2,552,048	4.33	0.5	2,777,433
14	4.34	1.0	2,715,520	4.33	1.0	2,819,824
14	4.34	5.0	2,993,821	4.33	5.0	2,927,547
14	4.34	10.0	3,125,458	4.33	10.0	2,952,345
14	4.34	25.0	3,287,074	4.33	25.0	2,887,709
40	4.34	0.1	1,102,676	4.33	0.1	1,410,959
40	4.34	0.5	1,478,732	4.33	0.5	1,569,152
40	4.34	1.0	1,626,368	4.33	1.0	1,616,472
40	4.34	5.0	1,971,270	4.33	5.0	1,726,375
40	4.34	10.0	2,115,860	4.33	10.0	1,766,861
40	4.34	25.0	2,308,008	4.33	25.0	1,784,270
70	4.34	0.1	419,592	4.33	0.1	741,972
70	4.34	0.5	612,240	4.33	0.5	798,542
70	4.34	1.0	718,956	4.33	1.0	829,525
70	4.34	5.0	1,033,117	4.33	5.0	933,560
70	4.34	10.0	1,160,227	4.33	10.0	979,608
70	4.34	25.0	1,365,361	4.33	25.0	1,040,371
100	4.34	0.1	118,786	4.33	0.1	249,877
100	4.34	0.5	164,296	4.33	0.5	229,392
100	4.34	1.0	196,754	4.33	1.0	224,225
100	4.34	5.0	336,224	4.33	5.0	270,947
100	4.34	10.0	433,606	4.33	10.0	325,392
100	4.34	25.0	593,022	4.33	25.0	402,766
130	4.34	0.1	48,505	4.33	0.1	86,415
130	4.34	0.5	50,017	4.33	0.5	71,808
130	4.34	1.0	60,095	4.33	1.0	72,427
130	4.34	5.0	95,607	4.33	5.0	86,894
130	4.34	10.0	119,200	4.33	10.0	103,773
130	4.34	25.0	178,629	4.33	25.0	136,075

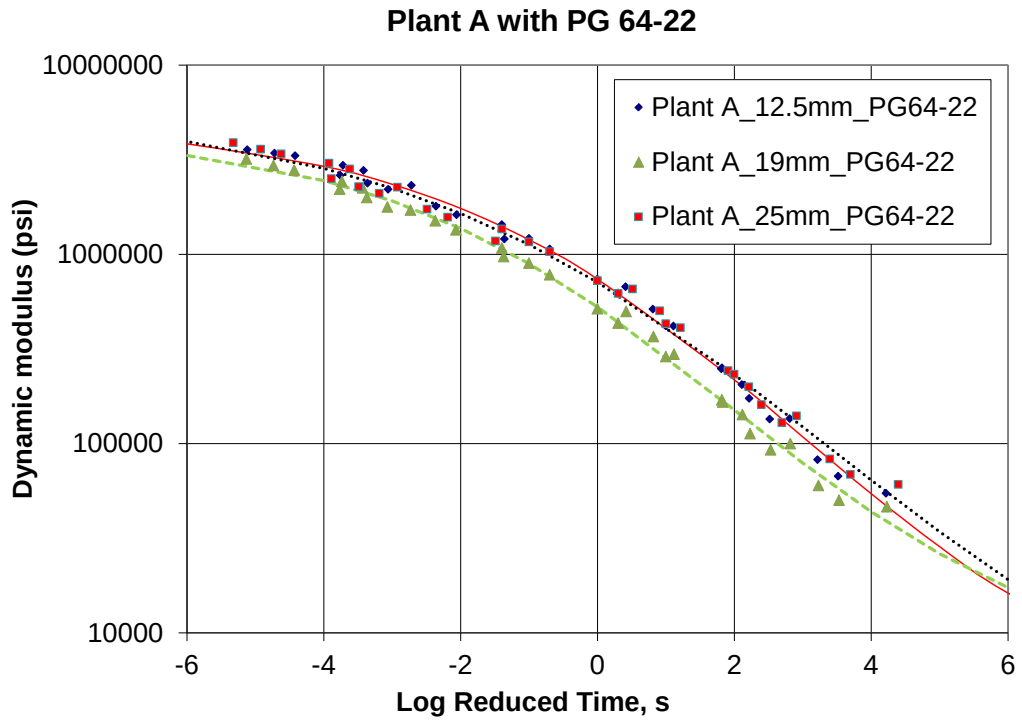

Fig. 4.4 Master Curve (Plant A JMF with PG 64-22)

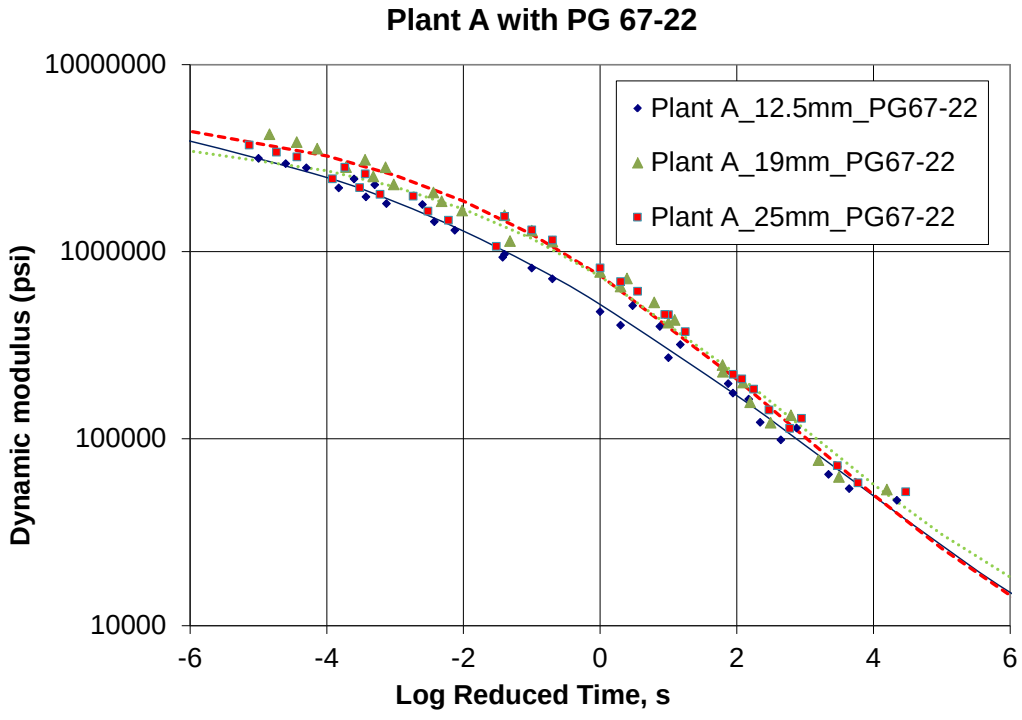

Fig. 4.5 Master Curve (Plant A JMF with PG 67-22)

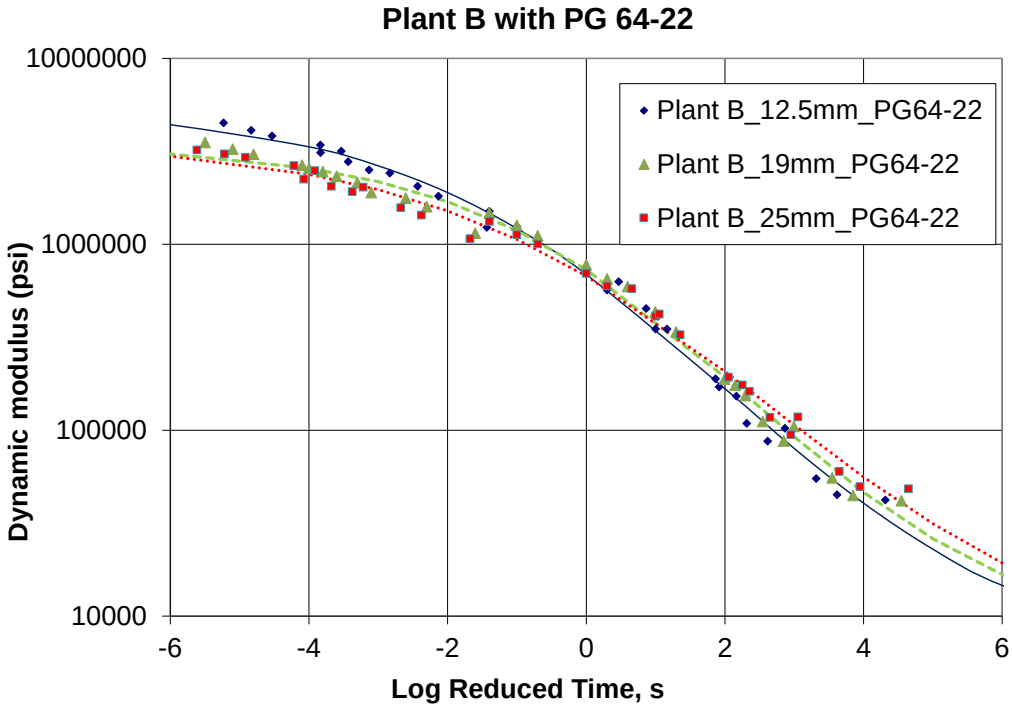

Fig. 4.6 Master Curve (Plant B JMF with PG 64-22)

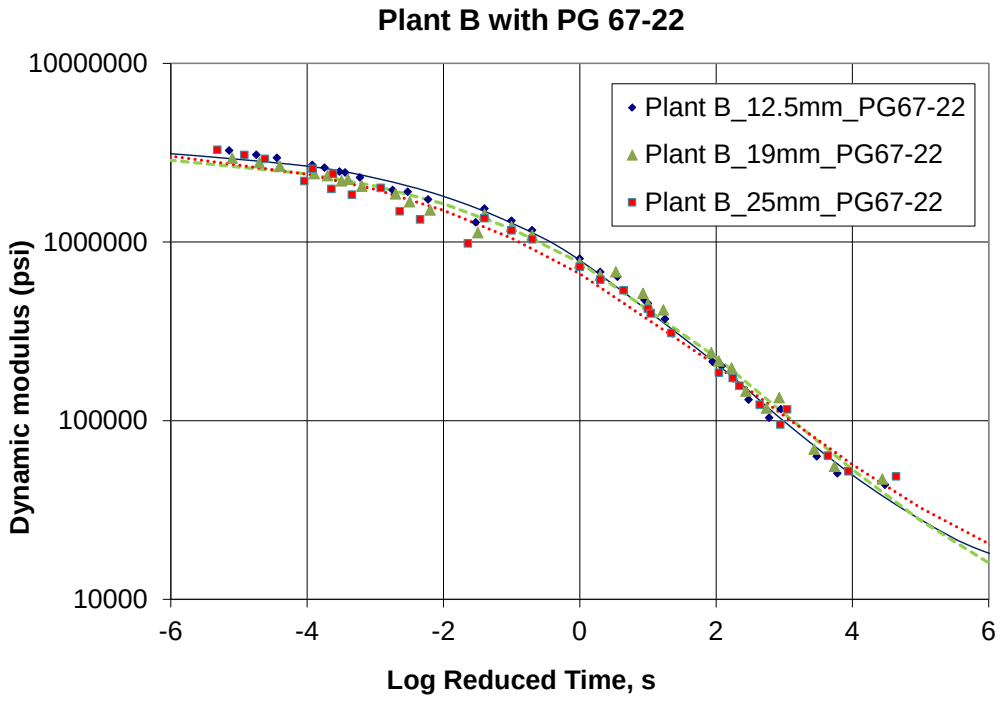

Fig. 4.7 Master Curve (Plant B JMF with PG 67-22)

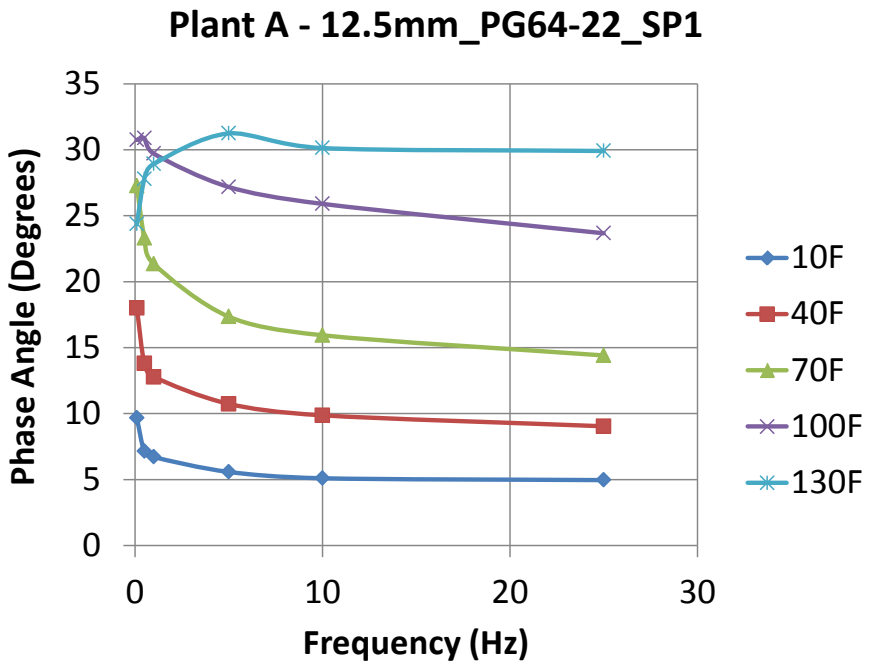

Fig. 4.8 Relationship between Phase Angle and Loading Frequency (Plant A, 12.5 mm NMAS, PG 64-22)

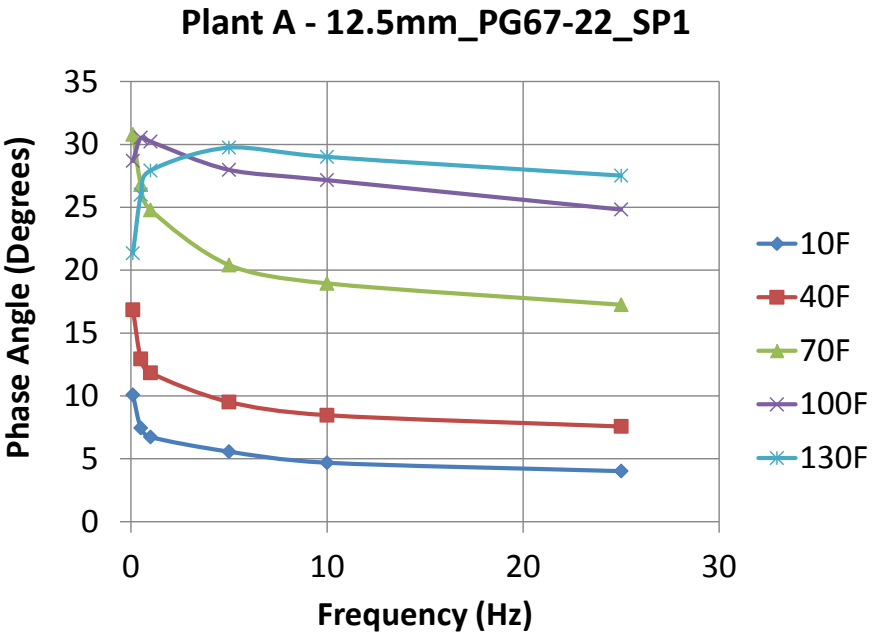

Fig. 4.9 Relationship between Phase Angle and Loading Frequency (Plant A, 12.5 mm NMAS, PG 67-22)

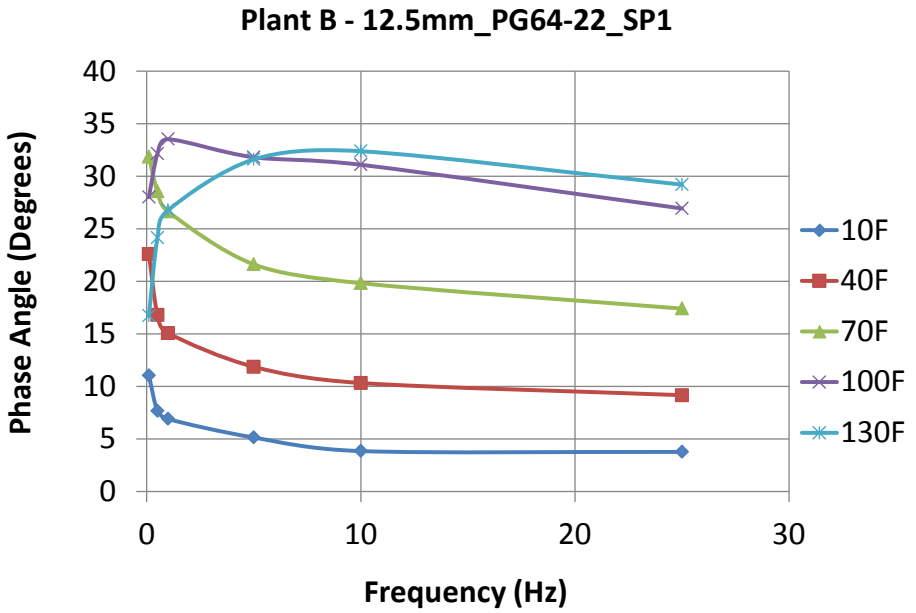

Fig. 4.10 Relationship between Phase Angle and Loading Frequency (Plant B, 12.5 mm NMAS, PG 64-22)

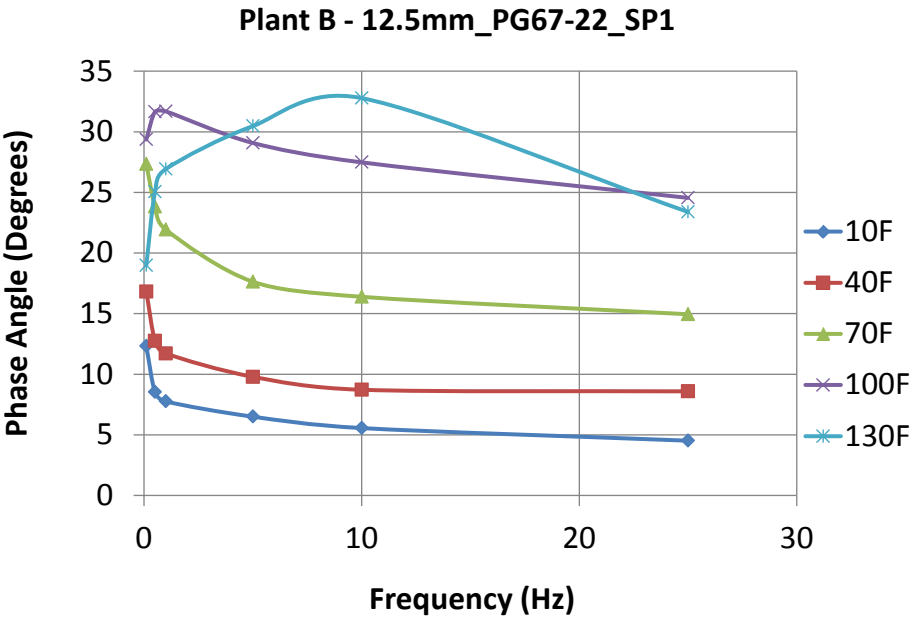

Fig. 4.11 Relationship between Phase Angle and Loading Frequency (Plant B, 12.5 mm NMAS, PG 67-22)

4.2 Graded Aggregate Base

4.2.1 Background

Unbound granular layer that is composed of odd-shaped aggregate particles with different size plays a structurally important role, especially for thin asphalt pavement subjected to the medium and low volume traffic loadings by providing load distribution through consolidation, distortion and attrition. For a reliable unbound pavement foundation, characterization of load-deformation behavior of unbound granular material is extremely important. In 1993, the American Association of State Highway and Transportation Officials (AASHTO) proposed a new pavement design procedure using the resilient modulus concept to describe the behavior of pavement materials under surface traffic loadings.

The deformation response of granular layers due to the surface traffic loading consists of resilient and permanent deformations. In the repeated triaxial test, considerable permanent deformation is observed at the initial stage of load applications and the increment of permanent deformation becomes smaller compared to the increment of resilient deformation after few load applications as shown in Fig. 4.12. Consequently, a properly designed granular layer accumulates very small amount of permanent deformation and most deformation is resilient deformation after repeated load test. For the characterization of this resilient behavior, the concept of resilient modulus (M_R) has been introduced and this concept gained the recognition as a useful property describing the resilient behavior of granular materials. Therefore, it is important to understand the factors affecting the M_R for design purposes and investigate the M_R changes when the influencing factors vary in certain amounts.

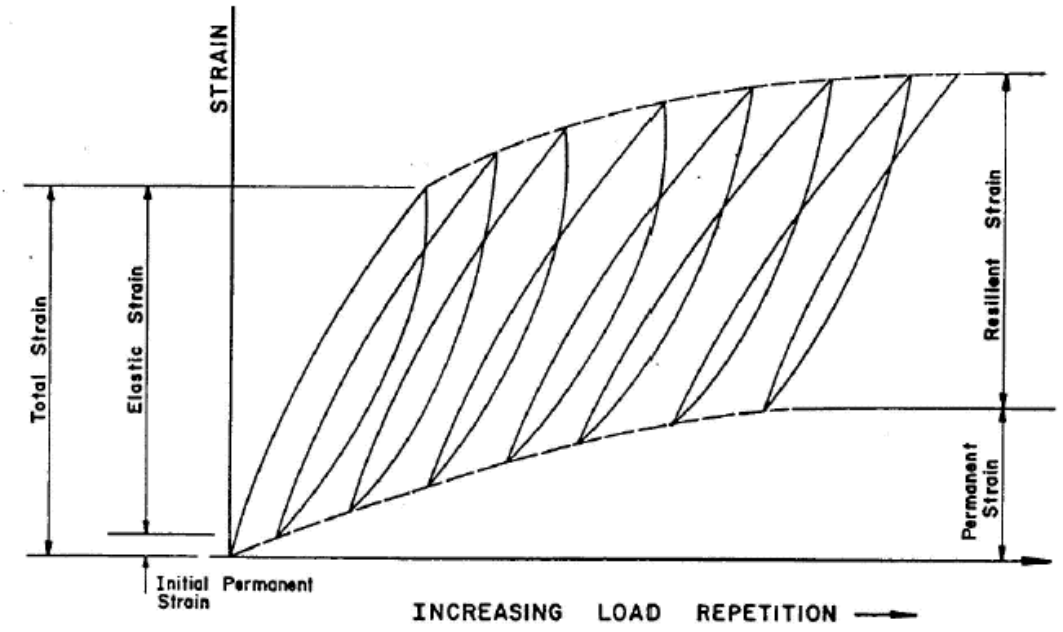

Fig. 4.12 Strains Under Repeated Loads (Huang, 1993)

4.2.2 Factors Affecting Resilient Behavior of Unbound Materials

Over five decades, many researchers who have investigated the nonlinear stress-dependent resilient behavior of unbound materials placed a relatively high degree of importance on the effect of deviatoric stress, dry density, moisture content, gradation and shape, fines content, and stress state, etc (Kim, 2004). The increase of dry density or degree of compaction of granular materials makes the aggregate medium stronger and stiffer. Previous researches indicated that the effect of dry density or degree of compaction has been considered as the significant influencing factors for the resilient behavior of unbound granular materials, by increasing the M_R with increasing dry density (Kim 2004). Kim et al. (2005) mentioned that the effect of the dry density decreases with increase of fine content and varies with the aggregate types and stress states.

A change in aggregate gradation produces a change in moisture content and dry density to form an appropriate aggregate assembly and the moisture content of unbound granular materials significantly affects the resilient response (Kim et al, 2007). Kim et al.

(2007) explained that the initial increase of stiffness is due to the increase of the contacts as voids are filled with fines and the decrease of stiffness is due to the displacement among coarse particles as excess fines are added. This results in the loss of aggregate particle interlocks and load carrying ability lies only on the fines. To investigate the effect of gradation on M_R, Kim et al. (2007) proposed the use of a three-parameter equation to quantify the full-scale particle size distributions. This three-parameter equation used to fit cumulative distribution functions of aggregate gradations is shown in Eq. (5):

$$P_p = \frac{100}{\ln\left[\exp(1) + \left(\frac{g_a}{d}\right)^{g_n}\right]^{g_m}} \quad (5)$$

Where,

P_p= the percent passing a particular grain size diameter, d, measured in mm,
g_a = fitting parameter corresponding to the initial break in the grain-size curve,
g_n = fitting parameter corresponding to the maximum slope of the grain-size curve,
g_m is a fitting parameter corresponding to the curvature of the grain-size curve.

Non-linear regression analyses were performed to obtain a set of parameters that fit a specific gradation. When the g_n and g_m are fixed, the parameter g_a is related to the percent of coarse aggregates. The parameter g_n controls the slope of the gradation curve, which determines if the gradation curve is open, gap or well graded. When the value of the parameter g_n increases, the gradation moves toward a gap-gradation, and differences between the slopes in the early and latter portion of the curves become more severe.

It has been also known that the stress state is an important factor influencing resilient properties of unbound granular materials. They have shown that the M_R of unbound granular materials depends on the confining stress and sum of principal stresses. It is generally agreed that the M_R increases with increasing confining stress and decreasing deviatoric stress.

4.2.3 Materials and Laboratory Test

To correctly characterize aggregate behavior, it is important to properly simulate the actual loading conditions in the laboratory. In this study, repeated load triaxial test was conducted for a prepared specimen in accordance with AASHTO T 307-99. Fig. 4.13 is a photograph of the test setup. IPC system supports automated control of cell movement and computer control of both confining and axial stress with Linear Variable Differential Transducers (LVDTs) for vertical strain. The apparatus can perform the test at multiple frequencies and stress states. This operation helps to measure resilient response not only time-dependent responses, but also stress-dependent responses of materials.

Fig 4.13 IPC Repeated Load Triaxial Test Setup

Fig. 4.13 and Table 4.8 show the selected aggregate sources to determine resilient properties. The selected materials possess substantially different shape, form and texture properties. Fig. 4.15 shows the different gradations of each Graded Aggregate Base (GAB) source used in this study. As shown in Fig. 4.15, the gradations of each source of GAB satisfy the GDOT

GAB specification. A 6-inch in diameter by 12-inch high cylindrical GAB specimen was prepared for testing. The aggregate sources in Table 4.8 were compacted with impact compaction method. Samples prepared with the impact compaction method were compacted with AASHTO T-180 using a 10-lb hammer and a 18-inch drop. The samples were compacted in 6 layers with high compaction effort. The GAB specimens were attempted to be compacted with 100% maximum dry density for Group II GAB and 98% maximum dry density for Group I GAB, respectively. Some of Group II GAB specimens were not compacted with 100% maximum dry density, but all specimens achieved more than 98% compaction efforts. The percent compaction is also shown in Table 4.8. Twenty two (22) specimens (11 materials by 2 replicates) were then subjected to resilient modulus test in accordance with AASHTO T 307-99. A total of 22 samples (11 materials by 2 replicates) were tested.

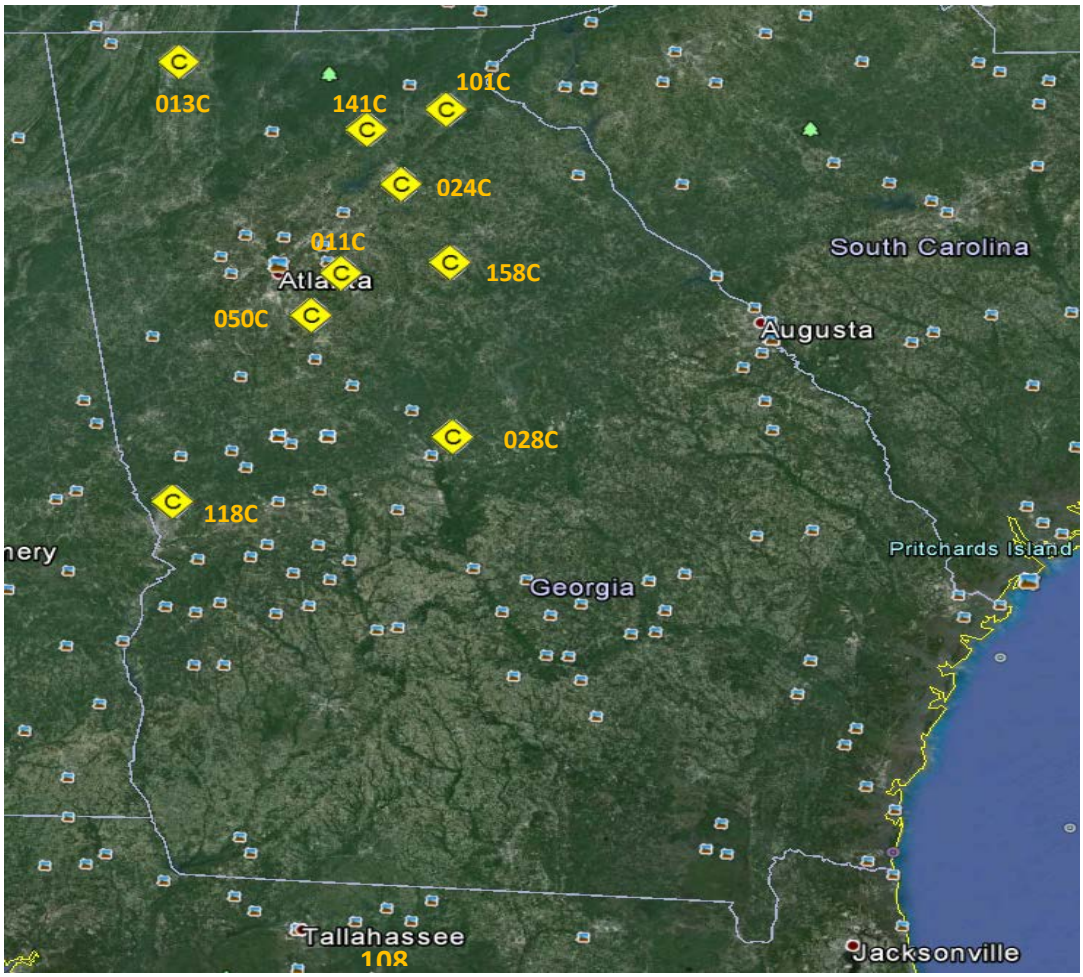

Fig 4.14 GAB Source Locations

TABLE 4.8 Aggregate Sources and Physical Properties

QPL ID	Aggregate Group	Source Location	GAB Character	w_{opt} (%)	Max. γ_d (pcf)	w_{actual} (%)	Actual γ_d (pcf)	Percent Compaction	LA Abrasion (%)	Bulk Specify Gravity
011C	II	Lithonia	Granite Gneiss	5.7	133.9	4.3	133	99	50	2.614
013C	I	Dalton	Limestone	6.6	142.5	4.7	139	98	25	2.702
024C	II	Gainesville	Mylonitic Gneiss	6	136.6	6.7	134	98	39	2.605
028C	II	Hitchcock	Mylonitic Gneiss	6.2	141.2	5.6	138	98	18	2.697
050C	II	Stockbridge	Granite Gneiss	5.9	134.2	5.9	134	100	42	2.611
101C	II	Demorest	Meta-sandstone	5.3	137.4	5	137	100	32	2.642
108T	I	Mayo Mine	Lime rock	13.6	112.6	11.5	110	98	N/A	N/A
118C	II	Columbus	Granite Gneiss	6	137.2	6.5	135	98	33	2.677
141C	II	Dahlonega	Granite Gneiss	5.6	135.2	4	132	98	34	2.646
158C	II	Walton County	Biotite Gneiss	6.4	135	4.5	132	98	41	2.64
165T	II	I-75 Unadilla	Recycled Concrete	7	134	8.5	131	98	N/A	N/A

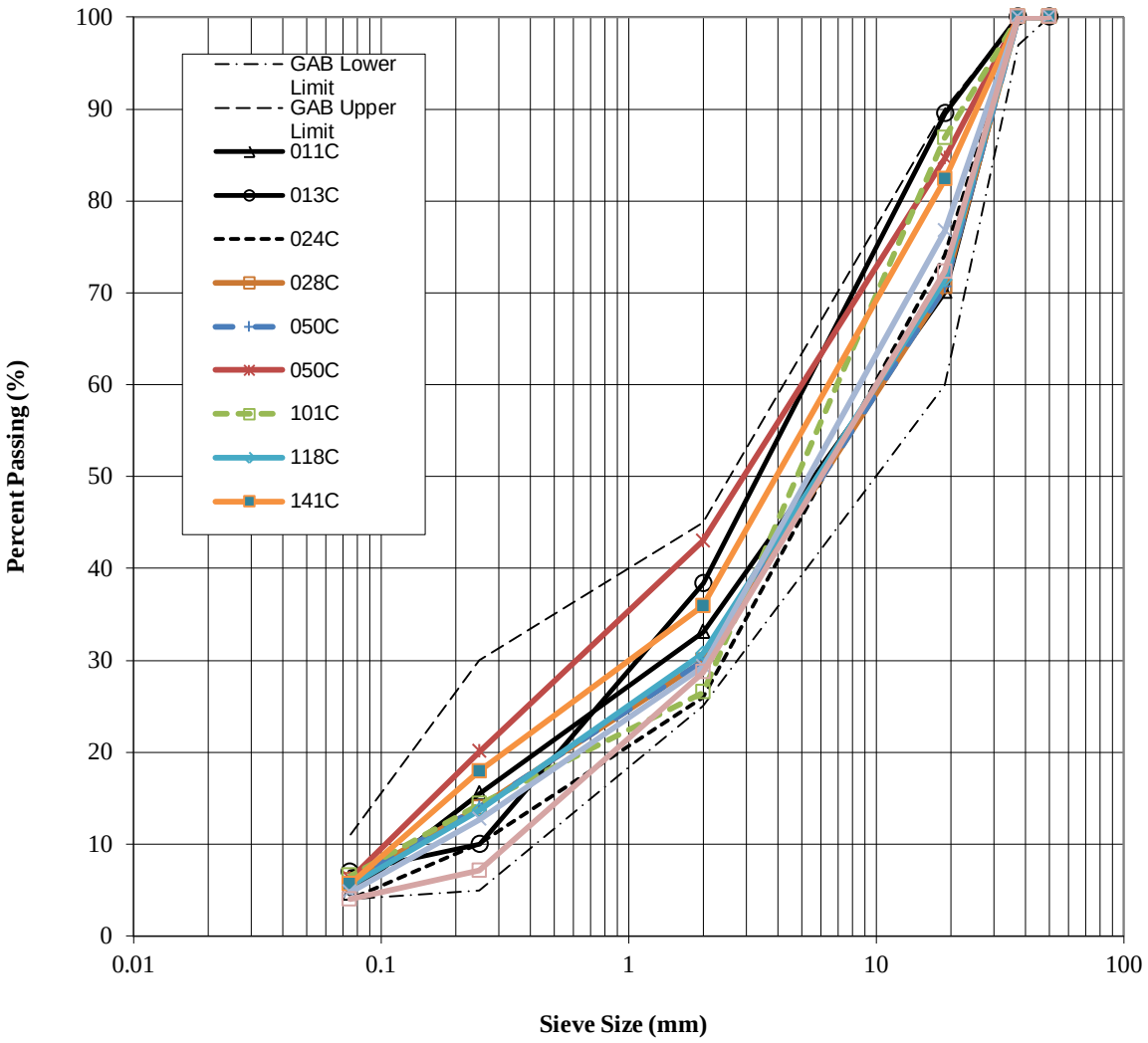

Fig. 4.15 GAB Gradations

4.2.4 Resilient Modulus Testing Protocol

The AASHTO protocol uses fifteen (15) stress states to determine stress sensitivity. At each static stress state, dynamic changes in stresses are applied to specimen and resilient strain are measured. A loading cycle of dynamic stress consists of 0.1 seconds loading and 0.9 seconds unloading period. Five-hundred (500) to One-thousand (1000) load repetitions were applied for conditioning of the specimens, and the deviator and confining stress were held at 15 psi to eliminate the effects of initial permanent deformation. After the conditioning

of the specimen, one hundred (100) load repetitions were applied to specimen for each load sequence as shown in Table 4.9. The mean deviator stress and mean recovered deflection were recorded and used for the calculation of the mean resilient modulus at each tress state. Two replicates of each aggregate system were molded and were in turn subjected to AASHTO T 307-99. The average values of two replicates were reported.

TABLE 4.9 AASHTO T307-99 Stress States for GAB Layer

Test Sequence	σ_1 (kPa)	σ_3 (kPa)	σ_1 (psi)	σ_3 (psi)	Number of Cycles
1	41.4	20.7	6	3	500-1000
2	62.1	20.7	9	3	100
3	82.8	20.7	12	3	100
4	69.0	34.5	10	5	100
5	103.5	34.5	15	5	100
6	137.9	34.5	20	5	100
7	137.9	68.9	20	10	100
8	206.8	68.9	30	10	100
9	275.8	68.9	40	10	100
10	172.4	103.4	25	15	100
11	206.8	103.4	30	15	100
12	310.3	103.4	45	15	100
13	241.3	137.9	35	20	100
14	275.8	137.9	40	20	100
15	413.7	137.9	60	20	100

4.2.5 Test Results and Analyses

The MEPDG suggests that the resilient behavior of the granular material systems has two components namely a hardening and a softening component. The hardening component is responsible for stress hardening and for improvements in stiffness properties of the system through soil particle interlocking effect. The softening component is related to the loss of stiffness due to generation of shear bands in the specimen. Eq. (6) presents the stress-sensitive and nonlinear relationship used to calculate the resilient modulus in this research effort.

$$M_R = k_1 p_a \left(\frac{\theta}{p_a} \right)^{k_2} \left(\frac{\tau_{oct}}{p_a} + 1 \right)^{k_3} \quad (6)$$

where:

M_R = resilient modulus,

σ_1, σ_2, σ_3 = principal stresses,

σ_d = deviatoric stress ($\sigma_1 - \sigma_3$),

θ = the bulk stress = $\sigma_1 + \sigma_2 + \sigma_3 = 3\sigma_3 + \sigma_d$,

τ_{oct} = octahedral shear stress = $\frac{1}{3}\sqrt{(\sigma_1 - \sigma_2)^2 + (\sigma_1 - \sigma_3)^2 + (\sigma_2 - \sigma_3)^2} = \frac{\sqrt{2}}{3}\sigma_d$,

P_a = atmospheric pressure, and

k-values = regression coefficients (dimension less).

Resilient modulus test results are shown in Table 4.10 and Figs. 4.16 through 4.26. The figures show the variations of vertical resilient modulus with respect to bulk stress. As evidenced in those figures, the resilient modulus increases with bulk stress, which demonstrates the stress-hardening behavior of the aggregate base materials. As illustrated in the figures, stiffness properties of the aggregate samples were improved with increasing stress magnitude. This could be due to reduction of the air voids in the continuum, which in turn results in higher friction forces between aggregate particles and therefore better orthogonal load bearing capacity of the mix.

The modulus values of the aggregate systems showed softening behavior when subjected to more taxing stress states. The softening behavior of the aggregate systems is indicated by the negative values of the k_3 regression coefficient. Aggregate systems with higher k_3 values are known to be more susceptible to develop shear rutting at elevated stress states (Kim et al. 2004; Kim et al 2005, Ashtiani 2008).

Table 4.10 GAB Resilient Modulus Test Results

QPL ID	k_1	k_2	k_3	R^2
011C	1049	0.716	-0.041	1.00
013C	1031	0.659	-0.145	0.99
024C	739	0.797	-0.012	0.98
028C	996	0.591	-0.046	0.99
050C	969	0.522	-0.022	0.99
101C	674	0.734	-0.014	0.99
108T	803	0.862	-0.012	0.96
118C	782	0.801	-0.084	0.99
141C	643	0.767	-0.111	0.99
158C	965	0.564	-0.010	0.99
165T	1173	0.626	-0.019	0.99

Note: k-values are dimensionless.

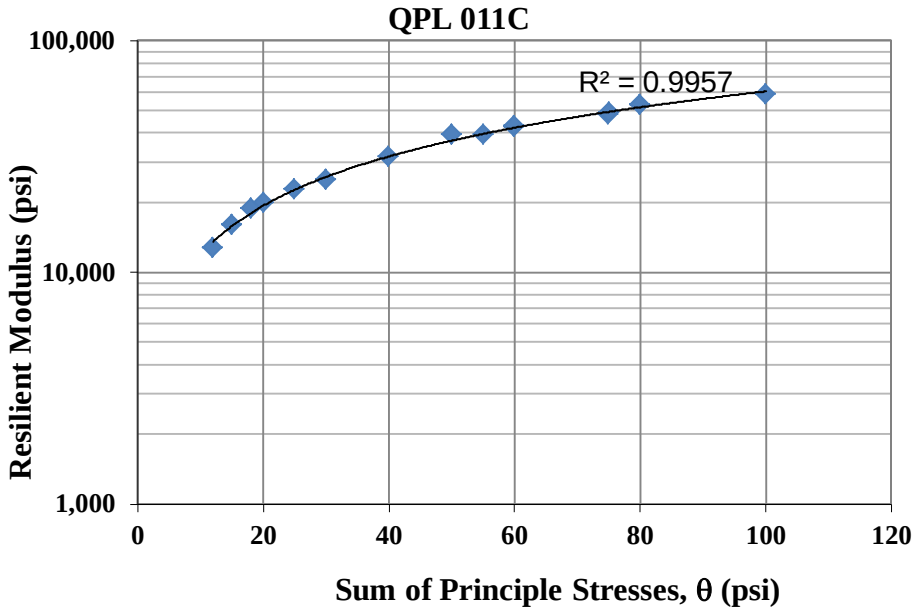

Fig. 4.16 Resilient Modulus vs. Bulk Stress (QPL 011C)

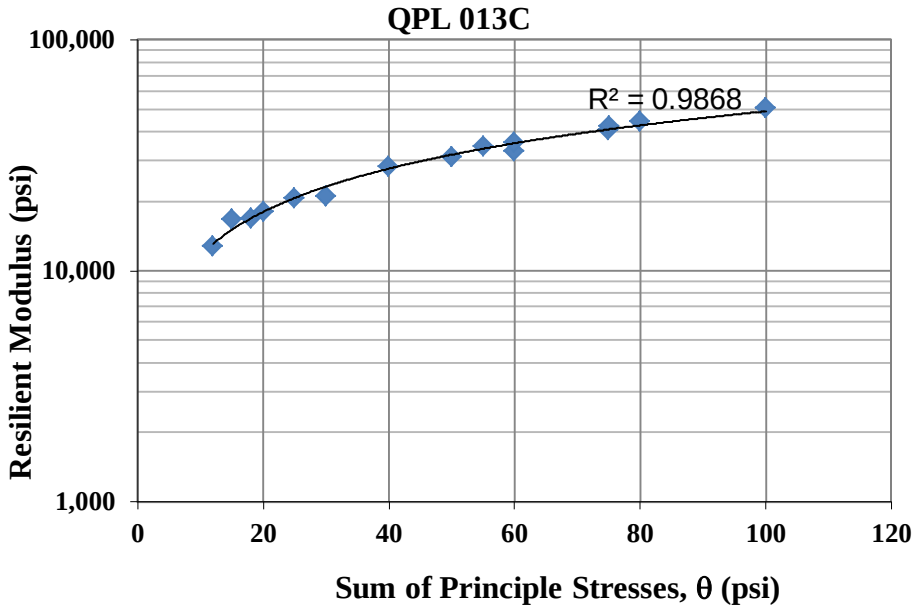

Fig. 4.17 Resilient Modulus vs. Bulk Stress (QPL 013C)

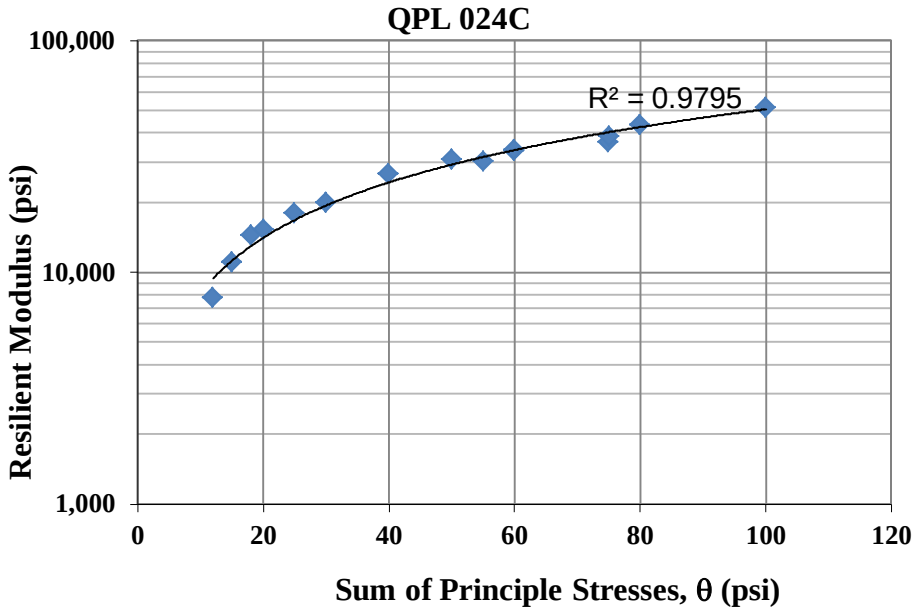

Fig. 4.18 Resilient Modulus vs. Bulk Stress (QPL 024C)

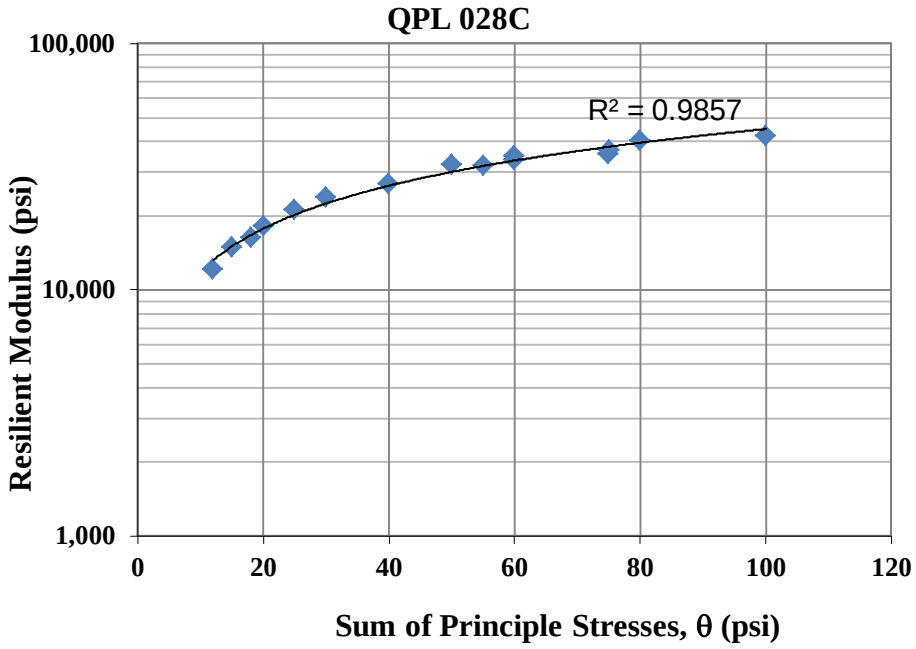

Fig. 4.19 Resilient Modulus vs. Bulk Stress (QPL 028C)

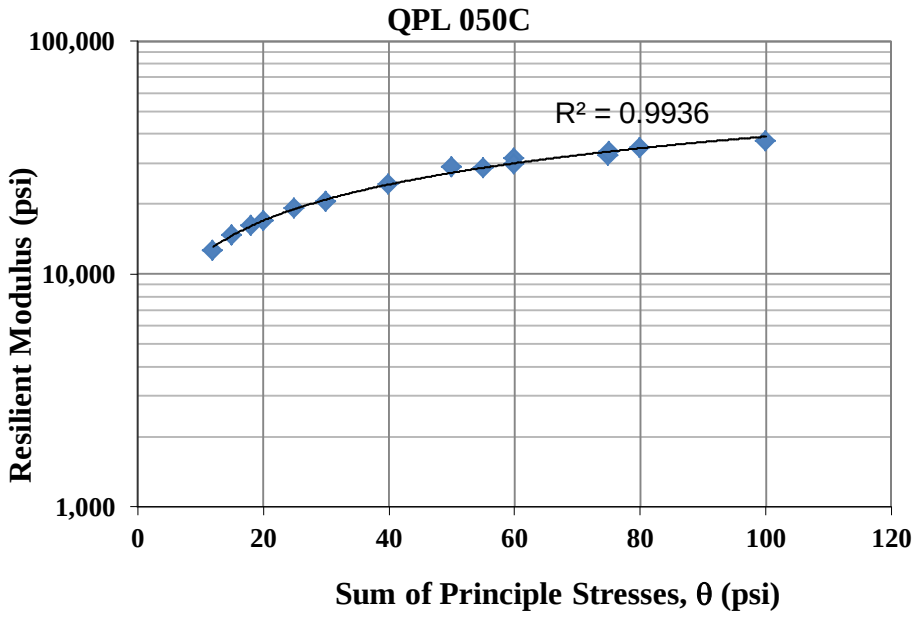

Fig. 4.20 Resilient Modulus vs. Bulk Stress (QPL 050C)

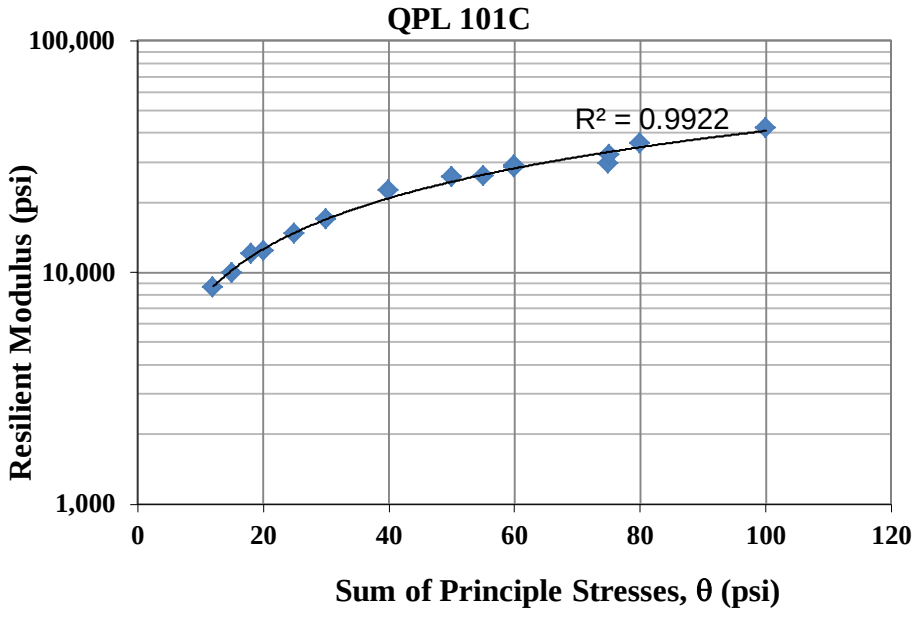

Fig. 4.21 Resilient Modulus vs. Bulk Stress (QPL 101C)

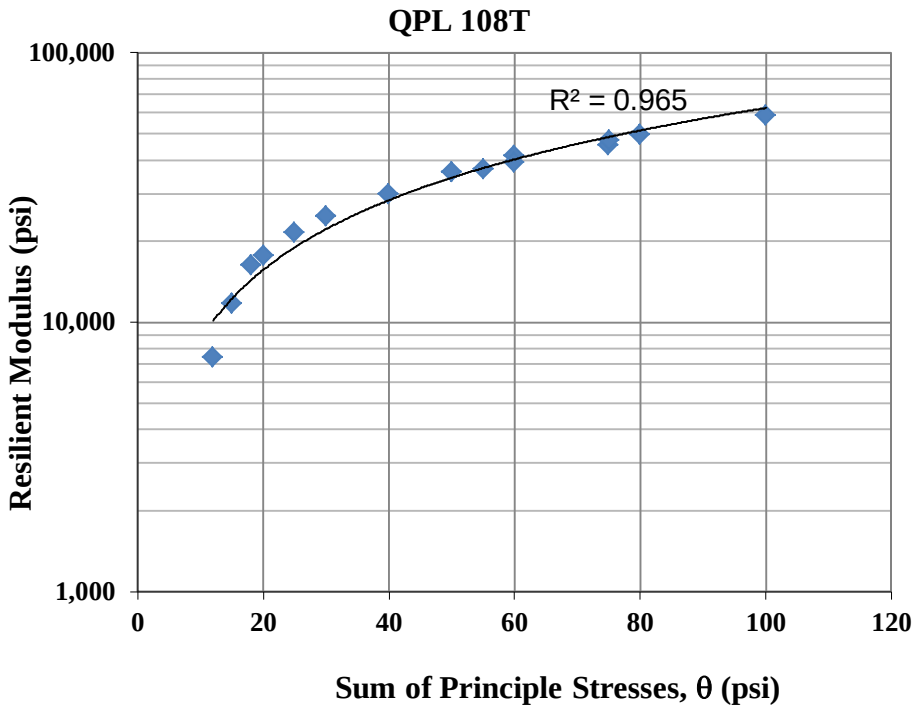

Fig. 4.22 Resilient Modulus vs. Bulk Stress (QPL 108T)

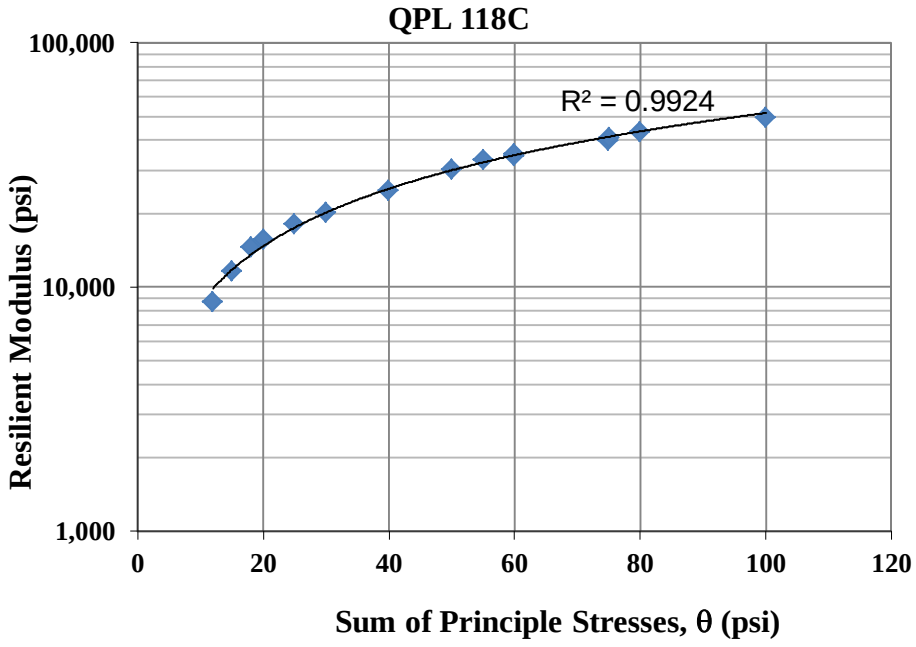

Fig. 4.23 Resilient Modulus vs. Bulk Stress (QPL 118C)

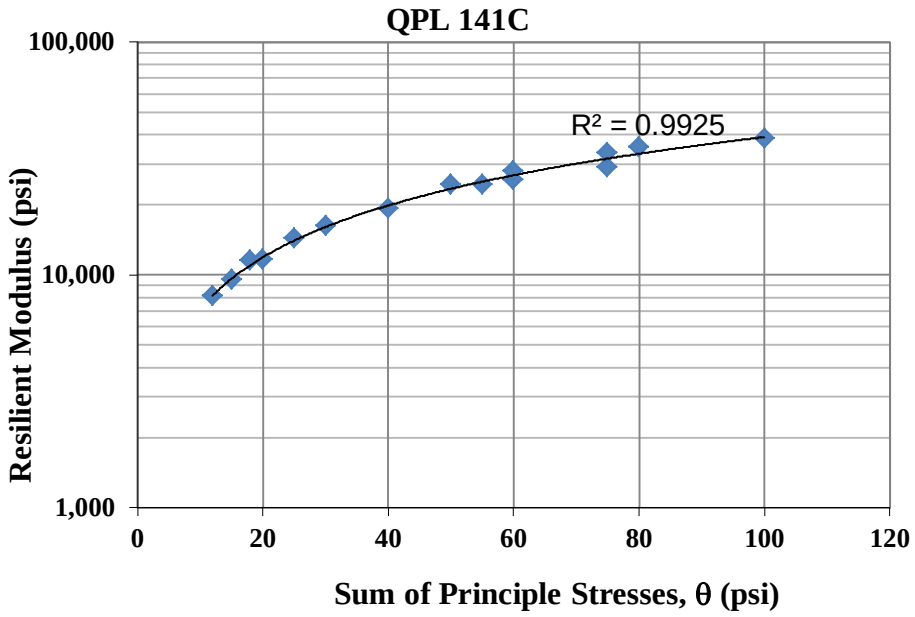

Fig. 4.24 Resilient Modulus vs. Bulk Stress (QPL 141C)

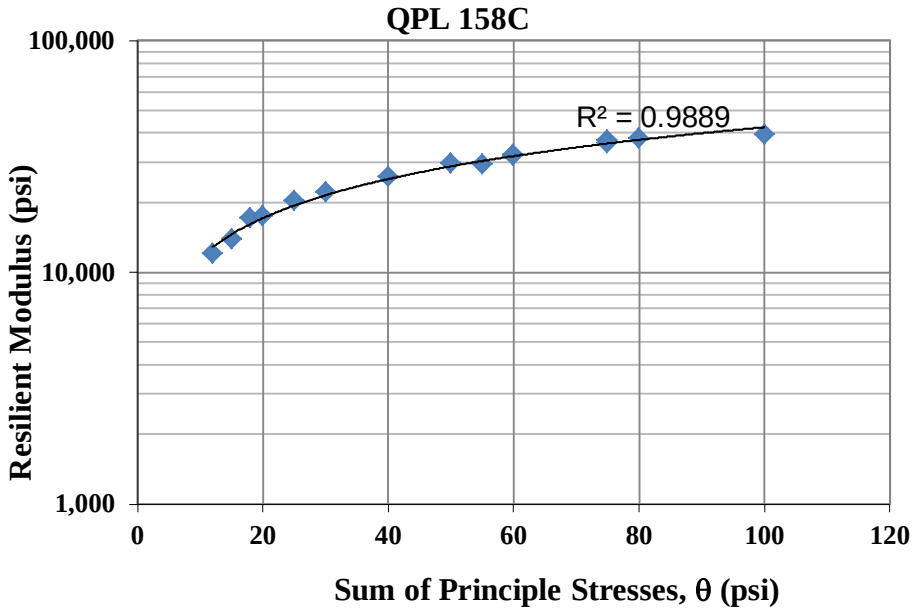

Fig. 4.25 Resilient Modulus vs. Bulk Stress (QPL 158C)

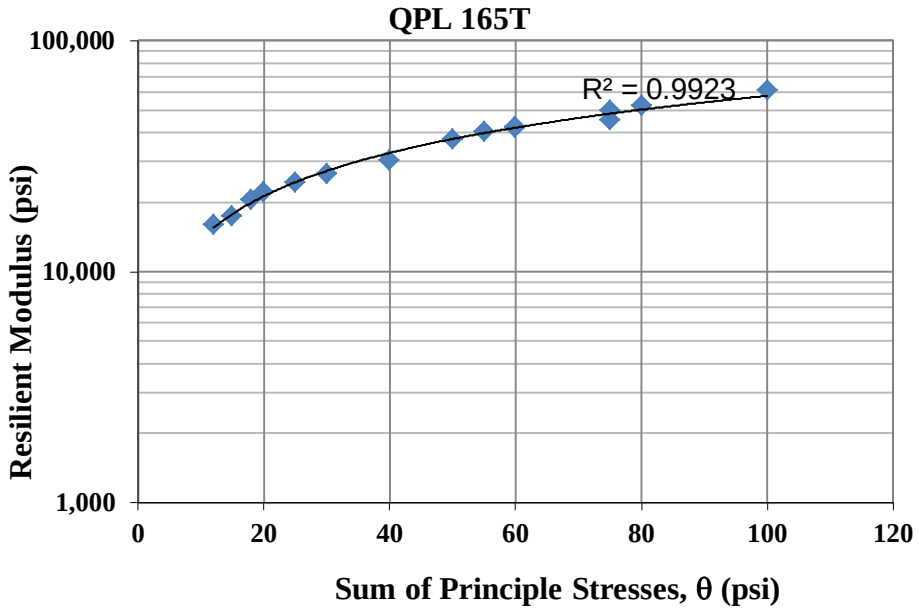

Fig. 4.26 Resilient Modulus vs. Bulk Stress (QPL 165T)

4.2.6 Moisture Susceptibility of Recycled Concrete as Unbound Base Materials

Resilient behavior of Unbound Aggregate Base (UAB) is significantly influenced by the aggregate physical properties and thus, good quality aggregate is desirable for construction of sustainable and perpetual flexible pavements. However, the ever-increasing cost of oil and gas byproducts has motivated road management agencies to pursue alternative construction techniques and materials to reduce the cost of pavement rehabilitation and construction. Recently, the use of Recycled Concrete (RC) materials as aggregate base layer has gained traction due to potential cost saving and reduction in undesirable environmental impacts, while maintaining the structural integrity of pavement foundations. It is well established in the literature that RC systems provide better resilient properties and superior rutting resistance compared to virgin aggregate systems (Ashtiani, 2012).

Although resilient properties of RC aggregate base factor significantly into flexible pavement design, the environmental aspect of RC aggregate base has been somewhat overlooked. RC aggregate base experiences significant moisture fluctuations due to rainfall, drainage, elevation of water table, and suction variation under repeated traffic loadings. Therefore, it is

essential to properly evaluate the effects of moisture and frost susceptibility of RC aggregate systems as well as the mechanical properties for the design and construction of pavements.

The propensity of recycled aggregate systems to hold moisture and therefore to cause moisture damage in the pavement structure needs to be considered. This type of damage manifests itself through the decay of resilient modulus and consequently results in loss of performance upon freezing and thawing cycles.

Previous research indicates that even small amount of free water in the UAB decreases resilient modulus by as much as 75 percent upon subjecting the samples to capillary rise conditions (Saarenketo, 1998). Also, RC aggregate base shows high moisture susceptibility, which significantly affects the resilient properties of aggregate base (Saeed, 2008, Ashtiani 2012). Therefore, it is imperative to consider both the effect of frost susceptibility and its impact on resilient behavior when RC is considered as an option for use in pavement foundations.

Guthrie and Scullion (2003) conducted a series of tube suction tests (TST) to assess the moisture susceptibility of UAB by measuring dielectric value using percometer. The percometer measures the dielectric value, which is an indication of the volumetric moisture content and the state of molecular bonding in a material. They employed statistical analysis on the TST laboratory data to establish acceptable thresholds for ranking the quality of the UAB materials. The interpretation of TST results were shown in Table 1.

TABLE 4.11 Interpretations of TST Results

Dielectric Value	Material Quality
< 10	Good
between 10 and 16	Marginal
> 16	Poor

This section presents the mechanical and environmental properties of three different aggregate sources as aggregate base materials. Aggregate specimens were prepared at optimum moisture content and at maximum dry density and were subjected to Tube Section Test (TST) to evaluate environmental properties. For TST, Aggregate specimens were compacted in 6-inch diameter and 8-inch in height molds and the dielectric values were measured at the top of each specimen at pre-determined time intervals using a percometer. Dielectric values of the specimen were measured in accordance with TX-144-E (Saarenketo and Scullion, 1995).

The variation of the dielectric value with respect to time is presented in Fig. 4.27. As shown in Fig. 4.27, it was observed that aggregate specimen composed of RC had higher frost susceptibility compared to control specimens composed of virgin aggregates.

The results indicate that the dielectric value of aggregate #3, consisted of 165T recycled RC materials, increased drastically from approximately 3.8 to 14.8 after 10 days, while virgin aggregate systems #2 and #3 had significantly lower variations. Based on TX-144 Tube Suction Test (TST) results, it was observed that the RC materials had higher affinity for moisture retention and therefore are more prone to performance degradation due to moisture damage in service. Results of this investigation indicate that RC provides good mechanical performance as a UAB, but the effects of increased moisture retention warrant careful observation of actual field performance over several climatic cycles.

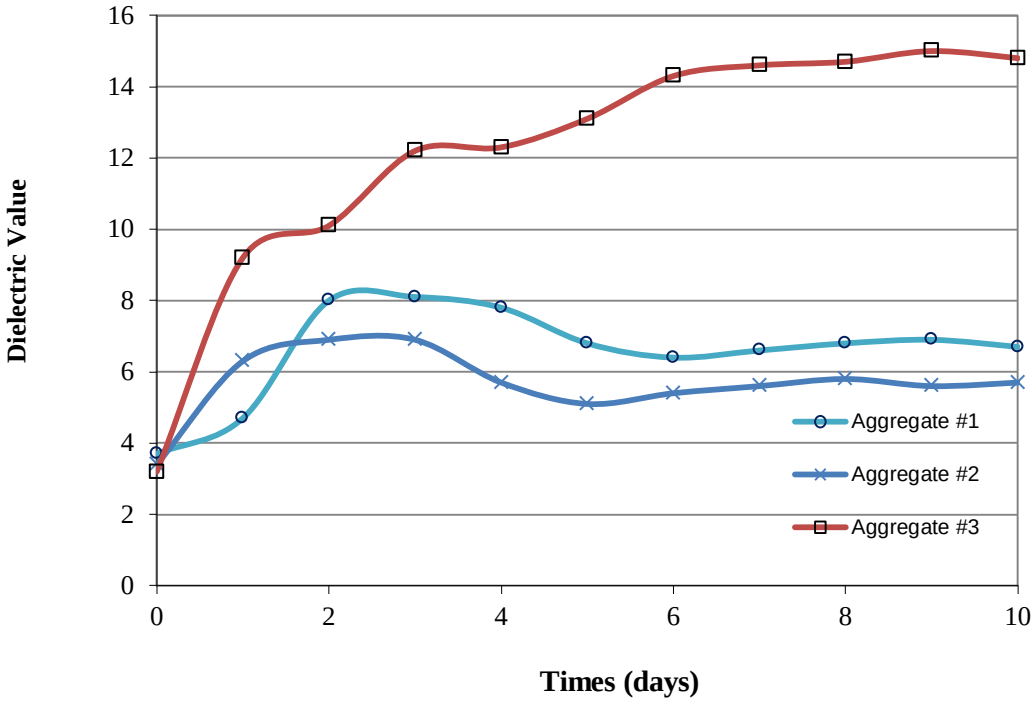

Fig. 4.27 Dielectric Value along with Times

4.2.7 Artificial Neural Network Modeling for GAB

Artificial Neural Network (ANN) has been extensively used in the engineering field especially for multidimensional function mapping. Given the exemplar data pairs, ANNs are capable of abstracting the relationship underlying the data. To construct an ANN for solving a particular problem, two key components must be identified: architecture and learning method.

Funahashi (1989) and Hornik et al. (1989) separately proved that any continuous function can be approximated with an arbitrary accuracy by using a three-layered network. Thus, from a theoretical viewpoint, the three-layer network is adequate for function approximation. As such, a three-layer ANN with one hidden layer was adopted in this study. Each neuron in an ANN is an independent processing element, having its own inputs and output. The commonly used neuron activation function, tansig (Eq.(7)), is used because it produces both positive and negative values and tends to speed training.

$$y = f(x) = \frac{2}{1 + e^{-2(\sum_{i=1}^{n} w_i x_i + b)}} - 1 \qquad (7)$$

where,

y = neuron output;

n = number of element in the input vector;

x_i = ith element in the input vector;

w_i = weight of link I;

b = bias

The learning capability of ANNs is achieved by adjusting the signs and magnitudes of their connection weights according to learning rules that seek to minimize a cost or an error function. The back-propagation method is selected because of its generality and versatility in function mapping. Several algorithms have proved to be effective in back-propagation training, such as gradient decedent with moment and adaptive learning rate, Levenberg-Marquardt, quasi-Newton, conjugate-gradient, and Bayesian regulation. Bayesian regulation

back-propagation (BRBP) algorithm is finally used for this study due to improved generalization and robustness to the notorious over-fitting problem.

Traditional network training algorithms, such as gradient decedent, aim to minimize the sum of square errors, such as the one in Eq. (8).

$$E_D = \frac{1}{2}\sum_{r=1}^{p}\sum_{k=1}^{m}\left(T_k^{(r)} - Y_k^{(r)}\right)^2 \quad (8)$$

where,

E_D = sum of square errors for all the patterns in the data sample;

p = the number of patterns in the data sample;

m = number of neurons in the output layer;

$T_k^{(r)}$ = target value of neuron k for pattern r; and

$Y_k^{(r)}$ =output of neuron k for pattern r

However, a dilemma often occurs during the network training process, dealing with whether the network is generalizing or memorizing the exemplar data. A memorizing network tends to produce smaller training errors, but large testing and validation errors, implying large prediction errors. BRBP aims to resolve this issue. Instead of minimizing the total squared network errors, BRBP minimizes a combination of squared errors and weights, an indicator of the "amount" of knowledge gained through training. As such, the BRBP objective function takes the form of Eq. (9).

$$F = \alpha E_W + \beta E_D \quad (9)$$

where,

α and β = parameters;

E_W = the sum of squares of errors;

E_D = the sum of squares of the network weights

As seen, BRBP takes consideration of both the goodness of fit in terms of data and the network fitness in terms of weights. By this way, the neural networks can be trained with

improved generalization ability. The weights are updated according to Levenberg-Marquardt algorithm using Eq. (10).

$$w_{i+1} = w_i - [J^T J + \mu I]^{-1} J^T e_k \quad (10)$$

Where,

J = the Jacobian matrix;

e_k = the vector of network errors;

μ = the damping factor.

Detailed discussion on the BRBP can be found in MacKay D. J. C. (1992). To establish the relationship between M_R and GAB physical properties, a three-layer back-propagation ANN was formulated with the lab-tested data described previously. For network training and testing purposes, the lab data were randomized and divided into two sets: training and testing. The training set contains 119 observations and the testing set contains 46 observations. Based on a statistical analysis, six factors show significance in explaining the variance of M_R and thus selected as inputs for the ANN model. The number of neurons in the hidden layer was based on Eq. (11), recommended in the NeuroShell 2 Software.

$$N = integer\left(\frac{n}{2} + \sqrt{R}\right) \quad (11)$$

Where,

n = the number of input and output neurons,

R = the size of the training data set.

As shown in Figure 4.29, the finally ANN architecture was selected, which are stress state and aggregate physical properties such as moisture content, dry density, and gradation parameters. The training and testing results are shown in Figs. 4.29 and 4.30. The high R^2 values indicate a good prediction of M_R by the ANN model. The mean absolute errors and root-mean-square errors are within 8% and 14% for training and testing, respectively. The relatively higher testing errors are expected due to unseen data pairs.

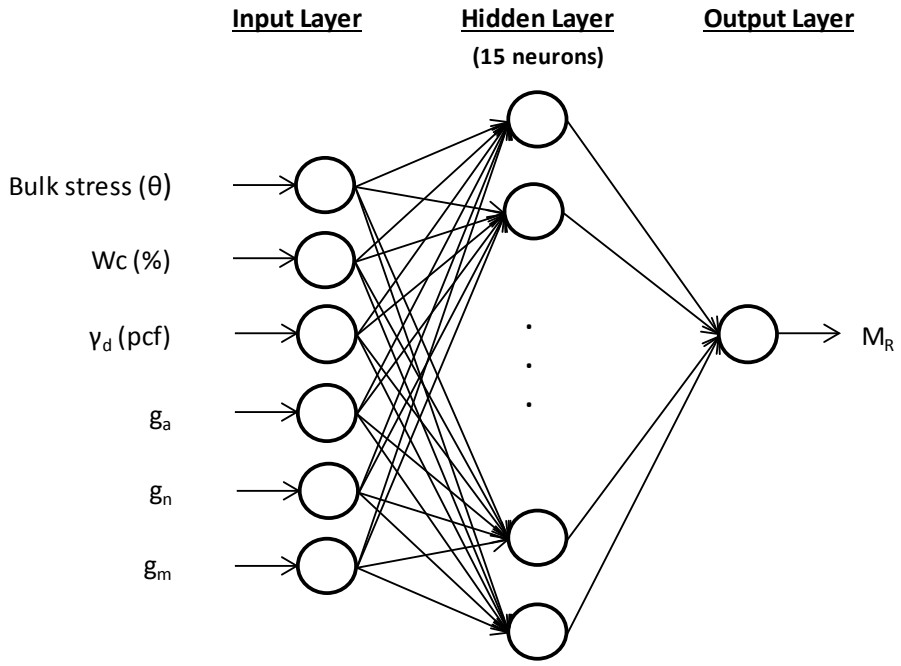

Fig. 4.28 Selected ANN Architecture

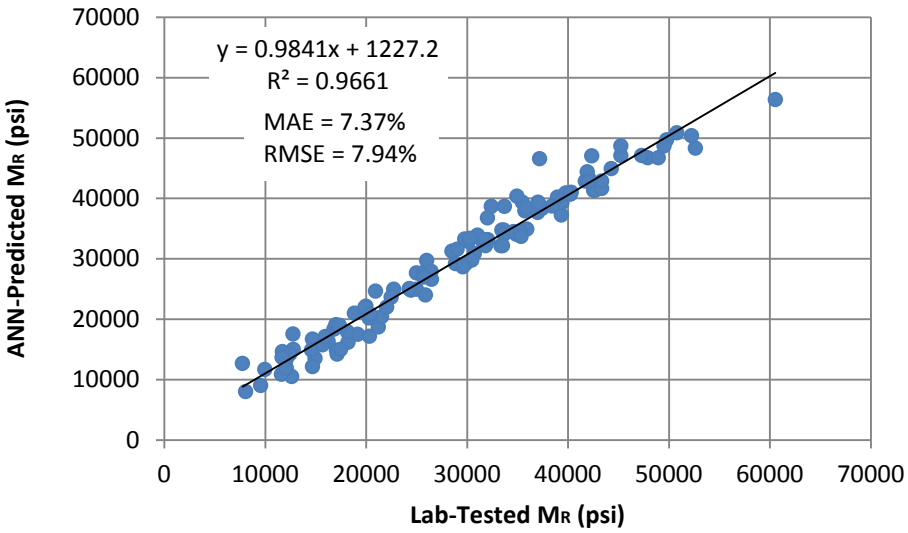

Fig. 4.29 Comparison of Lab-Tested M_R with ANN-Predicted M_R (Training Data)

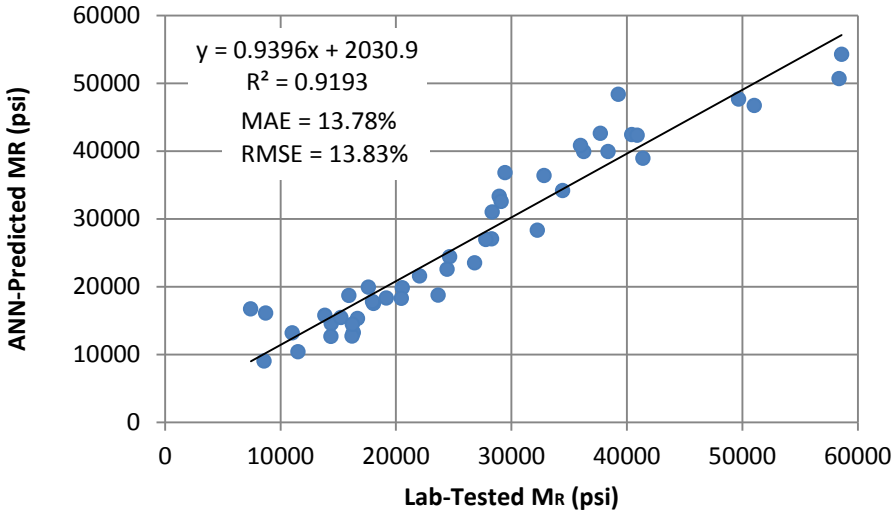

Fig. 4.30 Comparison of Lab-Tested M_R with ANN-Predicted M_R (Testing Data)

The training and testing results indicate that the ANN was able to generalize the relationship underlying GAB M_R and these explanatory variables considered. Good correlations between measured and predicted M_R were observed with the high R^2 values, which assures that aggregate physical properties and stress state are significant factors influencing the resilient behavior of aggregate base materials. Since the predicted M_R represents the knowledge generalized from the lab data, the developed model could be utilized to estimate the M_R needed for MEPDG level 2 input.

4.3 Subgrade

4.3.1 Background

A conventional flexible pavement is composed of Hot Mix Asphalt layer, base, and subbase on top of a prepared subgrade. Subgrade plays a structurally important role, especially for flexible pavement by providing foundation support through compaction, distortion and attrition. For a reliable flexible pavement foundation, characterization of load-deformation behavior of unbound materials is extremely important. Therefore, the MEPDG proposed a pavement design procedure using the resilient modulus to describe the behavior of subgrade under surface traffic loadings.

4.3.2 Materials and Laboratory Test

To develop subgrade M_R database and to investigate the factors affecting M_R of subgrade soils locally available in Georgia, nine (9) different sources of subgrade were selected for resilient modulus test. Fig. 4.31 and Table 4.12 show the selected subgrade source locations in Georgia and physical properties.

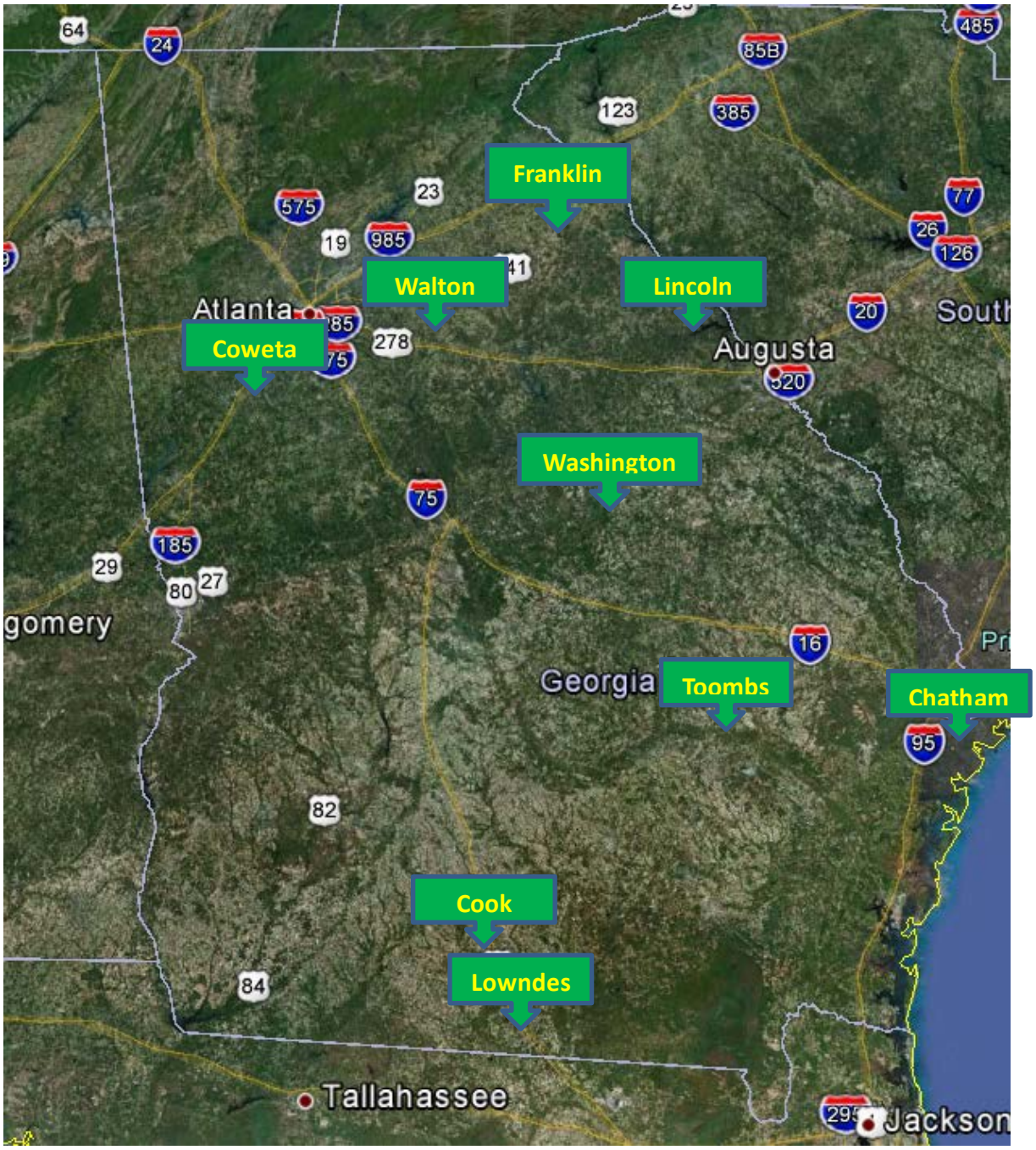

Fig. 4.31 Subgrade Source Locations

Table 4.12 Subgrade Sources and Properties

Subgrade No.	Location (County)	Percent Passing (%)				% Clay	% Volume Change	% Swell	% Shrink	Max. Dry Density (pcf)	Opt. Moisture Content (%)	LL (%)	PI (%)	Eros Index	GA Soil Class	USCS Soil Class	AASHTO Soil Class
		#10	#40	#60	#200												
1	Lincoln	99.3	96.8	93.8	48.9	40.7	24.5	20.5	4.0	93.4	23.5	39.9	8.6	4.23	IIB4	SC	A-4
2	Washington	99.8	84.6	56.1	23.8	20.6	4.7	4.5	0.2	117.8	11.0	23.0	6.6	7.30	IIB2	SM	A-2-4
3	Coweta	89.5	64.6	48.9	28.3	24.0	12.2	11.2	1.0	105.3	16.7	42.5	11.0	6.69	IIB3	SC	A-2-7
4	Walton	89.4	61.5	50.5	36.3	28.3	4.0	1.0	3.0	104.8	16.8	40.5	12.7	5.71	IIB4	SC	A-7-6
5	Chatham	99.9	97.4	93.5	3.6	1.8	0.0	3.6	0.0	97.4	12.7	0.0	0.0	9.76	IIB4	SM	A-2-4
6	Lowndes	99.0	74.9	52.9	12.2	4.5	0.0	0.0	0.0	113.1	4.7	0.0	0.0	8.65	IA2	SP	A-2-4
7	Franklin	97.3	89.4	70.9	31.1	19.6	5.2	3.0	2.2	105.1	22.6	39.3	9.8	6.32	IIB3	SC	A-2-4
8	Cook	79.9	66.4	46.6	25.0	18.4	0.6	0.6	0.0	113.1	9.9	0.0	0.0	7.06	IIB2	SM	A-2-4
9	Toombs	84.2	37.8	17.6	6.2	4.6	1.1	0.1	1.0	119.3	11.9	0.0	0.0	9.39	IA1	SP	A-1-b

Fig. 4.32 shows particle size distributions of each subgrade soil. The physical properties were determined from AASHTO T-89 (Liquid Limit Test), and AASHTO T-90 (Plastic Limit Test). The standard proctor test was conducted in accordance with AASHTO T-99 to obtain optimum moisture content and maximum dry density.

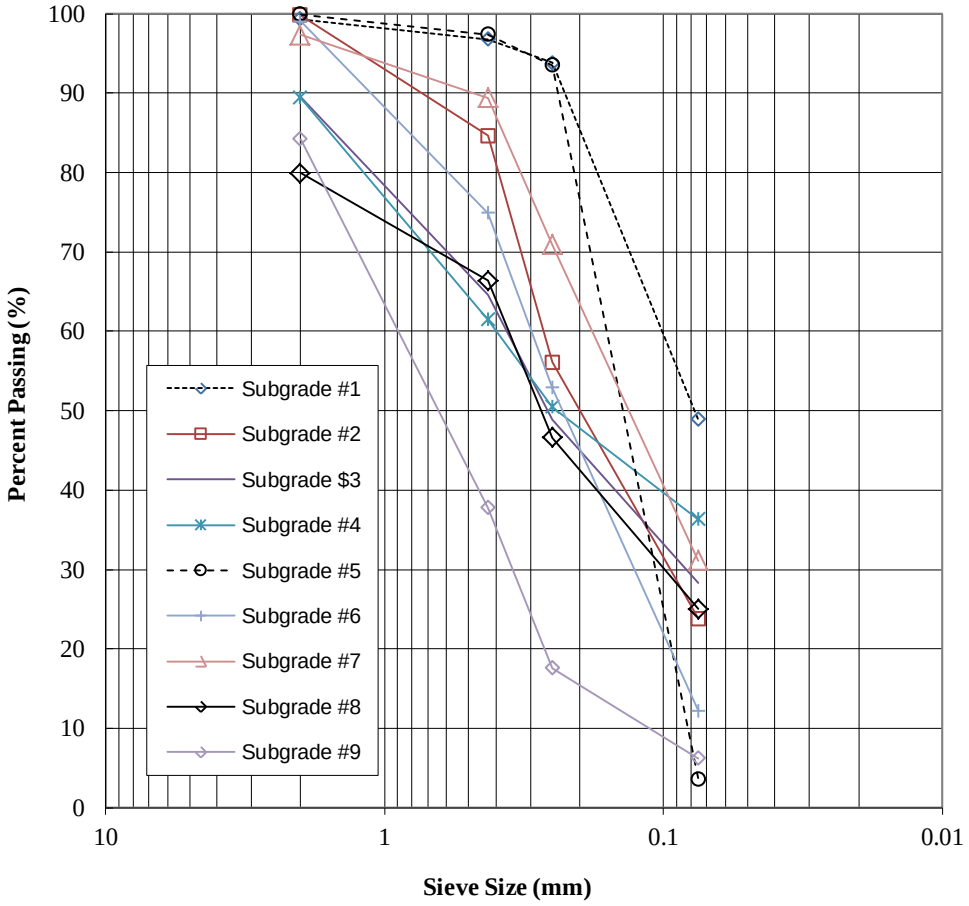

Fig. 4.32 Subgrade Gradations

Subgrade specimens were compacted with maximum dry density and optimum moisture content. A total of 27 samples (9 materials with 3 replicates) were tested. A 100-mm diameter by 200-mm high cylindrical specimen was prepared for M_R testing using impact compaction methods. The prepared specimens were then subjected to M_R test in accordance with AASHTO T 307-99. Initially, five-hundred (500) load repetitions were applied for conditioning of the prepared specimens, and the deviator of 4 psi and confining stress of 6 psi were held to eliminate the

effects of initial permanent deformation. After the initial conditioning of the specimen, one-hundred (100) load repetitions were applied to specimen for each load sequence as shown in Table 4.13. The mean deviator stress and mean recovered deflection were recorded and used for the calculation of the mean M_R at each stress state.

Table 4.13 AASHTO T307-99 Stress State for Subgrade Soil

Sequence Number	Confining Pressure (kPa)	Deviator Stress (kPa)	Confining Pressure (psi)	Deviator Stress (psi)	No. of Load Applications
0	41.4	27.6	6	4	500-1000
1	41.4	13.8	6	2	100
2	41.4	27.6	6	4	100
3	41.4	41.4	6	6	100
4	41.4	55.2	6	8	100
5	41.4	68.9	6	10	100
6	27.6	13.8	4	2	100
7	27.6	27.6	4	4	100
8	27.6	41.4	4	6	100
9	27.6	55.2	4	8	100
10	27.6	68.9	4	10	100
11	13.8	13.8	2	2	100
12	13.8	27.6	2	4	100
13	13.8	41.4	2	6	100
14	13.8	55.2	2	8	100
15	13.8	68.9	2	10	100

4.3.3 Test Results and Analyses

M_R test results are shown in Table 4.14. As expected, Positive k_2 and negative k_3 values were observed, which demonstrates the stress-hardening and stress-softening behavior of the subgrade soil.

Table 4.14 Average Subgrade k-values for Level 2 Input

Subgrade No.	Source Location	GA Soil Class	USCS Symbols	AASHTO Soil Class	Statistics	k-values		
						k1	k2	k3
1	Lincoln	IIB4	SC	A-4	Maximum	634	0.327	-1.884
					Minimum	559	0.026	-3.350
					Average	618	0.164	-2.831
2	Washing	IIB2	SM	A-2-4	Maximum	1209	0.542	-0.123
					Minimum	1079	0.182	-1.061
					Average	1156	0.330	-0.508
3	Coweta	IIB3	SC	A-2-7	Maximum	681	0.306	-1.724
					Minimum	578	0.231	-2.048
					Average	619	0.257	-1.836
4	Walton	IIB4	SC	A-7-6	Maximum	1217	0.352	-2.278
					Minimum	906	0.196	-2.906
					Average	1031	0.285	-2.679
5	Chatham	IIB4	SM	A-2-4	Maximum	1241	0.352	-2.852
					Minimum	1241	0.352	-2.852
					Average	1241	0.352	-2.852
6	Lownds	IA2	SP	A-2-4	Maximum	1298	0.535	-0.148
					Minimum	1288	0.509	-0.438
					Average	1293	0.522	-0.293
7	Franklin	IIB3	SC	A-2-4	Maximum	495	0.419	-2.773
					Minimum	357	0.341	-3.407
					Average	426	0.380	-3.090
8	Cook	IIB2	SM	A-2-4	Maximum	1153	0.255	-0.369
					Minimum	1153	0.255	-0.369
					Average	1153	0.255	-0.369
9	Toombs	IA1	SP	A-1-b	Maximum	1468	0.316	-2.476
					Minimum	1285	0.240	-2.521
					Average	1386	0.277	-2.499

As shown in Table 4.14, the type of soil that is classified as IA1 and IA2 by Georgia Soil Classification was stiffer than other IIB materials and relatively higher k_1 values were observed. Fig. 4.33 shows the resilient modulus along with bulk stress and the relatively lower resilient moduli were observed in subgrade source numbers 1, 3, 4, and 7. In comparison with Fig. 4.33, these subgrade sources contained higher passing #200 fine contents and it confirms that the resilient modulus decreases when higher fine content increases. Fig. 4.34 shows the typical resilient modulus variation along with stress changes, which was obtained from subgrade source # 7. It shows the resilient modulus decreases when the deviatoric stress is high and confining stress is low.

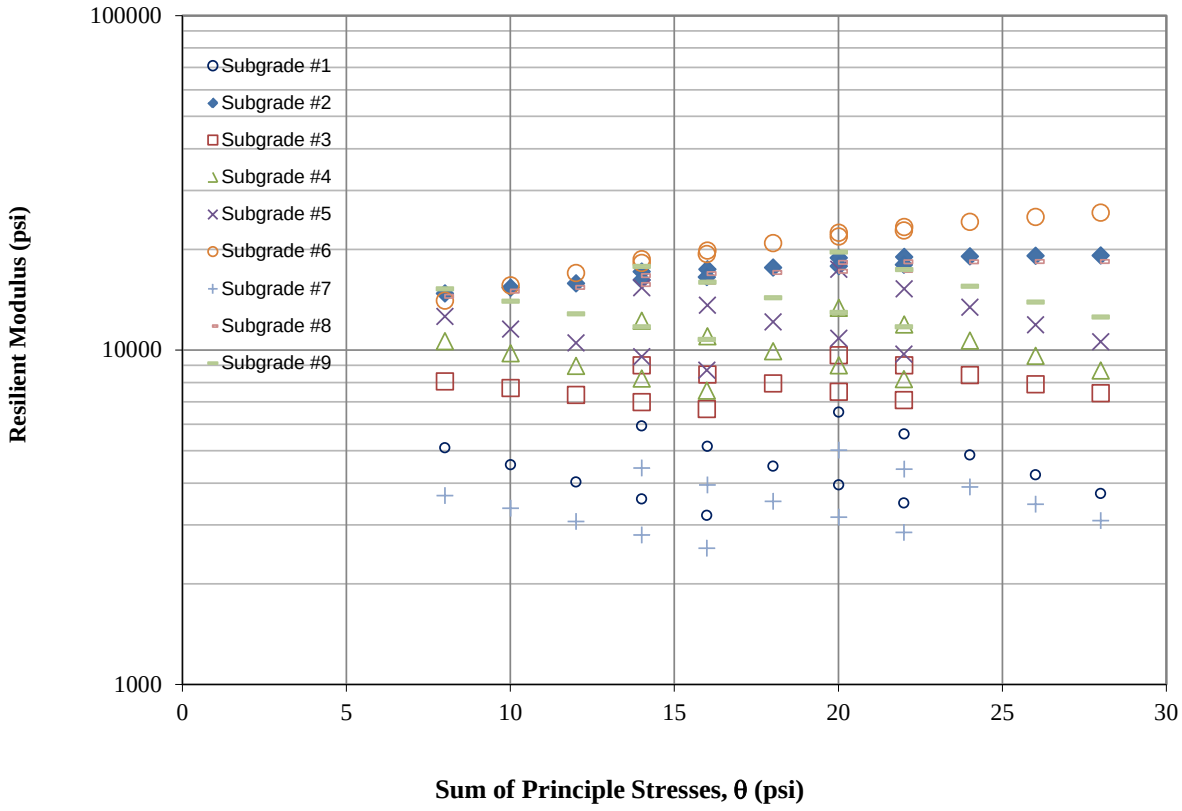

Fig. 4.33 Resilient Modulus Variation along with Bulk Stress

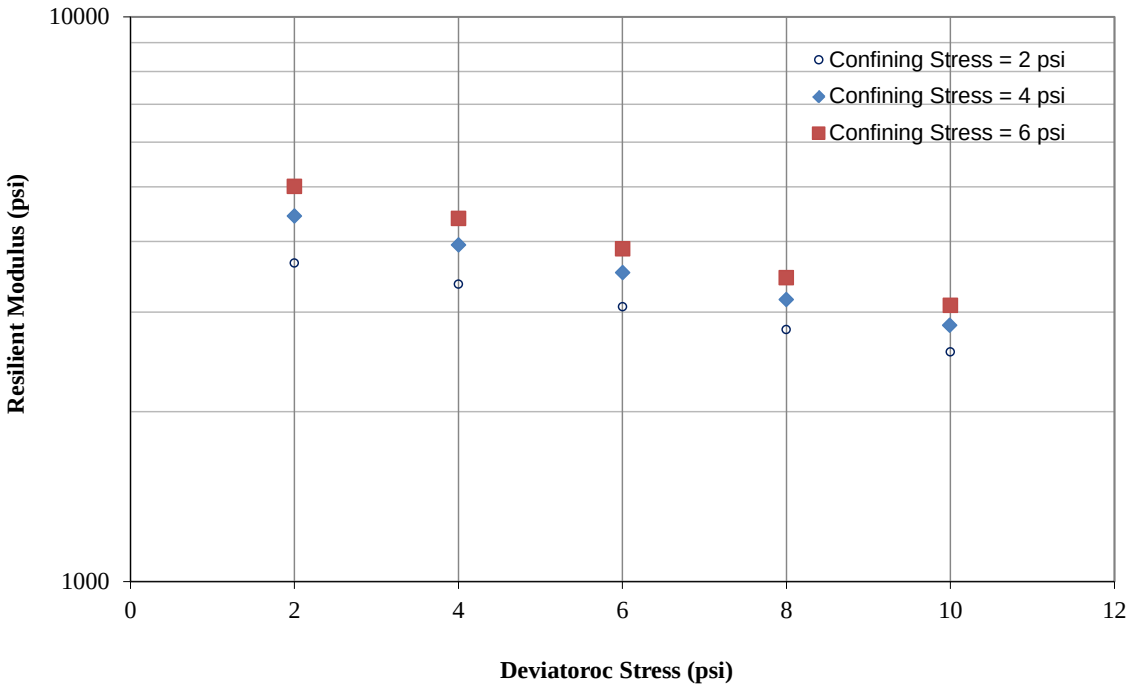

Fig. 4.34 Resilient Modulus Variation along with Deviatoric Stress and Confining Stress

Fig. 4.35 shows the resilient modulus variations along with deviatoric stress of subgrade sources containing higher fine contents. The results show that resilient modulus decreases when the deviatoric stress increases. In summary, it was observed that fine contents and stress state affect the resilient modulus of subgrade materials. It could be inferred that gradation and amount of fines has an indirect effect on the stress state and resilient behavior of subgrade by affecting the impact of moisture and density of the system.

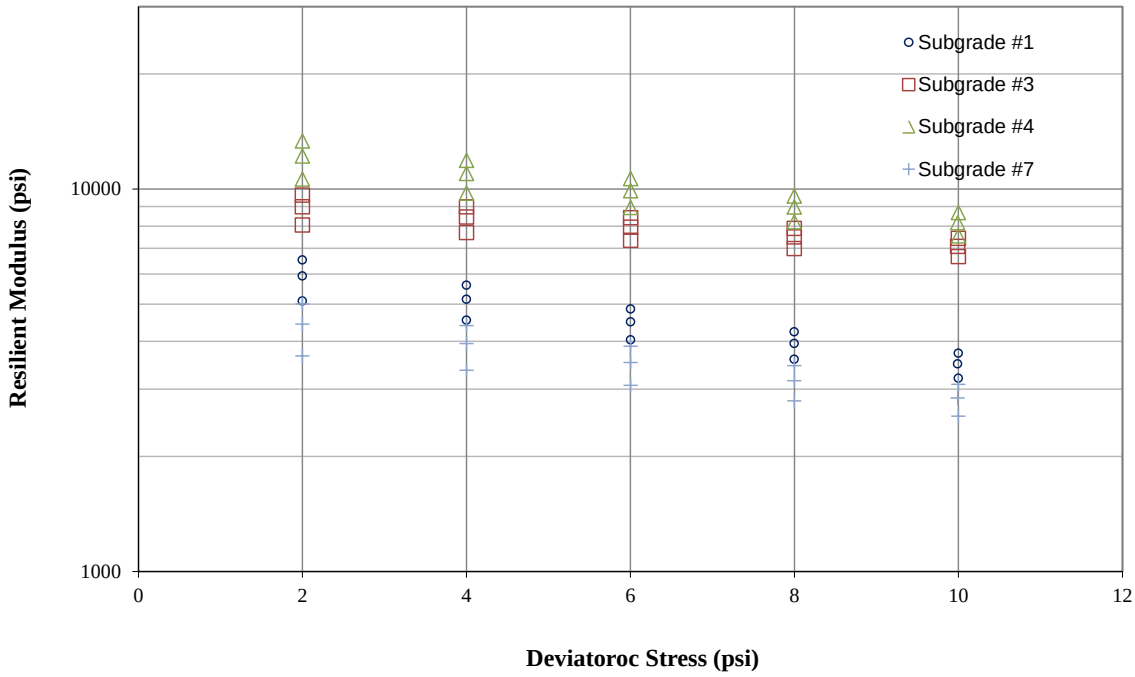

Fig. 4.35 Subgrade Resilient Modulus Variation along with deviatoric stress

The resilient modulus test doesn't provide a single specific value although a specific resilient modulus value is required as an input for MEPDG Level 3 pavement design. Thus, the combination of the confining and deviatoric stress states need to be identified to determine a MEPDG Level 3 resilient modulus input. Several researchers recommended the stress combination of 2 psi confining stress and 6 psi deviatoric stress to estimate a specific resilient modulus for pavement design (Ping et al., 1997; Houssain 2008). Table 4.15 shows the resilient modulus at the stress combination of 2 psi confining stress and 6 psi deviatoric stress. It shows that most of the calculated resilient modulus values are much less than the MEPDG Level 3 input ranges except the subgrade soil type of A-7-6. Further, soil with the same soil classification has a wide range of recommended modulus values for MEPDG Level 3 input. Thus, the accuracy of the pavement design would be questionable if the national default Level 3 value is directly used for pavement design without local calibration in Georgia.

Table 4.15 Calculated Subgrade Resilient Modulus for Level 3 Input

Subgrade No.	Source Location	GA Soil Class	USCS Symbols	AASHTO Soil Class	Calculated M_R* for Level 3 (psi)	MEPDG Default M_R Ranges (psi)
1	Lincoln	IIB4	SC	A-4	5,413	21,500-29,000
2	Washington	IIB2	SM	A-2-4	14,681	28,000-37,500
3	Coweta	IIB3	SC	A-2-7	6,237	21,500-28,000
4	Walton	IIB4	SC	A-7-6	8,919	5,000-13,500
5	Chatham	IIB4	SM	A-2-4	10,285	28,000-37,500
6	Lowndes	IA2	SP	A-2-4	16,244	28,000-37,500
7	Franklin	IIB3	SC	A-2-4	3,339	28,000-37,500
8	Cook	IIB2	SM	A-2-4	15,086	28,000-37,500
9	Toombs	IA1	SP	A-1-b	12,407	38,500-40,000

* Confining stress = 2 psi, deviatoric stress = 6 psi

4.3.4 ANN Modeling for Subgrade

A three-layer back-propagation ANN was developed to forecast subgrade resilient modulus using the subgrade physical properties and stress state. For network training and testing purposes, the lab data were divided into two sets: training and testing. The training set contains 195 observations and the testing set contains 75 observations. Selection of the number of neurons in the hidden layer is an experimental process. The number of hidden neurons represents the complexity of an ANN. Too many hidden neurons allow an ANN to memorize rather than generalize, in other words, the ANN is over-specified. Conversely, too few hidden neurons prevent an ANN from learning sufficiently and reduce the robustness of the ANN. Fig. 4.36 shows the mean square error with respect to the number of hidden neurons. It indicates that the ANN with nine hidden neurons results in minimum mean square error and thus is chosen. The final ANN architecture is summarized in Table 4.16.

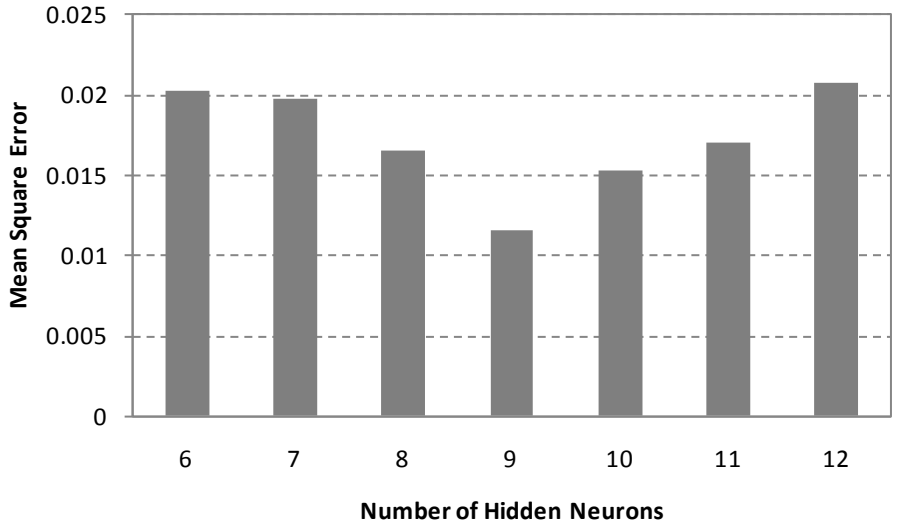

Fig. 4.36 Selection of the number of neurons in the hidden layer

Table 4.16. ANN Architecture

ANN Layer	Neuron	Sieve #	Min	Max
Input	Percent Passing (%)	#10	79.9	99.9
		#40	37.8	97.4
		#60	17.6	93.8
		#200	3.6	48.9
	Clay (%)		1.8	40.7
	Swell (%)		0.0	20.5
	Shrink (%)		0.0	4.0
	Max. Dry Density (pcf)		93.5	119.4
	Opt. Moisture Content (%)		4.7	23.5
	Liquid Limit (%)		0.0	42.5
	Plastic Index (%)		0.0	12.7
	Erosion Index		4.2	9.8
	σ_1 (psi)		4	16
	σ_3 (psi)		2	6
	θ (psi)		8	28
Hidden	9 neurons		n/a	n/a
Output	M_R (psi)		3,174	25,886

The ANN-estimated M_R were plotted against the lab measured M_R for both training and test sets. As shown in Figs. 4.37 and 4.38, there is a fairly good alignment between the ANN-estimated M_R and the lab-measured M_R. The slightly lower R^2 for test set is intuitive as the test data were not seen by the neural network as part of the training. As shown, both the training and

testing results indicate a fairly high accuracy of the ANN model in estimating M_R based on the subgrade physical properties and the stress state.

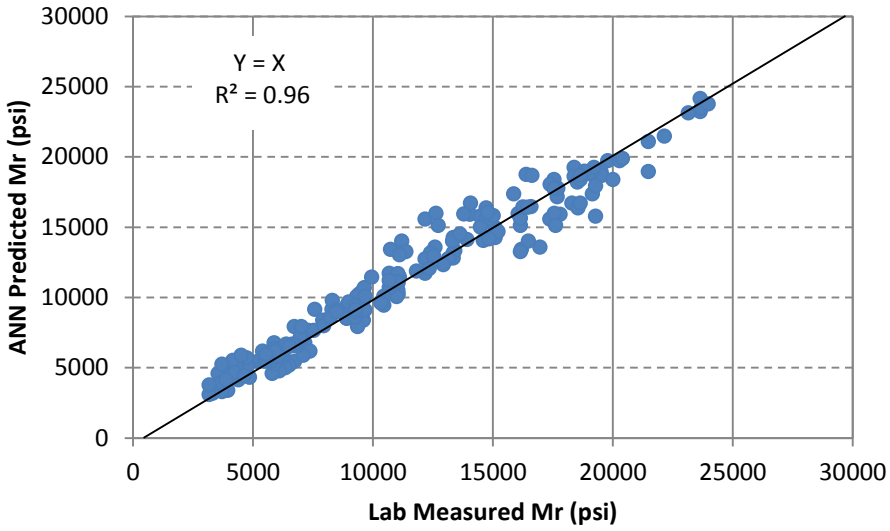

Fig. 4.37. Goodness of Fit (Training Set)

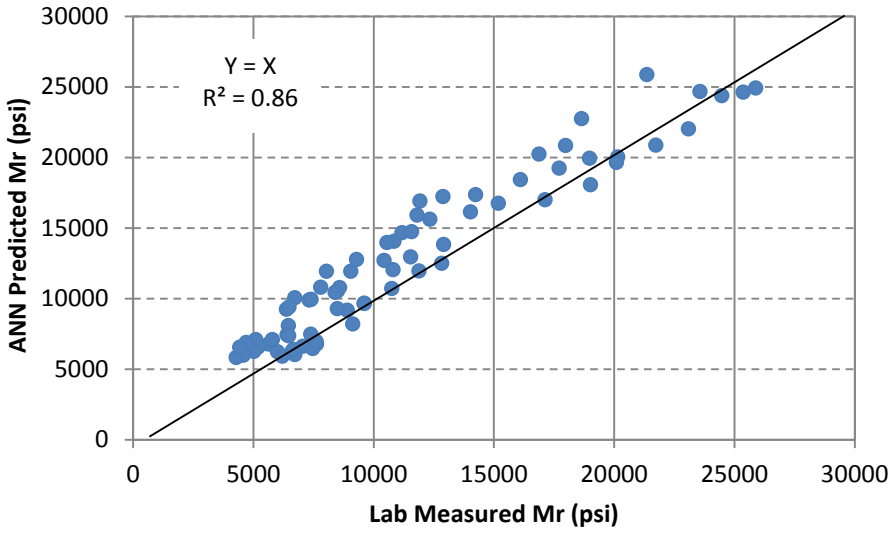

Fig. 4.38. Goodness of Fit (Testing Set)

Further, Table 4.17 shows the average k-values estimated from the laboratory database and calculated from ANN prediction model, separately. The comparisons show the potential of ANN model to reasonably estimate the k-values and explain the subgrade resilient behavior based on physical properties. With better and more accurate predictions of subgrade resilient modulus, a structurally more adequate pavement can be designed.

Table 4.17. Measured and Calculated k-values

Subgrade No.	Source Location	Estimated from MR test data			Calculated from ANN Model		
		k1	k2	k3	k1	k2	k3
1	Lincoln	618	0.164	-2.831	620	0.156	-2.360
2	Washington	1156	0.330	-0.508	1133	0.375	-0.503
3	Coweta	619	0.257	-1.836	631	0.198	-1.967
4	Walton	1031	0.285	-2.679	1123	0.234	-2.549
5	Chatham	1241	0.352	-2.852	1209	0.352	-2.787
6	Lowndes	1293	0.522	-0.293	1380	0.474	-0.387
7	Franklin	426	0.380	-3.090	486	0.350	-3.239
8	Cook	1153	0.255	-0.369	1127	0.295	-0.396
9	Toombs	1386	0.277	-2.499	1556	0.227	-2.717

5.0 SUMMARY AND CONCLUSIONS

The primary objective of this research was to develop E* and M_R database based on local materials commonly used in Georgia.

To develop HMA E* database, JMFs for 25mm, 19mm, and 12.5 mm NMAS with two types of binder (PG 64-22 and PG 67-22) were provided from Plant A and Plant B in Georgia. Both JMFs contained 25% of RAP. Thirty six (36) HMA specimens were prepared and subjected to E* measurements in accordance with AASHTO T 342. Based on E* measurements at five different temperatures and six different frequencies, twelve (12) master curves were constructed for the MEPDG implementation.

To develop M_R database for GAB materials, eleven (11) different GAB materials were collected. To investigate the factors affecting M_R and correctly characterize aggregate behavior, repeated load triaxial test was conducted for a prepared specimen in accordance with AASHTO T 307-99. The gradations of each source of GAB satisfied the GDOT GAB specification. A 150-mm in diameter by 300-mm high cylindrical GAB specimen was prepared for testing. Twenty two (22) specimens (11 materials with 2 replicates) were then subjected to M_R test in accordance with AASHTO T 307-99 and GAB M_R database was developed.

Nine (9) different sources of subgrade soils were selected for M_R database development. The physical properties were determined from AASHTO T-89 (Liquid Limit Test), and AASHTO T-90 (Plastic Limit Test). Subgrade specimens were compacted with maximum dry density and optimum moisture content. A total of 27 samples (9 materials with 3 replicates) were tested. A 100-mm in diameter by 200-mm high cylindrical specimen was prepared for M_R testing using impact compaction methods. The prepared specimens were then subjected to M_R test in accordance with AASHTO T 307-99 and subgrade M_R database was developed.

An ANN model was developed to estimate GAB and subgrade resilient modulus for the MEPDG using the physical properties and stress state. The developed ANN model has the potential to reasonably estimate resilient modulus of granular materials based on physical properties and the stress state. The accurately calculated resilient modulus input of granular materials impacts the stress and strain distributions in the base and subgrade. Since the developed ANN model sets forth in the report defines how to estimate granular resilient modulus as a function of physical

properties and stress; in essence, it provides a tool or guide for the reasonable estimation of the resilient properties of GAB and subgrade materials locally available in Georgia.

6.0 RECOMMENDATIONS

1. It is recommended to conduct sensitivity analysis using Pavement ME software to verify the E* and M_R results.
2. It is recommended to develop the database for E* with 9.5 NMAS and Stone Matrix Asphalt (SMA) which was not a scope of this special research study.
3. The effect of RAP on the E* needed additional investigations.
4. The measurements of binder stiffness from the Dynamic Shear Rheometer test (DSR) are not in the scope of this research. When the binder stiffness data is available, the prediction model can be compared with the measured E* values.

7.0 REFERENCES

1. American Association of State and Highway Officials (AASHTO). *AASHTO Guide for Design of Pavement Structures*. American Association of State and Highway Officials, Washington, DC, 1993.
2. Kim, S.H. *Determination of Aggregate Physical Properties and Its Effect on Cross-Anisotropic Behavior of Unbound Aggregate Materials*. Ph.D. Dissertation, Texas A&M University, College Station, TX, 2004.
3. Witzack, M.W. *Development of Performance Related Specifications for Asphalt Pavements in the State of Arizona*, Report No. FHWA-SPR-08-402-2, Arizona Department of Transportation, 2008.
4. Birgisson, B., R.Roque, J.Kim, and L.V. Pham. *The Use of Complex Modulus to Characterize the Performance of Asphalt Mixtures and Pavements in Florida*, Report No. UF Proj 4910-4504-784-12, submitted to Florida Department of Transportation, Tallahassee, FL, 2004.
5. Bayomy, Fouad, Sherif M. El-Badawy, and Ahmed Awed. *Implementation of the MEPDG for Flexible Pavements in Idaho*. Report No. FHWA-ID-12-193, Submitted to the Idaho Department of Transportation, 2012.
6. Carpenter, S.H. *Dynamic Modulus Performance of IDOT Mixtures*, Report No. FHWA-ICT-07-008, Submitted to Illinois Department of Transportation, Springfield, IL, 2007.
7. Romanoschi, S.A. and S. Bethu. *Implementation of the 2002 AASHTO Design Guide for Pavement Structures in KDOT*, Part-II: Asphalt Concrete Pavements, K-TRAN: KSU-04-4 Part 2, Kansas Department of Transportation, Topeka, KS, 2009
8. Schwartz, C.W, R. Li, S.J. Kim, H. Ccylan and K. Gopalakrishnan, *Sensitivity Evaluation of MEPDG Performance Prediction*, NCHRP Project 1-47, National Cooperative Highway Research Program, Transportation Research Board, Washington, DC, 2011
9. Marasteanu,M.O, T.R.Clyne, X.Li and E.L.Skok. *Dynamic and Resilient Modulus of Mn/DOT Asphalt Mixtures*, Report No. MN/RC-2003-09, Minnesota Department of Transportation, Minneapolis, MN, 2003

10. Im, S., Y.R.Kim and H.Ban, *Layer Moduli of Nebraska Pavements for the New Mechanistic Empirical Pavement Design Guide (MEPDG)*, Report No. MPH-08, Nebraska Department of Roads, Lincoln, NE, 2010
11. Bennert, T. *Dynamic Modulus of Hot Mix Asphalt*, Report No. FHWA-NJ-2009-011, New Jersey Department of Transportation, Trenton, NJ, 2009
12. Kim, Y.R., M.King and M.Momen, *Typical Dynamic Moduli for North Carolina Asphalt Concrete Mixes*, Report No. FHWA/NC/2005-03, North Carolina Department of Transportation, Raleigh, NC, 2007
13. Cross, S.A., R.Gibbe and N. Aryal. Development of a Flexible Pavement Database for Local Calibration of the MEPDG Part 2 Evaluation of ODOT SMA Mixtures. FHWA-OK-11-06(2), Submitted to Oklahoma Department of Transportation, Oklahoma City, OK, 2011
14. Apeagyei, Alex K., and Stacey D. Diefenderfer. *Asphalt Material Design Inputs for Use with the MEPDG in Virginia*. Report No. FHWA/VCTIR 12-R6, Submitted to the Virginia Department of Transportation, 2011
15. Tashman,L., M.A. Elangovan. *Dynamic Modulus Test-Laboratory Investigation and Future Implementation in the state of Washington*. Report No. WA-RD 704.1, Submitted to Washington State Department of Transportation, Olympia, Washington, 2007
16. Bonaquist, R. *Wisconsin Mixture Characterization Using the Asphalt Mixture Performance Tester (AMPT) on Historical Aggregate Structures*. REPORT No. WHRP 09-03, Submitted to Wisconsin Department of Transportation, Madison, WI, 2011
17. Ping, W.V., W.Xiong and Z. Yang. *Implementing Resilient Modulus Test for Design of Pavement Structures in Florida*. Report No. FL/DOT/RMC/BC-352-6(F), Submitted to Florida Department of Transportation, Tallahassee, FL, 2003.
18. Kim, D. and N.Z.Siddiki, *Simplification of Resilient Modulus Testing for Subgrades*, Report No. FHWA/IN/JTRP-2005/23. Indiana Department of Transportation, Indianapolis, IN, 2006.
19. Hopkins, T.C., T.L.Beckham and C.Sun. *Resilient Modulus of Compacted Crushed Stone Aggregate Bases*, Report No. KTC-05-27/SPR-229-01-1F, Submitted to Kentucky Transportation Cabinet, Frankfort, KY, 2007.

20. Ceylan, H., K.Gopalakrishnan, and S.Kim. *MEPDG Work Plan Task No.5: Characterization of Unbound Materials (Soils/Aggregates) for MEPDG*. Report No. CTRE Project 06-271, Iowa Department of Transportation, Ames, IA2009.
21. George, K.P. *Falling Weight Deflectometer for Estimating Subgrade Moduli,* Report No. FHWA/MS-DOT-RD-03-153, Submitted to Mississippi Department of Transportation, Jackson, MS, 2003
22. Richarson, D., T.Petry, L.Ge, Y.Han and S.M.Lusher. *Resilient Moduli of Typical Missouri Soils and Unbound Granular Base*, Contract/Grant No.: RI06-001, Submitted to Missouri Department of Transportation, Jefferson City, MO, 2009.
23. Hossain, M.S. *Characterization of Subgrade Resilient Modulus for Virginia Soils and Its Correlation with the Results of Other Soil Tests*, Report No. VTRC 09-R04, Submitted to Virginia Transportation Research Council, Charlottesville, VA 2008.
24. Hossain, Z., M.Zaman, C.Doiron and S.A.Cross. *Development of Flexible Pavement Database for Local Calibration of MEPDG – Volume I*. FHWA-OK-11-06(1), Submitted to Oklahoman Department of Transportation, Oklahoma City, OK, 2011.
25. Titi, H.H., M.B.Elias and S. Helwany. *Determination of Typical Resilient Modulus Values for Selected Soils in Wisconsin*, Report No. WHRP 0092-03-11, Submitted to Wisconsin Department of Transportation, Madison, WI, 2006.
26. Huang, Y. H. *Pavement Analysis and Design*. 1st Edition, Prentice Hall, Englewood Cliffs, NJ, 1993.
27. Kim, S. H., Little, D. N., and Masad, E. *Simple Methods to Estimate Inherent and Stress-Induced Anisotropic Level of Aggregate Base*. Transportation Research Record 1913, TRB, National Research Council, Washington D.C, 24-31.
28. S. H. Kim, D. N. Little, and E. Tutumluer, *Effect of Gradation on Nonlinear Stress-Dependent Behavior of a Sandy Flexible Pavement Subgrade*, Journal of Transportation Engineering, Volume 133, Issue 10, 2007, pp. 582-589.
29. AASHTO T 307-99. *Standard Method of Test for Determining the Resilient Modulus of Soils and Aggregate Materials*, American Association of State and Highway Transportation Officials, 2007

30. Ashtiani, S. R. and Little D., and Masad E. *Material Factors that Influence the Anisotropy Level of Aggregate Bases*, Transportation Research Record, Journal of Transportation Research Board, Vol. 2059 Washington DC, pp. 20-30, 2008
31. Ashtiani, S. R. and Saeed A. *Laboratory Performance Characterization of Pavements Incorporating Recycled materials*, American Society of Civil Engineers (ASCE) Geo-Congress-2012 proceeding, Vol.3 Auckland, CA, pp. 1582-1591, 2012
32. Saeed, A. *Performance-Related Tests of Recycled Aggregates for Use in Unbound Pavement Layers*. NCHRP Report 598, Transporation Research Board, National Research Council, Washington, DC, pp. 23-37, 2008
33. Saeed, A. *Performance-Related Tests of Recycled Aggregates for Use in Unbound Pavement Layers*. *NCHRP Report 598*, Transportation Research Board, National Research Council, Washington, DC, pp. 23-37, 2008.
34. Saarenketo, T. and Scullion, T. *Using Electrical Properties to Classify the Strength Properties of Base Course Aggregates*, Research Report 1341-2. Project No. 1341. Texas Transportation Institute, College Station, TX. July 1995.
35. Saarenketo, T., T. Scullion, and P. Kolisoja. *Moisture Susceptibility and Electrical Properties of Base Course Aggregates*. In Proceedings of the Fifth International Conference on the Bearing Capacity of Roads and Airfields, Trondheim, Norway, pp. 1401-1410, 1998
36. Guthrie, W. S. and Scullion, T., *Interlaboratory Study of the Tube Suction Test*, FHWA/TX-03/0-4114-2, 2003
37. Funahashi, K. *On the Approximate Realization of Continuous Mappings by Neural Networks*. Neural Networks, Vol. 2, No. 3, pp. 183–192, 1989
38. Hornik, K., M. Stinchcombe, and H. White. *Multilayer Feedforward Networks Are Universal Approximators*. Neural Networks, Vol. 2, No. 5, pp. 359–366, 1989
39. Mehta, P. K., Monteiro, P. J., *Concrete: Microstructure, Properties, and Materials*, McGraw-Hill, Third Edition, 2006

APPENDIX A

HMA E* Test Results (Plant A JMF, 12.5 mm NMAS, PG 64-22)

Temp. (F)	PLANT A											
	12.5 mm NMAS											
	PG64-22											
	Specimen 1				Specimen 2				Specimen 3			
	COAC(%)	Hz	E* (psi)	ϕ (Deg)	COAC(%)	Hz	E* (psi)	ϕ (Deg)	COAC(%)	Hz	E* (psi)	ϕ (Deg)
14	5.42	0.1	2,460,901	9.7	5.42	0.1	2,022,502	10.3	5.42	0.1	2,500,786	9.0
14	5.42	0.5	3,005,410	7.2	5.42	0.5	2,459,703	7.3	5.42	0.5	2,903,057	6.9
14	5.42	1.0	3,217,893	6.7	5.42	1.0	2,617,527	6.7	5.42	1.0	3,061,632	6.3
14	5.42	5.0	3,623,933	5.6	5.42	5.0	2,942,956	5.4	5.42	5.0	3,433,749	5.5
14	5.42	10.0	3,799,160	5.1	5.42	10.0	3,052,931	4.8	5.42	10.0	3,455,883	5.1
14	5.42	25.0	4,027,458	5.0	5.42	25.0	3,192,394	4.2	5.42	25.0	3,540,577	4.3
40	5.42	0.1	1,248,586	18.0	5.42	0.1	981,051	19.0	5.42	0.1	1,433,514	15.6
40	5.42	0.5	1,672,006	13.8	5.42	0.5	1,348,011	14.3	5.42	0.5	1,876,837	12.1
40	5.42	1.0	1,863,243	12.8	5.42	1.0	1,506,532	13.1	5.42	1.0	2,058,512	11.2
40	5.42	5.0	2,297,813	10.7	5.42	5.0	1,871,736	10.8	5.42	5.0	2,490,057	9.4
40	5.42	10.0	2,482,245	9.9	5.42	10.0	2,034,396	10.0	5.42	10.0	2,671,619	8.7
40	5.42	25.0	2,705,240	9.0	5.42	25.0	2,252,985	8.5	5.42	25.0	2,926,487	8.1
70	5.42	0.1	487,555	27.3	5.42	0.1	312,215	30.0	5.42	0.1	483,770	28.1
70	5.42	0.5	729,400	23.3	5.42	0.5	464,750	26.3	5.42	0.5	722,854	23.4
70	5.42	1.0	858,679	21.4	5.42	1.0	551,482	24.2	5.42	1.0	853,742	21.8
70	5.42	5.0	1,227,549	17.4	5.42	5.0	821,268	20.2	5.42	5.0	1,208,674	17.6
70	5.42	10.0	1,387,433	15.9	5.42	10.0	942,474	18.8	5.42	10.0	1,367,966	16.3
70	5.42	25.0	1,628,062	14.4	5.42	25.0	1,134,683	16.4	5.42	25.0	1,605,455	14.7
100	5.42	0.1	147,050	30.8	5.42	0.1	121,609	29.8	5.42	0.1	138,891	31.6
100	5.42	0.5	224,503	30.9	5.42	0.5	179,045	29.5	5.42	0.5	214,382	31.0
100	5.42	1.0	270,487	29.7	5.42	1.0	214,914	29.1	5.42	1.0	263,847	30.2
100	5.42	5.0	459,278	27.2	5.42	5.0	348,822	27.0	5.42	5.0	456,638	27.3
100	5.42	10.0	558,414	25.9	5.42	10.0	435,809	25.8	5.42	10.0	557,427	25.9
100	5.42	25.0	727,854	23.7	5.42	25.0	578,093	21.9	5.42	25.0	725,236	24.1
130	5.42	0.1	67,562	24.4	5.42	0.1	46,954	21.6	5.42	0.1	51,163	22.2
130	5.42	0.5	89,181	27.8	5.42	0.5	54,491	25.8	5.42	0.5	62,404	26.2
130	5.42	1.0	108,796	28.9	5.42	1.0	67,670	27.3	5.42	1.0	75,586	28.6
130	5.42	5.0	181,756	31.2	5.42	5.0	106,587	28.8	5.42	5.0	125,866	31.0
130	5.42	10.0	246,372	30.1	5.42	10.0	131,579	29.2	5.42	10.0	160,274	30.6
130	5.42	25.0	349,156	29.9	5.42	25.0	191,570	28.2	5.42	25.0	237,851	31.0

HMA E* Test Results (Plant A JMF, 12.5 mm NMAS, PG 67-22)

Temp. (F)	PLANT A											
	12.5 mm NMAS											
	PG67-22											
	Specimen 1				Specimen 2				Specimen 3			
	COAC(%)	Hz	E* (psi)	ϕ (Deg)	COAC(%)	Hz	E* (psi)	ϕ (Deg)	COAC(%)	Hz	E* (psi)	ϕ (Deg)
14	5.52	0.1	2,381,656	10.1	5.52	0.1	1,354,400	14.6	5.52	0.1	1,765,935	11.6
14	5.52	0.5	2,979,877	7.5	5.52	0.5	1,785,827	10.5	5.52	0.5	2,221,941	8.0
14	5.52	1.0	3,201,353	6.7	5.52	1.0	1,923,706	9.2	5.52	1.0	2,377,621	7.0
14	5.52	5.0	3,590,358	5.6	5.52	5.0	2,272,672	7.6	5.52	5.0	2,701,983	5.8
14	5.52	10.0	3,838,999	4.7	5.52	10.0	2,405,343	6.8	5.52	10.0	2,799,811	5.2
14	5.52	25.0	4,191,085	4.0	5.52	25.0	2,597,269	5.6	5.52	25.0	2,879,958	4.2
40	5.52	0.1	1,320,008	16.9	5.52	0.1	910,661	17.7	5.52	0.1	673,262	23.3
40	5.52	0.5	1,797,165	12.9	5.52	0.5	1,261,951	13.2	5.52	0.5	967,562	18.2
40	5.52	1.0	1,979,830	11.8	5.52	1.0	1,406,280	11.8	5.52	1.0	1,085,812	16.2
40	5.52	5.0	2,391,645	9.5	5.52	5.0	1,728,847	9.8	5.52	5.0	1,428,483	13.4
40	5.52	10.0	2,598,940	8.5	5.52	10.0	1,858,408	9.1	5.52	10.0	1,564,287	12.0
40	5.52	25.0	2,913,173	7.6	5.52	25.0	2,052,125	8.3	5.52	25.0	1,765,120	10.3
70	5.52	0.1	269,669	30.8	5.52	0.1	269,669	30.8	5.52	0.1	273,954	30.1
70	5.52	0.5	406,757	26.8	5.52	0.5	406,757	26.8	5.52	0.5	399,463	26.5
70	5.52	1.0	482,827	24.8	5.52	1.0	482,827	24.8	5.52	1.0	467,650	24.6
70	5.52	5.0	724,779	20.4	5.52	5.0	724,779	20.4	5.52	5.0	695,694	20.4
70	5.52	10.0	827,658	19.0	5.52	10.0	827,658	19.0	5.52	10.0	797,652	19.2
70	5.52	25.0	978,181	17.3	5.52	25.0	978,181	17.3	5.52	25.0	944,791	17.4
100	5.52	0.1	134,822	28.7	5.52	0.1	101,398	29.0	5.52	0.1	108,274	28.4
100	5.52	0.5	196,187	30.5	5.52	0.5	140,583	29.8	5.52	0.5	155,591	28.9
100	5.52	1.0	243,451	30.2	5.52	1.0	167,650	29.2	5.52	1.0	186,241	28.4
100	5.52	5.0	408,773	28.0	5.52	5.0	270,615	27.8	5.52	5.0	291,275	26.7
100	5.52	10.0	500,847	27.2	5.52	10.0	338,782	26.8	5.52	10.0	370,392	25.1
100	5.52	25.0	659,687	24.8	5.52	25.0	418,703	19.8	5.52	25.0	490,821	22.3
130	5.52	0.1	53,835	21.4	5.52	0.1	41,449	20.3	5.52	0.1	45,849	19.6
130	5.52	0.5	71,883	26.0	5.52	0.5	43,825	24.9	5.52	0.5	50,231	24.1
130	5.52	1.0	83,099	27.9	5.52	1.0	53,604	26.9	5.52	1.0	60,098	25.8
130	5.52	5.0	131,889	29.8	5.52	5.0	83,827	28.7	5.52	5.0	86,566	27.6
130	5.52	10.0	169,301	29.0	5.52	10.0	102,815	28.0	5.52	10.0	104,962	27.9
130	5.52	25.0	237,496	27.5	5.52	25.0	146,543	12.1	5.52	25.0	154,022	22.7

HMA E* Test Results (Plant A JMF, 19 mm NMAS, PG 64-22)

Temp. (F)	PLANT A											
	19 mm NMAS											
	PG64-22											
	Specimen 1				Specimen 2				Specimen 3			
	COAC(%)	Hz	E* (psi)	ϕ (Deg)	COAC(%)	Hz	E* (psi)	ϕ (Deg)	COAC(%)	Hz	E* (psi)	ϕ (Deg)
14	4.62	0.1	1,679,147	12.3	4.62	0.1	1,716,993	13.8	4.62	0.1	1,751,009	11.6
14	4.62	0.5	2,144,580	8.5	4.62	0.5	2,284,107	9.7	4.62	0.5	2,305,614	8.1
14	4.62	1.0	2,312,628	7.5	4.62	1.0	2,503,269	8.6	4.62	1.0	2,488,231	7.3
14	4.62	5.0	2,641,904	6.1	4.62	5.0	2,892,036	7.0	4.62	5.0	2,829,855	5.9
14	4.62	10.0	2,778,991	5.5	4.62	10.0	3,091,282	6.1	4.62	10.0	2,977,442	5.3
14	4.62	25.0	2,968,676	4.5	4.62	25.0	3,310,699	7.3	4.62	25.0	3,307,014	3.3
40	4.62	0.1	1,076,781	16.7	4.62	0.1	1,107,124	19.1	4.62	0.1	773,210	21.0
40	4.62	0.5	1,451,479	12.1	4.62	0.5	1,549,378	14.3	4.62	0.5	1,083,796	15.7
40	4.62	1.0	1,606,505	11.3	4.62	1.0	1,736,186	13.0	4.62	1.0	1,218,993	13.9
40	4.62	5.0	1,729,269	11.1	4.62	5.0	2,135,587	10.6	4.62	5.0	1,521,681	10.9
40	4.62	10.0	2,072,624	8.5	4.62	10.0	2,326,496	9.4	4.62	10.0	1,645,427	10.0
40	4.62	25.0	2,291,720	7.5	4.62	25.0	2,566,490	8.1	4.62	25.0	1,833,646	8.4
70	4.62	0.1	290,398	30.0	4.62	0.1	367,300	30.8	4.62	0.1	224,622	27.1
70	4.62	0.5	435,437	26.6	4.62	0.5	570,334	26.4	4.62	0.5	326,947	27.5
70	4.62	1.0	518,268	24.4	4.62	1.0	679,503	24.5	4.62	1.0	390,321	26.5
70	4.62	5.0	766,314	20.3	4.62	5.0	1,006,522	19.8	4.62	5.0	613,596	22.8
70	4.62	10.0	876,206	19.0	4.62	10.0	1,144,545	18.4	4.62	10.0	721,066	21.4
70	4.62	25.0	1,040,974	16.9	4.62	25.0	1,351,602	16.0	4.62	25.0	895,134	18.8
100	4.62	0.1	95,791	26.6	4.62	0.1	95,725	29.0	4.62	0.1	108,894	27.3
100	4.62	0.5	133,450	29.5	4.62	0.5	140,531	31.4	4.62	0.5	153,202	29.8
100	4.62	1.0	158,922	30.0	4.62	1.0	170,269	32.1	4.62	1.0	182,724	30.2
100	4.62	5.0	273,774	28.9	4.62	5.0	305,507	30.1	4.62	5.0	312,233	27.9
100	4.62	10.0	332,396	29.3	4.62	10.0	383,649	29.4	4.62	10.0	388,310	26.7
100	4.62	25.0	462,981	26.2	4.62	25.0	515,498	26.1	4.62	25.0	521,184	24.5
130	4.62	0.1	45,160	18.5	4.62	0.1	41,887	19.1	4.62	0.1	52,743	17.1
130	4.62	0.5	49,282	23.0	4.62	0.5	47,271	23.4	4.62	0.5	54,174	21.8
130	4.62	1.0	58,961	25.2	4.62	1.0	57,454	25.5	4.62	1.0	63,917	23.8
130	4.62	5.0	91,872	29.0	4.62	5.0	88,650	30.1	4.62	5.0	97,722	28.1
130	4.62	10.0	113,247	30.0	4.62	10.0	107,511	33.5	4.62	10.0	118,235	29.0
130	4.62	25.0	170,200	28.9	4.62	25.0	151,032	28.4	4.62	25.0	177,337	28.7

HMA E* Test Results (Plant A JMF, 19 mm NMAS, PG 67-22)

Temp. (F)	PLANT A											
	19 mm NMAS											
	PG67-22											
	Specimen 1				Specimen 2				Specimen 3			
	COAC(%)	Hz	E* (psi)	ϕ (Deg)	COAC(%)	Hz	E* (psi)	ϕ (Deg)	COAC(%)	Hz	E* (psi)	ϕ (Deg)
14	4.72	0.1	1,646,309	14.8	4.72	0.1	2,060,152	11.4	4.72	0.1	2,611,846	11.1
14	4.72	0.5	2,290,777	10.1	4.72	0.5	2,778,908	8.2	4.72	0.5	3,535,063	8.2
14	4.72	1.0	2,556,904	9.1	4.72	1.0	3,019,375	7.5	4.72	1.0	3,842,277	7.4
14	4.72	5.0	3,006,702	7.2	4.72	5.0	3,433,075	6.0	4.72	5.0	4,357,474	5.9
14	4.72	10.0	3,281,761	5.8	4.72	10.0	3,685,114	5.2	4.72	10.0	4,716,339	4.8
14	4.72	25.0	3,702,840	5.8	4.72	25.0	4,009,411	4.2	4.72	25.0	5,129,674	4.1
40	4.72	0.1	1,167,829	19.0	4.72	0.1	1,323,539	16.0	4.72	0.1	955,796	22.8
40	4.72	0.5	1,696,106	14.2	4.72	0.5	1,855,118	11.6	4.72	0.5	1,449,506	17.7
40	4.72	1.0	1,903,443	12.6	4.72	1.0	2,047,191	10.6	4.72	1.0	1,651,098	16.0
40	4.72	5.0	2,347,133	9.9	4.72	5.0	2,418,210	8.8	4.72	5.0	2,111,201	12.6
40	4.72	10.0	2,577,330	8.9	4.72	10.0	2,629,131	8.1	4.72	10.0	2,374,202	11.3
40	4.72	25.0	2,883,753	8.5	4.72	25.0	2,882,515	6.9	4.72	25.0	2,729,330	10.4
70	4.72	0.1	401,545	30.8	4.72	0.1	398,410	29.4	4.72	0.1	453,751	29.6
70	4.72	0.5	627,209	26.5	4.72	0.5	612,678	24.8	4.72	0.5	719,008	25.7
70	4.72	1.0	755,178	24.6	4.72	1.0	727,993	23.0	4.72	1.0	861,299	23.9
70	4.72	5.0	1,116,763	19.7	4.72	5.0	1,042,215	18.7	4.72	5.0	1,242,172	19.2
70	4.72	10.0	1,281,583	18.3	4.72	10.0	1,187,747	17.5	4.72	10.0	1,427,117	17.7
70	4.72	25.0	1,536,769	15.9	4.72	25.0	1,466,638	15.0	4.72	25.0	1,697,075	15.7
100	4.72	0.1	122,435	29.4	4.72	0.1	128,405	29.5	4.72	0.1	150,928	27.9
100	4.72	0.5	182,002	31.9	4.72	0.5	196,550	31.1	4.72	0.5	221,379	30.3
100	4.72	1.0	226,636	31.9	4.72	1.0	242,261	31.1	4.72	1.0	275,754	30.4
100	4.72	5.0	407,850	30.2	4.72	5.0	416,519	27.9	4.72	5.0	470,943	28.2
100	4.72	10.0	507,986	29.4	4.72	10.0	516,190	26.4	4.72	10.0	585,330	27.1
100	4.72	25.0	706,820	25.5	4.72	25.0	677,885	24.0	4.72	25.0	776,457	22.0
130	4.72	0.1	48,814	19.7	4.72	0.1	51,060	20.7	4.72	0.1	61,054	17.9
130	4.72	0.5	55,561	26.2	4.72	0.5	63,417	24.9	4.72	0.5	69,081	23.6
130	4.72	1.0	69,657	27.4	4.72	1.0	77,478	26.8	4.72	1.0	83,688	26.3
130	4.72	5.0	112,405	30.8	4.72	5.0	123,222	30.4	4.72	5.0	130,390	29.7
130	4.72	10.0	147,362	30.6	4.72	10.0	157,208	30.3	4.72	10.0	165,938	29.6
130	4.72	25.0	221,416	31.3	4.72	25.0	223,691	29.7	4.72	25.0	238,568	20.4

HMA E* Test Results (Plant A JMF, 25 mm NMAS, PG 64-22)

Temp. (F)	PLANT A											
	25 mm NMAS											
	PG64-22											
	Specimen 1				Specimen 2				Specimen 3			
	COAC(%)	Hz	E* (psi)	ϕ (Deg)	COAC(%)	Hz	E* (psi)	ϕ (Deg)	COAC(%)	Hz	E* (psi)	ϕ (Deg)
14	4.47	0.1	1,898,133	11.0	4.47	0.1	2,812,117	10.1	4.47	0.1	2,183,681	7.4
14	4.47	0.5	2,414,145	8.1	4.47	0.5	3,513,434	7.7	4.47	0.5	2,655,154	7.5
14	4.47	1.0	2,616,892	7.3	4.47	1.0	3,755,262	7.0	4.47	1.0	2,836,553	6.6
14	4.47	5.0	2,958,020	6.1	4.47	5.0	4,186,934	5.5	4.47	5.0	3,154,521	5.7
14	4.47	10.0	3,193,037	5.4	4.47	10.0	4,417,275	5.0	4.47	10.0	3,292,445	4.8
14	4.47	25.0	3,580,331	4.7	4.47	25.0	4,736,421	3.9	4.47	25.0	3,477,833	3.4
40	4.47	0.1	1,148,933	16.3	4.47	0.1	1,271,389	18.9	4.47	0.1	1,114,260	16.3
40	4.47	0.5	1,505,224	12.6	4.47	0.5	1,761,221	14.8	4.47	0.5	1,469,378	12.5
40	4.47	1.0	1,651,049	11.8	4.47	1.0	1,958,396	13.7	4.47	1.0	1,613,199	11.4
40	4.47	5.0	1,996,653	9.9	4.47	5.0	2,386,483	11.0	4.47	5.0	1,946,322	9.6
40	4.47	10.0	2,158,396	9.3	4.47	10.0	2,651,566	10.3	4.47	10.0	2,073,459	8.8
40	4.47	25.0	2,393,186	8.2	4.47	25.0	2,963,440	9.2	4.47	25.0	2,235,790	7.1
70	4.47	0.1	483,741	23.7	4.47	0.1	444,609	28.3	4.47	0.1	368,983	28.2
70	4.47	0.5	653,522	20.9	4.47	0.5	666,963	24.8	4.47	0.5	548,504	24.7
70	4.47	1.0	753,456	19.8	4.47	1.0	791,083	23.2	4.47	1.0	643,834	22.9
70	4.47	5.0	1,039,740	16.6	4.47	5.0	1,133,894	19.1	4.47	5.0	935,448	18.7
70	4.47	10.0	1,152,816	15.6	4.47	10.0	1,295,119	17.7	4.47	10.0	1,054,857	17.2
70	4.47	25.0	1,327,456	14.0	4.47	25.0	1,541,632	15.7	4.47	25.0	1,235,246	15.7
100	4.47	0.1	157,658	28.1	4.47	0.1	145,777	27.4	4.47	0.1	119,825	27.9
100	4.47	0.5	216,302	28.4	4.47	0.5	210,951	29.1	4.47	0.5	174,904	29.9
100	4.47	1.0	259,407	28.4	4.47	1.0	258,398	29.2	4.47	1.0	213,749	30.2
100	4.47	5.0	427,990	25.5	4.47	5.0	436,883	27.1	4.47	5.0	368,445	27.6
100	4.47	10.0	517,509	24.7	4.47	10.0	539,128	26.0	4.47	10.0	455,386	26.4
100	4.47	25.0	657,508	22.8	4.47	25.0	714,845	23.1	4.47	25.0	602,257	24.2
130	4.47	0.1	65,126	20.0	4.47	0.1	59,529	18.1	4.47	0.1	58,313	15.3
130	4.47	0.5	73,244	24.8	4.47	0.5	69,077	23.2	4.47	0.5	63,993	22.0
130	4.47	1.0	89,861	26.1	4.47	1.0	81,950	25.3	4.47	1.0	77,432	24.2
130	4.47	5.0	140,327	27.1	4.47	5.0	125,713	28.4	4.47	5.0	121,835	27.6
130	4.47	10.0	174,677	26.8	4.47	10.0	156,375	28.4	4.47	10.0	152,130	27.7
130	4.47	25.0	252,807	26.8	4.47	25.0	229,457	27.8	4.47	25.0	217,319	25.6

HMA E* Test Results (Plant A JMF, 25 mm NMAS, PG 67-22)

Temp. (F)	PLANT A											
	25 mm NMAS											
	PG67-22											
	Specimen 1				Specimen 2				Specimen 3			
	COAC(%)	Hz	E* (psi)	ϕ (Deg)	COAC(%)	Hz	E* (psi)	ϕ (Deg)	COAC(%)	Hz	E* (psi)	ϕ (Deg)
14	4.56	0.1	1,636,274	14.0	4.56	0.1	2,026,715	11.0	4.56	0.1	2,341,344	10.7
14	4.56	0.5	2,224,638	9.8	4.56	0.5	2,669,885	7.8	4.56	0.5	2,976,503	7.6
14	4.56	1.0	2,436,999	8.7	4.56	1.0	2,884,210	6.9	4.56	1.0	3,205,536	6.9
14	4.56	5.0	2,833,378	7.0	4.56	5.0	3,255,978	5.6	4.56	5.0	3,600,827	5.6
14	4.56	10.0	3,005,504	6.1	4.56	10.0	3,485,224	4.5	4.56	10.0	3,768,722	4.9
14	4.56	25.0	3,254,883	4.5	4.56	25.0	3,864,097	3.8	4.56	25.0	4,067,270	4.1
40	4.56	0.1	1,071,773	18.7	4.56	0.1	1,140,036	17.1	4.56	0.1	992,881	21.1
40	4.56	0.5	1,451,275	14.4	4.56	0.5	1,579,855	12.5	4.56	0.5	1,395,228	16.3
40	4.56	1.0	1,617,981	13.0	4.56	1.0	1,755,159	11.2	4.56	1.0	1,568,252	14.9
40	4.56	5.0	1,999,082	10.6	4.56	5.0	2,101,562	9.0	4.56	5.0	1,982,637	12.0
40	4.56	10.0	2,154,896	9.3	4.56	10.0	2,278,908	8.1	4.56	10.0	2,166,350	11.0
40	4.56	25.0	2,407,518	8.7	4.56	25.0	2,506,996	7.1	4.56	25.0	2,449,620	9.7
70	4.56	0.1	441,250	27.5	4.56	0.1	406,424	28.7	4.56	0.1	542,308	27.2
70	4.56	0.5	660,203	23.8	4.56	0.5	622,127	24.4	4.56	0.5	807,205	22.8
70	4.56	1.0	783,019	22.1	4.56	1.0	742,144	22.6	4.56	1.0	946,609	20.9
70	4.56	5.0	1,108,506	17.8	4.56	5.0	1,060,973	18.2	4.56	5.0	1,311,418	16.8
70	4.56	10.0	1,248,519	16.7	4.56	10.0	1,211,314	16.8	4.56	10.0	1,473,598	15.5
70	4.56	25.0	1,482,738	14.8	4.56	25.0	1,427,929	14.9	4.56	25.0	1,732,531	13.5
100	4.56	0.1	113,125	26.7	4.56	0.1	126,590	28.3	4.56	0.1	147,496	28.9
100	4.56	0.5	160,487	28.9	4.56	0.5	178,345	28.9	4.56	0.5	216,845	29.7
100	4.56	1.0	190,464	29.7	4.56	1.0	211,198	29.4	4.56	1.0	266,923	29.4
100	4.56	5.0	317,620	28.0	4.56	5.0	360,276	27.3	4.56	5.0	456,069	26.6
100	4.56	10.0	397,091	27.4	4.56	10.0	443,310	26.4	4.56	10.0	557,224	25.5
100	4.56	25.0	545,015	25.6	4.56	25.0	583,669	22.6	4.56	25.0	726,902	23.6
130	4.56	0.1	45,497	18.2	4.56	0.1	54,364	18.9	4.56	0.1	56,980	20.5
130	4.56	0.5	48,181	23.7	4.56	0.5	58,680	24.4	4.56	0.5	69,180	24.5
130	4.56	1.0	60,237	25.8	4.56	1.0	72,942	26.0	4.56	1.0	83,919	26.2
130	4.56	5.0	94,995	29.5	4.56	5.0	115,262	28.7	4.56	5.0	133,148	28.5
130	4.56	10.0	118,482	29.3	4.56	10.0	142,142	28.3	4.56	10.0	171,055	27.9
130	4.56	25.0	177,820	29.9	4.56	25.0	206,545	24.6	4.56	25.0	247,508	27.4

HMA E* Test Results (Plant B JMF, 12.5 mm NMAS, PG 64-22)

Temp. (F)	PLANT B											
	12.5 mm NMAS											
	PG64-22											
	Specimen 1				Specimen 2				Specimen 3			
	COAC(%)	Hz	E* (psi)	ϕ (Deg)	COAC(%)	Hz	E* (psi)	ϕ (Deg)	COAC(%)	Hz	E* (psi)	ϕ (Deg)
14	5.45	0.1	2,474,863	11.0	5.45	0.1	2,464,861	11.0	5.45	0.1	2,295,649	11.1
14	5.45	0.5	3,281,475	7.7	5.45	0.5	3,280,475	7.8	5.45	0.5	2,954,867	8.0
14	5.45	1.0	3,540,503	6.9	5.45	1.0	3,540,521	7.1	5.45	1.0	3,191,162	7.3
14	5.45	5.0	3,943,304	5.1	5.45	5.0	3,943,321	5.3	5.45	5.0	3,591,500	5.7
14	5.45	10.0	4,241,640	3.9	5.45	10.0	4,240,621	4.3	5.45	10.0	3,829,234	4.8
14	5.45	25.0	4,682,866	3.8	5.45	25.0	4,681,568	4.0	5.45	25.0	4,140,149	4.1
40	5.45	0.1	1,086,294	22.6	5.45	0.1	1,432,715	17.8	5.45	0.1	1,203,600	18.7
40	5.45	0.5	1,659,127	16.8	5.45	0.5	2,063,212	12.9	5.45	0.5	1,749,172	13.7
40	5.45	1.0	1,904,788	15.1	5.45	1.0	2,302,119	11.8	5.45	1.0	1,972,303	12.3
40	5.45	5.0	2,405,716	11.9	5.45	5.0	2,748,287	8.1	5.45	5.0	2,406,835	9.8
40	5.45	10.0	2,676,780	10.3	5.45	10.0	3,022,307	7.4	5.45	10.0	2,653,253	8.4
40	5.45	25.0	3,046,090	9.2	5.45	25.0	3,342,273	6.8	5.45	25.0	2,954,038	7.3
70	5.45	0.1	349,986	31.8	5.45	0.1	356,440	32.2	5.45	0.1	342,540	31.5
70	5.45	0.5	569,613	28.6	5.45	0.5	585,880	28.6	5.45	0.5	547,860	27.5
70	5.45	1.0	704,698	26.6	5.45	1.0	720,608	26.0	5.45	1.0	669,933	25.5
70	5.45	5.0	1,085,001	21.6	5.45	5.0	1,094,654	21.1	5.45	5.0	1,019,002	20.3
70	5.45	10.0	1,275,732	19.8	5.45	10.0	1,274,890	19.4	5.45	10.0	1,182,352	18.7
70	5.45	25.0	1,558,222	17.4	5.45	25.0	1,529,149	17.2	5.45	25.0	1,427,693	16.2
100	5.45	0.1	101,362	28.0	5.45	0.1	100,354	27.5	5.45	0.1	105,254	29.0
100	5.45	0.5	150,453	32.2	5.45	0.5	148,887	32.2	5.45	0.5	157,564	31.8
100	5.45	1.0	187,122	33.5	5.45	1.0	185,062	33.7	5.45	1.0	195,605	32.6
100	5.45	5.0	347,785	31.8	5.45	5.0	343,916	32.2	5.45	5.0	359,047	30.6
100	5.45	10.0	450,828	31.1	5.45	10.0	446,979	30.9	5.45	10.0	456,787	28.9
100	5.45	25.0	631,877	26.9	5.45	25.0	630,647	27.3	5.45	25.0	626,888	25.6
130	5.45	0.1	40,553	16.7	5.45	0.1	42,245	16.6	5.45	0.1	43,506	17.9
130	5.45	0.5	42,961	24.1	5.45	0.5	44,141	24.1	5.45	0.5	47,709	24.1
130	5.45	1.0	52,461	26.8	5.45	1.0	53,204	26.4	5.45	1.0	59,147	26.4
130	5.45	5.0	84,007	31.6	5.45	5.0	85,851	31.7	5.45	5.0	92,159	31.3
130	5.45	10.0	109,395	32.4	5.45	10.0	108,502	33.6	5.45	10.0	108,517	35.4
130	5.45	25.0	172,605	29.2	5.45	25.0	172,524	30.9	5.45	25.0	167,318	14.8

HMA E* Test Results (Plant B JMF, 12.5 mm NMAS, PG 67-22)

Temp. (F)	PLANT B											
	12.5 mm NMAS											
	PG67-22											
	Specimen 1				Specimen 2				Specimen 3			
	COAC(%)	Hz	E* (psi)	ϕ (Deg)	COAC(%)	Hz	E* (psi)	ϕ (Deg)	COAC(%)	Hz	E* (psi)	ϕ (Deg)
14	5.44	0.1	2,051,382	12.3	5.44	0.1	1,862,898	11.3	5.44	0.1	1,950,719	11.6
14	5.44	0.5	2,816,976	8.5	5.44	0.5	2,210,526	8.1	5.44	0.5	2,360,197	8.4
14	5.44	1.0	3,050,847	7.8	5.44	1.0	2,303,366	7.3	5.44	1.0	2,519,653	7.5
14	5.44	5.0	3,475,236	6.5	5.44	5.0	2,613,881	6.1	5.44	5.0	2,855,278	6.4
14	5.44	10.0	3,739,916	5.6	5.44	10.0	2,622,815	5.5	5.44	10.0	2,978,010	5.5
14	5.44	25.0	4,039,476	4.5	5.44	25.0	2,723,350	4.2	5.44	25.0	3,137,945	4.2
40	5.44	0.1	1,304,868	16.8	5.44	0.1	1,241,454	16.4	5.44	0.1	1,317,983	16.8
40	5.44	0.5	1,840,715	12.8	5.44	0.5	1,612,930	12.2	5.44	0.5	1,746,463	12.5
40	5.44	1.0	2,044,183	11.7	5.44	1.0	1,769,308	11.1	5.44	1.0	1,923,614	11.3
40	5.44	5.0	2,433,336	9.8	5.44	5.0	2,146,999	9.0	5.44	5.0	2,323,720	9.3
40	5.44	10.0	2,689,771	8.7	5.44	10.0	2,276,094	8.2	5.44	10.0	2,482,196	8.4
40	5.44	25.0	2,980,358	8.6	5.44	25.0	2,454,689	6.9	5.44	25.0	2,680,867	7.2
70	5.44	0.1	525,533	27.3	5.44	0.1	409,891	28.2	5.44	0.1	434,097	29.3
70	5.44	0.5	799,244	23.8	5.44	0.5	594,222	25.4	5.44	0.5	658,175	25.2
70	5.44	1.0	949,039	21.9	5.44	1.0	701,873	23.5	5.44	1.0	788,599	23.3
70	5.44	5.0	1,334,865	17.6	5.44	5.0	1,042,689	19.1	5.44	5.0	1,135,425	18.6
70	5.44	10.0	1,520,360	16.4	5.44	10.0	1,165,371	17.4	5.44	10.0	1,281,199	17.1
70	5.44	25.0	1,748,640	15.0	5.44	25.0	1,387,517	15.4	5.44	25.0	1,498,396	14.9
100	5.44	0.1	122,635	29.4	5.44	0.1	122,280	29.0	5.44	0.1	103,665	28.8
100	5.44	0.5	184,138	31.7	5.44	0.5	184,066	30.7	5.44	0.5	150,564	31.4
100	5.44	1.0	230,291	31.7	5.44	1.0	227,588	31.0	5.44	1.0	186,271	31.9
100	5.44	5.0	402,234	29.1	5.44	5.0	384,451	28.6	5.44	5.0	330,742	29.9
100	5.44	10.0	514,373	27.5	5.44	10.0	487,386	26.6	5.44	10.0	424,126	28.5
100	5.44	25.0	680,278	24.6	5.44	25.0	651,012	23.7	5.44	25.0	591,961	25.5
130	5.44	0.1	46,333	19.0	5.44	0.1	42,460	19.1	5.44	0.1	42,447	19.5
130	5.44	0.5	55,106	25.0	5.44	0.5	47,466	25.3	5.44	0.5	49,849	26.9
130	5.44	1.0	67,809	26.9	5.44	1.0	58,410	27.4	5.44	1.0	63,523	28.6
130	5.44	5.0	108,782	30.5	5.44	5.0	95,212	30.2	5.44	5.0	107,951	31.9
130	5.44	10.0	136,014	32.8	5.44	10.0	121,754	30.4	5.44	10.0	135,305	33.4
130	5.44	25.0	204,461	23.4	5.44	25.0	184,755	29.9	5.44	25.0	217,960	30.1

HMA E* Test Results (Plant B JMF, 19 mm NMAS, PG 64-22)

Temp. (F)	PLANT B											
	19 mm NMAS											
	PG64-22											
	Specimen 1				Specimen 2				Specimen 3			
	COAC(%)	Hz	E* (psi)	ϕ (Deg)	COAC(%)	Hz	E* (psi)	ϕ (Deg)	COAC(%)	Hz	E* (psi)	ϕ (Deg)
14	4.74	0.1	1,943,050	12.4	4.74	0.1	1,859,971	12.8	4.74	0.1	1,892,692	12.0
14	4.74	0.5	2,567,855	8.8	4.74	0.5	2,484,080	9.2	4.74	0.5	2,333,843	9.0
14	4.74	1.0	2,785,951	7.7	4.74	1.0	2,709,372	8.1	4.74	1.0	2,502,834	8.2
14	4.74	5.0	3,188,798	5.8	4.74	5.0	3,095,115	6.2	4.74	5.0	2,869,527	6.4
14	4.74	10.0	3,391,703	4.8	4.74	10.0	3,341,018	5.1	4.74	10.0	3,028,158	5.7
14	4.74	25.0	3,642,888	3.8	4.74	25.0	3,661,455	4.8	4.74	25.0	3,305,328	4.3
40	4.74	0.1	1,305,111	16.8	4.74	0.1	994,811	20.0	4.74	0.1	1,160,624	17.4
40	4.74	0.5	1,809,917	12.7	4.74	0.5	1,434,857	14.8	4.74	0.5	1,557,143	13.1
40	4.74	1.0	2,007,955	11.4	4.74	1.0	1,602,032	13.1	4.74	1.0	1,726,358	11.8
40	4.74	5.0	2,383,243	8.8	4.74	5.0	1,961,749	10.3	4.74	5.0	2,098,357	9.4
40	4.74	10.0	2,592,753	7.5	4.74	10.0	2,143,800	9.4	4.74	10.0	2,259,324	8.5
40	4.74	25.0	2,853,898	6.7	4.74	25.0	2,356,271	7.9	4.74	25.0	2,505,365	6.9
70	4.74	0.1	596,417	26.3	4.74	0.1	307,824	30.3	4.74	0.1	426,802	29.2
70	4.74	0.5	902,860	21.5	4.74	0.5	473,268	27.5	4.74	0.5	645,984	24.7
70	4.74	1.0	1,051,772	19.3	4.74	1.0	574,695	25.8	4.74	1.0	772,946	22.9
70	4.74	5.0	1,412,770	15.2	4.74	5.0	868,907	21.1	4.74	5.0	1,116,622	18.4
70	4.74	10.0	1,583,533	13.9	4.74	10.0	1,005,255	19.6	4.74	10.0	1,264,535	16.9
70	4.74	25.0	1,813,350	12.5	4.74	25.0	1,185,578	18.3	4.74	25.0	1,494,413	15.0
100	4.74	0.1	115,621	28.9	4.74	0.1	91,909	26.9	4.74	0.1	107,871	28.6
100	4.74	0.5	172,949	31.5	4.74	0.5	131,907	30.7	4.74	0.5	158,106	31.3
100	4.74	1.0	212,819	32.3	4.74	1.0	161,281	32.0	4.74	1.0	193,758	31.9
100	4.74	5.0	383,855	29.6	4.74	5.0	288,824	30.8	4.74	5.0	346,478	29.8
100	4.74	10.0	488,335	27.8	4.74	10.0	371,096	29.6	4.74	10.0	444,373	28.3
100	4.74	25.0	657,381	25.6	4.74	25.0	521,037	26.1	4.74	25.0	607,508	26.2
130	4.74	0.1	44,210	16.1	4.74	0.1	38,165	16.9	4.74	0.1	43,067	18.6
130	4.74	0.5	47,308	22.8	4.74	0.5	39,935	23.5	4.74	0.5	46,603	25.5
130	4.74	1.0	58,402	24.9	4.74	1.0	48,920	25.7	4.74	1.0	59,454	27.6
130	4.74	5.0	89,195	30.4	4.74	5.0	75,871	31.2	4.74	5.0	98,390	32.0
130	4.74	10.0	108,457	34.3	4.74	10.0	100,200	31.5	4.74	10.0	126,694	32.6
130	4.74	25.0	178,519	31.9	4.74	25.0	147,988	32.4	4.74	25.0	200,526	31.1

HMA E* Test Results (Plant B JMF, 19 mm NMAS, PG 67-22)

Temp. (F)	PLANT B											
	19 mm NMAS											
	PG67-22											
	Specimen 1				Specimen 2				Specimen 3			
	COAC(%)	Hz	E* (psi)	ϕ (Deg)	COAC(%)	Hz	E* (psi)	ϕ (Deg)	COAC(%)	Hz	E* (psi)	ϕ (Deg)
14	4.73	0.1	1,622,991	11.1	4.73	0.1	2,543,304	9.8	4.73	0.1	1,550,113	12.6
14	4.73	0.5	1,837,672	8.2	4.73	0.5	3,155,817	7.1	4.73	0.5	1,939,759	8.6
14	4.73	1.0	1,876,248	7.2	4.73	1.0	3,369,427	6.5	4.73	1.0	2,053,294	7.9
14	4.73	5.0	2,126,840	6.1	4.73	5.0	3,755,054	5.3	4.73	5.0	2,368,052	6.2
14	4.73	10.0	2,186,809	5.3	4.73	10.0	3,965,532	4.5	4.73	10.0	2,485,621	5.4
14	4.73	25.0	2,310,843	4.4	4.73	25.0	4,198,566	4.2	4.73	25.0	2,634,167	4.5
40	4.73	0.1	984,631	17.2	4.73	0.1	1,569,355	15.5	4.73	0.1	924,417	19.9
40	4.73	0.5	1,295,845	12.9	4.73	0.5	2,098,432	11.7	4.73	0.5	1,265,401	15.5
40	4.73	1.0	1,438,923	11.6	4.73	1.0	2,300,819	10.7	4.73	1.0	1,432,359	13.6
40	4.73	5.0	1,758,690	9.7	4.73	5.0	2,737,275	8.5	4.73	5.0	1,792,754	10.7
40	4.73	10.0	1,853,893	8.6	4.73	10.0	2,959,037	7.7	4.73	10.0	1,939,355	9.8
40	4.73	25.0	2,039,935	7.3	4.73	25.0	3,192,099	7.1	4.73	25.0	2,149,359	8.8
70	4.73	0.1	412,621	27.3	4.73	0.1	545,565	26.9	4.73	0.1	402,866	28.5
70	4.73	0.5	585,584	23.3	4.73	0.5	801,095	23.4	4.73	0.5	588,573	24.5
70	4.73	1.0	675,849	21.3	4.73	1.0	947,482	21.4	4.73	1.0	696,607	22.8
70	4.73	5.0	968,217	17.5	4.73	5.0	1,332,563	17.4	4.73	5.0	1,012,610	18.2
70	4.73	10.0	1,070,123	16.0	4.73	10.0	1,503,498	15.8	4.73	10.0	1,134,093	16.7
70	4.73	25.0	1,240,961	14.1	4.73	25.0	1,735,614	14.1	4.73	25.0	1,355,704	15.8
100	4.73	0.1	119,681	31.0	4.73	0.1	159,807	29.0	4.73	0.1	127,143	29.8
100	4.73	0.5	171,202	31.2	4.73	0.5	238,207	30.5	4.73	0.5	186,943	31.5
100	4.73	1.0	205,435	31.0	4.73	1.0	298,848	30.2	4.73	1.0	226,271	32.1
100	4.73	5.0	348,912	28.3	4.73	5.0	508,002	27.0	4.73	5.0	406,931	28.6
100	4.73	10.0	438,526	25.8	4.73	10.0	623,842	25.4	4.73	10.0	502,360	27.0
100	4.73	25.0	588,057	23.2	4.73	25.0	784,303	23.4	4.73	25.0	682,982	23.9
130	4.73	0.1	48,676	21.1	4.73	0.1	51,394	21.2	4.73	0.1	41,735	19.3
130	4.73	0.5	58,714	26.1	4.73	0.5	61,688	27.3	4.73	0.5	47,055	26.5
130	4.73	1.0	72,905	28.2	4.73	1.0	78,290	28.9	4.73	1.0	58,194	28.4
130	4.73	5.0	123,121	30.7	4.73	5.0	134,026	30.6	4.73	5.0	98,553	31.3
130	4.73	10.0	146,471	31.9	4.73	10.0	171,983	30.0	4.73	10.0	124,179	31.6
130	4.73	25.0	219,400	26.3	4.73	25.0	243,364	30.1	4.73	25.0	187,768	31.4

HMA E* Test Results (Plant B JMF, 25 mm NMAS, PG 64-22)

Temp. (F)	PLANT B											
	25 mm NMAS											
	PG64-22											
	Specimen 1				Specimen 2				Specimen 3			
	COAC(%)	Hz	E* (psi)	ϕ (Deg)	COAC(%)	Hz	E* (psi)	ϕ (Deg)	COAC(%)	Hz	E* (psi)	ϕ (Deg)
14	4.34	0.1	2,527,382	9.5	4.34	0.1	2,287,284	7.1	4.34	0.1	1,447,950	13.0
14	4.34	0.5	3,099,304	7.0	4.34	0.5	2,728,641	4.7	4.34	0.5	1,828,200	9.2
14	4.34	1.0	3,310,075	5.5	4.34	1.0	2,884,410	4.5	4.34	1.0	1,952,075	8.2
14	4.34	5.0	3,610,158	4.6	4.34	5.0	3,143,607	3.0	4.34	5.0	2,227,697	6.5
14	4.34	10.0	3,792,702	3.9	4.34	10.0	3,267,240	2.9	4.34	10.0	2,316,431	5.4
14	4.34	25.0	3,977,102	3.7	4.34	25.0	3,440,931	2.5	4.34	25.0	2,443,188	5.0
40	4.34	0.1	1,457,356	17.4	4.34	0.1	1,030,180	16.4	4.34	0.1	820,493	18.9
40	4.34	0.5	1,949,094	13.1	4.34	0.5	1,420,066	12.1	4.34	0.5	1,067,036	14.3
40	4.34	1.0	2,147,619	11.7	4.34	1.0	1,573,936	10.5	4.34	1.0	1,157,551	12.8
40	4.34	5.0	2,567,462	9.1	4.34	5.0	1,909,765	8.3	4.34	5.0	1,436,582	10.4
40	4.34	10.0	2,762,048	8.0	4.34	10.0	2,067,600	7.6	4.34	10.0	1,517,932	9.3
40	4.34	25.0	3,000,171	6.7	4.34	25.0	2,274,526	6.7	4.34	25.0	1,649,327	8.1
70	4.34	0.1	522,350	28.2	4.34	0.1	420,375	27.4	4.34	0.1	316,051	27.6
70	4.34	0.5	775,288	24.6	4.34	0.5	623,443	22.7	4.34	0.5	437,990	24.7
70	4.34	1.0	920,091	22.5	4.34	1.0	738,031	20.7	4.34	1.0	498,745	23.2
70	4.34	5.0	1,314,136	18.0	4.34	5.0	1,051,925	16.4	4.34	5.0	733,290	18.8
70	4.34	10.0	1,488,789	16.4	4.34	10.0	1,181,639	14.9	4.34	10.0	810,254	17.7
70	4.34	25.0	1,740,145	14.5	4.34	25.0	1,389,699	12.9	4.34	25.0	966,238	15.3
100	4.34	0.1	132,725	28.6	4.34	0.1	122,822	29.0	4.34	0.1	100,812	23.1
100	4.34	0.5	193,403	31.3	4.34	0.5	171,692	31.1	4.34	0.5	127,794	26.3
100	4.34	1.0	237,757	32.5	4.34	1.0	206,359	30.5	4.34	1.0	146,144	28.0
100	4.34	5.0	423,260	30.6	4.34	5.0	350,365	27.9	4.34	5.0	235,048	28.2
100	4.34	10.0	539,159	28.8	4.34	10.0	455,243	25.3	4.34	10.0	306,418	27.1
100	4.34	25.0	753,201	25.5	4.34	25.0	598,292	18.6	4.34	25.0	427,572	25.1
130	4.34	0.1	52,429	18.1	4.34	0.1	46,080	19.4	4.34	0.1	47,007	12.7
130	4.34	0.5	56,951	25.1	4.34	0.5	47,744	26.1	4.34	0.5	45,355	18.2
130	4.34	1.0	66,688	28.0	4.34	1.0	59,240	27.5	4.34	1.0	54,356	20.3
130	4.34	5.0	112,309	31.2	4.34	5.0	95,569	29.8	4.34	5.0	78,942	24.1
130	4.34	10.0	148,762	31.2	4.34	10.0	114,778	30.0	4.34	10.0	94,059	26.2
130	4.34	25.0	225,939	31.7	4.34	25.0	171,209	24.1	4.34	25.0	138,740	23.9

HMA E* Test Results (Plant B JMF, 25 mm NMAS, PG 67-22)

Temp. (F)	PLANT B											
	25 mm NMAS											
	PG67-22											
	Specimen 1				Specimen 2				Specimen 3			
	COAC(%)	Hz	E* (psi)	ϕ (Deg)	COAC(%)	Hz	E* (psi)	ϕ (Deg)	COAC(%)	Hz	E* (psi)	ϕ (Deg)
14	4.33	0.1	1,788,756	12.0	4.33	0.1	2,229,861	9.8	4.33	25.0	3,535,985	7.0
14	4.33	0.5	2,178,000	8.5	4.33	0.5	2,736,409	7.3	4.33	10.0	3,417,890	4.6
14	4.33	1.0	2,293,923	7.7	4.33	1.0	2,913,102	6.5	4.33	5.0	3,252,445	5.0
14	4.33	5.0	2,617,092	6.2	4.33	5.0	3,252,445	5.0	4.33	1.0	2,913,102	6.5
14	4.33	10.0	2,702,735	5.7	4.33	10.0	3,417,890	4.6	4.33	0.5	2,736,409	7.3
14	4.33	25.0	2,897,282	4.4	4.33	25.0	3,535,985	-1.7	4.33	0.1	2,229,861	9.8
40	4.33	0.1	951,382	20.2	4.33	0.1	1,178,885	16.5	4.33	25.0	2,102,611	9.7
40	4.33	0.5	1,269,384	15.4	4.33	0.5	1,569,314	12.6	4.33	10.0	1,868,757	10.9
40	4.33	1.0	1,409,344	13.8	4.33	1.0	1,730,103	11.3	4.33	5.0	1,709,968	12.3
40	4.33	5.0	1,756,141	11.2	4.33	5.0	2,073,970	9.1	4.33	1.0	1,349,014	15.5
40	4.33	10.0	1,862,566	10.2	4.33	10.0	2,240,670	8.2	4.33	0.5	1,197,349	17.3
40	4.33	25.0	2,012,394	8.6	4.33	25.0	2,496,168	7.1	4.33	0.1	844,248	22.4
70	4.33	0.1	433,917	27.6	4.33	0.1	442,743	26.5	4.33	25.0	1,349,256	15.2
70	4.33	0.5	623,970	23.9	4.33	0.5	636,204	23.4	4.33	10.0	1,135,451	17.5
70	4.33	1.0	733,851	22.2	4.33	1.0	750,662	21.8	4.33	5.0	1,004,061	18.9
70	4.33	5.0	1,048,165	17.9	4.33	5.0	1,055,817	17.8	4.33	1.0	696,699	23.5
70	4.33	10.0	1,166,536	16.6	4.33	10.0	1,183,989	16.6	4.33	0.5	588,299	25.2
70	4.33	25.0	1,334,193	14.4	4.33	25.0	1,391,151	14.5	4.33	0.1	395,770	28.8
100	4.33	0.1	115,435	25.7	4.33	0.1	121,281	25.4	4.33	25.0	512,915	26.3
100	4.33	0.5	156,713	29.1	4.33	0.5	163,715	27.7	4.33	10.0	367,749	28.3
100	4.33	1.0	187,239	30.3	4.33	1.0	192,850	28.5	4.33	5.0	292,587	29.1
100	4.33	5.0	319,074	29.5	4.33	5.0	317,305	28.0	4.33	1.0	176,463	29.3
100	4.33	10.0	414,901	27.7	4.33	10.0	411,544	26.1	4.33	0.5	149,729	28.2
100	4.33	25.0	545,729	25.0	4.33	25.0	552,028	24.9	4.33	0.1	110,541	26.6
130	4.33	0.1	48,851	16.7	4.33	0.1	53,668	16.6	4.33	25.0	156,724	29.4
130	4.33	0.5	53,273	23.8	4.33	0.5	54,981	22.5	4.33	10.0	107,169	28.0
130	4.33	1.0	64,144	25.9	4.33	1.0	68,627	24.1	4.33	5.0	84,510	27.6
130	4.33	5.0	96,934	30.9	4.33	5.0	105,145	26.1	4.33	1.0	58,604	24.2
130	4.33	10.0	127,799	29.4	4.33	10.0	135,554	27.5	4.33	0.5	47,965	22.8
130	4.33	25.0	174,456	20.5	4.33	25.0	189,737	25.3	4.33	0.1	44,030	18.8

APPENDIX B

GAB Resilient Modulus Test Results

Georgia Pavement Research Center

Southern Polytechnic State University

		Test Date:	8/28/2012
QPL ID:	011C	Specimen Preparation Date:	8/27/2012
Source Location	Lithonia	Specimen Diameter (in):	6
GAB Character:	Granite Gneiss	Specimen Height (in.)	12.5
w_{opt} (%):	5.7	Compaction w_c (%)	5.5
Max. γ_d (pcf):	133.9	w_c after Testing (%):	
		Tested By:	sk

Test Seq.	σ_1 (kPa)	σ_3 (kPa)	θ (kPa)	τ_{oct} (kPa)	I/Pa	τ_{oct}/Pa	Log(I/Pa)	Log(τ_{oct}/Pa+1)	M_R (kPa)	Log M_R
1	41.39	20.70	82.79	9.75	0.82	0.10	-0.09	0.04	87,983	4.944
2	62.07	20.70	103.47	19.50	1.02	0.19	0.01	0.08	109,911	5.041
3	82.76	20.70	124.16	29.25	1.23	0.29	0.09	0.11	129,846	5.113
4	68.98	34.50	137.98	16.25	1.36	0.16	0.13	0.06	137,797	5.139
5	103.45	34.50	172.45	32.50	1.70	0.32	0.23	0.12	156,797	5.195
6	137.93	34.50	206.93	48.76	2.04	0.48	0.31	0.17	172,262	5.236
7	137.85	68.90	275.65	32.50	2.72	0.32	0.43	0.12	218,139	5.339
8	206.80	68.90	344.60	65.01	3.40	0.64	0.53	0.22	271,241	5.433
9	275.75	68.90	413.55	97.51	4.08	0.96	0.61	0.29	293,328	5.467
10	172.35	103.40	379.15	32.50	3.74	0.32	0.57	0.12	271,800	5.434
11	206.83	103.40	413.63	48.76	4.08	0.48	0.61	0.17	294,185	5.469
12	310.25	103.40	517.05	97.51	5.10	0.96	0.71	0.29	330,193	5.519
13	241.33	137.90	517.13	48.76	5.10	0.48	0.71	0.17	337,379	5.528
14	275.80	137.90	551.60	65.01	5.44	0.64	0.74	0.22	362,916	5.560
15	413.70	137.90	689.50	130.01	6.80	1.28	0.83	0.36	402,505	5.605

Generalized NCHRP 1-28A Model (M-E Design Guide)

k1	k2	k3	R^2
1049	0.716	-0.041	1.00

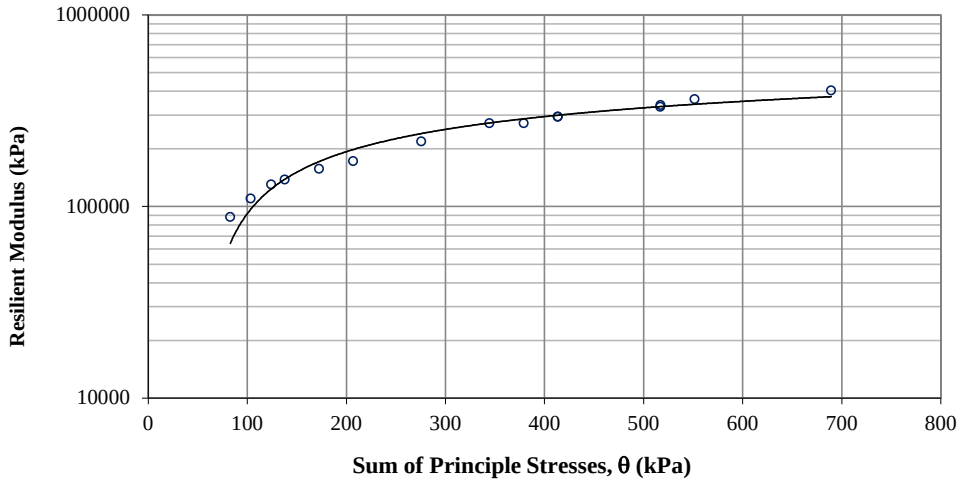

GAB Resilient Modulus Test Results

Georgia Pavement Research Center
Southern Polytechnic State University

		Test Date:	2/6/2013
QPL ID:	013C	Specimen Preparation Date:	2/6/2013
Source Location	Dalton, GA	Specimen Diameter (in):	6
GAB Character:	Limestone	Specimen Height (in.)	12
w_{opt} (%):	6.6	Compaction w_c (%)	6.6
Max. γ_d (pcf):	142.5	w_c after Testing (%):	6.6
		Tested By:	sk

Test Seq.	σ_1 (kPa)	σ_3 (kPa)	θ (kPa)	τ_{oct} (kPa)	I/Pa	τ_{oct}/Pa	Log(I/Pa)	Log(τ_{oct}/Pa+1)	M_R (kPa)	Log M_R
1	41.39	20.70	82.79	9.75	0.82	0.10	-0.09	0.04	88,113	4.945
2	62.07	20.70	103.47	19.50	1.02	0.19	0.01	0.08	114,910	5.060
3	82.76	20.70	124.16	29.25	1.23	0.29	0.09	0.11	115,852	5.064
4	68.98	34.50	137.98	16.25	1.36	0.16	0.13	0.06	124,544	5.095
5	103.45	34.50	172.45	32.50	1.70	0.32	0.23	0.12	141,703	5.151
6	137.93	34.50	206.93	48.76	2.04	0.48	0.31	0.17	144,218	5.159
7	137.85	68.90	275.65	32.50	2.72	0.32	0.43	0.12	195,127	5.290
8	206.80	68.90	344.60	65.01	3.40	0.64	0.53	0.22	214,097	5.331
9	275.75	68.90	413.55	97.51	4.08	0.96	0.61	0.29	226,437	5.355
10	172.35	103.40	379.15	32.50	3.74	0.32	0.57	0.12	237,486	5.376
11	206.83	103.40	413.63	48.76	4.08	0.48	0.61	0.17	246,335	5.392
12	310.25	103.40	517.05	97.51	5.10	0.96	0.71	0.29	278,798	5.445
13	241.33	137.90	517.13	48.76	5.10	0.48	0.71	0.17	290,014	5.462
14	275.80	137.90	551.60	65.01	5.44	0.64	0.74	0.22	305,425	5.485
15	413.70	137.90	689.50	130.01	6.80	1.28	0.83	0.36	350,249	5.544

Generalized NCHRP 1-28A Model (M-E Design Guide)

k1	k2	k3	R^2
1031	0.659	-0.145	0.99

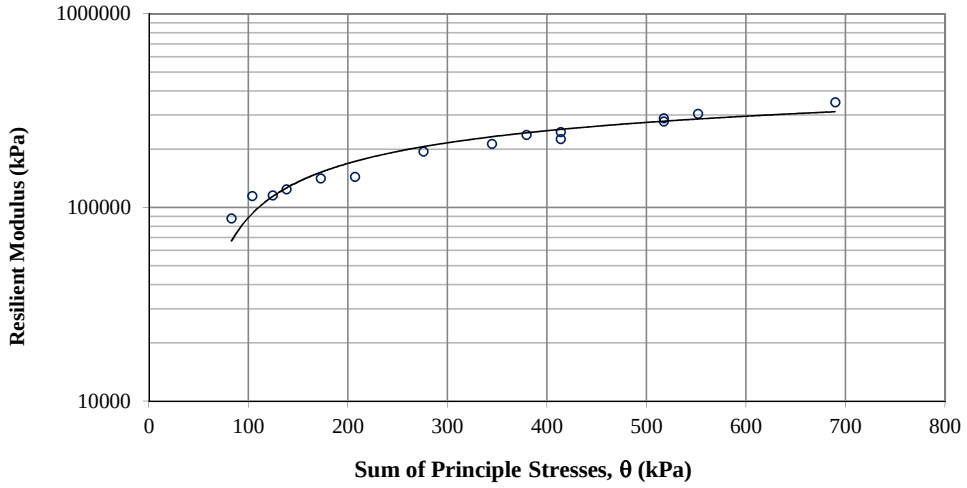

GAB Resilient Modulus Test Results

Georgia Pavement Research Center
Southern Polytechnic State University

		Test Date:	10/2/2012
QPL ID:	024C	Specimen Preparation Date:	10/1/2012
Source Location	Gainsville	Specimen Diameter (in):	6
GAB Character:	Mylonitic Gneiss	Specimen Height (in.)	12
w_{opt} (%):	6	Compaction w_c (%)	6
Max. γ_d (pcf):	136.6	w_c after Testing (%):	
		Tested By:	sk

Test Seq.	σ_1 (kPa)	σ_3 (kPa)	θ (kPa)	τ_{oct} (kPa)	I/Pa	τ_{oct}/Pa	Log(I/Pa)	Log(τ_{oct}/Pa+1)	M_R (kPa)	Log M_R
1	41.39	20.70	82.79	9.75	0.82	0.10	-0.09	0.04	53,372	4.727
2	62.07	20.70	103.47	19.50	1.02	0.19	0.01	0.08	76,028	4.881
3	82.76	20.70	124.16	29.25	1.23	0.29	0.09	0.11	99,318	4.997
4	68.98	34.50	137.98	16.25	1.36	0.16	0.13	0.06	104,950	5.021
5	103.45	34.50	172.45	32.50	1.70	0.32	0.23	0.12	124,011	5.093
6	137.93	34.50	206.93	48.76	2.04	0.48	0.31	0.17	137,159	5.137
7	137.85	68.90	275.65	32.50	2.72	0.32	0.43	0.12	182,500	5.261
8	206.80	68.90	344.60	65.01	3.40	0.64	0.53	0.22	211,840	5.326
9	275.75	68.90	413.55	97.51	4.08	0.96	0.61	0.29	230,664	5.363
10	172.35	103.40	379.15	32.50	3.74	0.32	0.57	0.12	207,640	5.317
11	206.83	103.40	413.63	48.76	4.08	0.48	0.61	0.17	232,020	5.366
12	310.25	103.40	517.05	97.51	5.10	0.96	0.71	0.29	250,171	5.398
13	241.33	137.90	517.13	48.76	5.10	0.48	0.71	0.17	264,627	5.423
14	275.80	137.90	551.60	65.01	5.44	0.64	0.74	0.22	298,856	5.475
15	413.70	137.90	689.50	130.01	6.80	1.28	0.83	0.36	351,853	5.546

Generalized NCHRP 1-28A Model (M-E Design Guide)

k1	k2	k3	R^2
739	0.797	-0.012	0.98

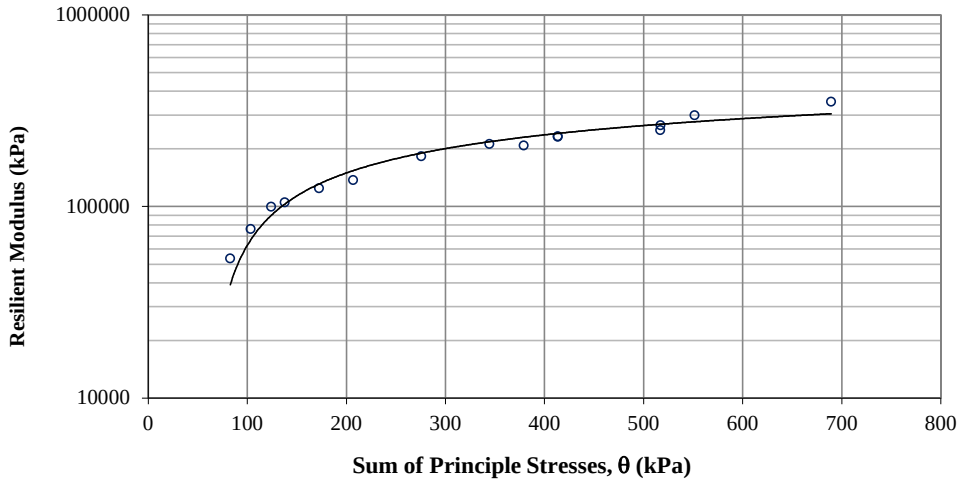

GAB Resilient Modulus Test Results

Georgia Pavement Research Center
Southern Polytechnic State University

		Test Date:	2/15/2013
QPL ID:	028C	Specimen Preparation Date:	2/15/2013
Source Location	Hitchcock	Specimen Diameter (in):	6
GAB Character:	Mylonitic Gneiss	Specimen Height (in.)	12
w_{opt} (%):	6.2	Compaction w_c (%)	6.2
Max. γ_d (pcf):	141.2	w_c after Testing (%):	
		Tested By:	sk

Test Seq.	σ_1 (kPa)	σ_3 (kPa)	θ (kPa)	τ_{oct} (kPa)	I/Pa	τ_{oct}/Pa	Log(I/Pa)	Log(τ_{oct}/Pa+1)	M_R (kPa)	Log M_R
1	41.39	20.70	82.79	9.75	0.82	0.10	-0.09	0.04	83,197	4.920
2	62.07	20.70	103.47	19.50	1.02	0.19	0.01	0.08	102,984	5.013
3	82.76	20.70	124.16	29.25	1.23	0.29	0.09	0.11	112,473	5.051
4	68.98	34.50	137.98	16.25	1.36	0.16	0.13	0.06	125,521	5.099
5	103.45	34.50	172.45	32.50	1.70	0.32	0.23	0.12	146,266	5.165
6	137.93	34.50	206.93	48.76	2.04	0.48	0.31	0.17	163,171	5.213
7	137.85	68.90	275.65	32.50	2.72	0.32	0.43	0.12	185,005	5.267
8	206.80	68.90	344.60	65.01	3.40	0.64	0.53	0.22	222,432	5.347
9	275.75	68.90	413.55	97.51	4.08	0.96	0.61	0.29	240,438	5.381
10	172.35	103.40	379.15	32.50	3.74	0.32	0.57	0.12	219,470	5.341
11	206.83	103.40	413.63	48.76	4.08	0.48	0.61	0.17	232,210	5.366
12	310.25	103.40	517.05	97.51	5.10	0.96	0.71	0.29	244,564	5.388
13	241.33	137.90	517.13	48.76	5.10	0.48	0.71	0.17	255,329	5.407
14	275.80	137.90	551.60	65.01	5.44	0.64	0.74	0.22	277,980	5.444
15	413.70	137.90	689.50	130.01	6.80	1.28	0.83	0.36	292,078	5.465

Generalized NCHRP 1-28A Model (M-E Design Guide)

k1	k2	k3	R^2
996	0.591	-0.046	0.99

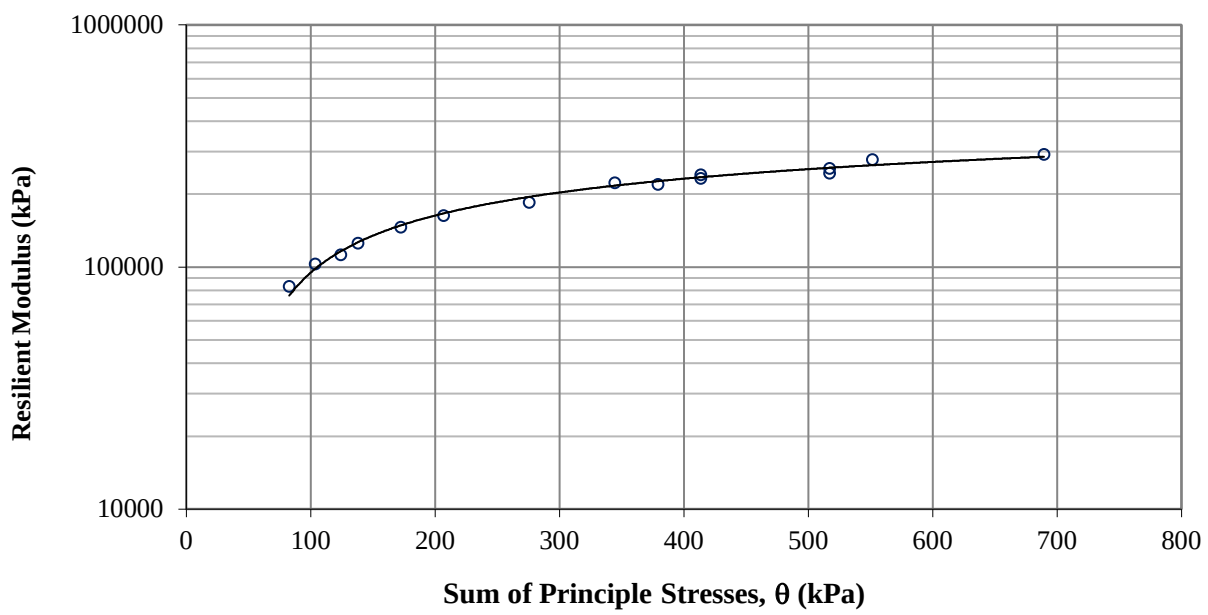

GAB Resilient Modulus Test Results

Georgia Pavement Research Center
Southern Polytechnic State University

		Test Date:	2/17/2013
QPL ID:	050C	Specimen Preparation Date:	2/17/2013
Source Location	Stockbridge, GA	Specimen Diameter (in):	6
GAB Character:	Granite Gneiss	Specimen Height (in.)	12
w_{opt} (%):	5.9	Compaction w_c (%)	5.9
Max. γ_d (pcf):	134.2	w_c after Testing (%):	
		Tested By:	sk

Test Seq.	σ_1 (kPa)	σ_3 (kPa)	θ (kPa)	τ_{oct} (kPa)	I/Pa	τ_{oct}/Pa	Log(I/Pa)	Log(τ_{oct}/Pa+1)	M_R (kPa)	Log M_R
1	41.39	20.70	82.79	9.75	0.82	0.10	-0.09	0.04	87,037	4.940
2	62.07	20.70	103.47	19.50	1.02	0.19	0.01	0.08	101,145	5.005
3	82.76	20.70	124.16	29.25	1.23	0.29	0.09	0.11	111,733	5.048
4	68.98	34.50	137.98	16.25	1.36	0.16	0.13	0.06	117,676	5.071
5	103.45	34.50	172.45	32.50	1.70	0.32	0.23	0.12	131,946	5.120
6	137.93	34.50	206.93	48.76	2.04	0.48	0.31	0.17	141,253	5.150
7	137.85	68.90	275.65	32.50	2.72	0.32	0.43	0.12	168,486	5.227
8	206.80	68.90	344.60	65.01	3.40	0.64	0.53	0.22	199,018	5.299
9	275.75	68.90	413.55	97.51	4.08	0.96	0.61	0.29	216,578	5.336
10	172.35	103.40	379.15	32.50	3.74	0.32	0.57	0.12	196,609	5.294
11	206.83	103.40	413.63	48.76	4.08	0.48	0.61	0.17	205,287	5.312
12	310.25	103.40	517.05	97.51	5.10	0.96	0.71	0.29	223,381	5.349
13	241.33	137.90	517.13	48.76	5.10	0.48	0.71	0.17	232,308	5.366
14	275.80	137.90	551.60	65.01	5.44	0.64	0.74	0.22	240,798	5.382
15	413.70	137.90	689.50	130.01	6.80	1.28	0.83	0.36	256,435	5.409

Generalized NCHRP 1-28A Model (M-E Design Guide)

k1	k2	k3	R^2
969	0.522	-0.022	0.99

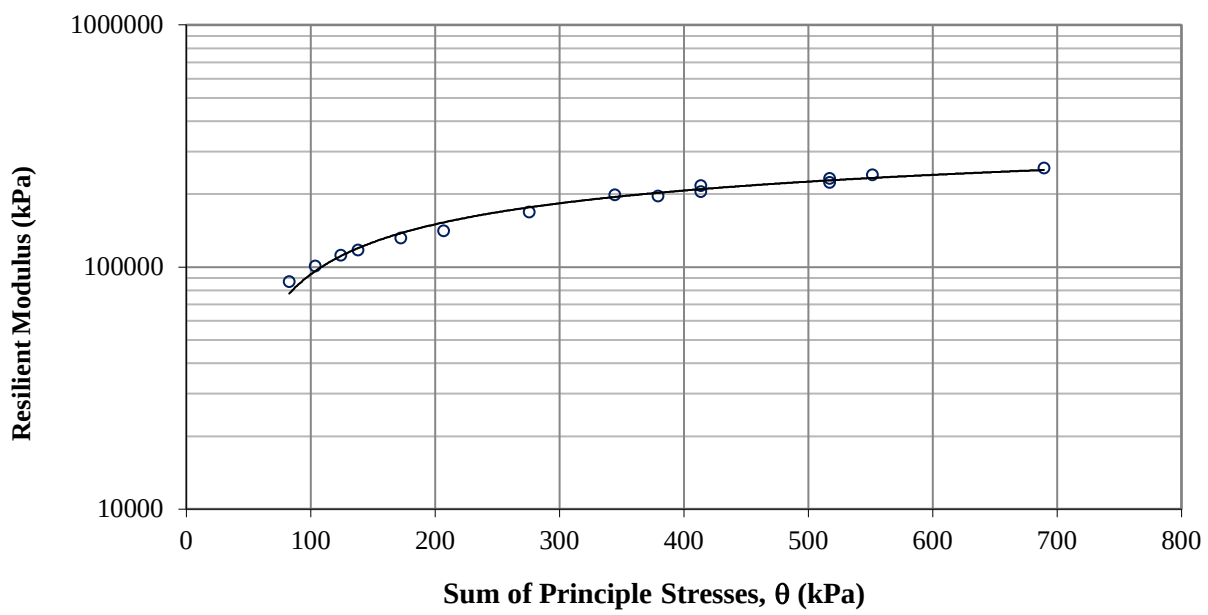

GAB Resilient Modulus Test Results

Georgia Pavement Research Center
Southern Polytechnic State University

		Test Date:	8/27/2012
QPL ID:	101C	Specimen Preparation Date:	8/26/2012
Source Location	Demorest, GA	Specimen Diameter (in):	6
GAB Character:	Metasandstone	Specimen Height (in.)	12
w_{opt} (%):	5.3	Compaction w_c (%)	5.3
Max. γ_d (pcf):	137.4	w_c after Testing (%):	
		Tested By:	sk

Test Seq.	σ_1 (kPa)	σ_3 (kPa)	θ (kPa)	τ_{oct} (kPa)	I/Pa	τ_{oct}/Pa	Log(I/Pa)	Log(τ_{oct}/Pa+1)	M_R (kPa)	Log M_R
1	41.38	20.69	82.76	9.75	0.82	0.10	-0.09	0.04	59,239	4.773
2	62.06	20.69	103.44	19.50	1.02	0.19	0.01	0.08	68,655	4.837
3	82.75	20.69	124.13	29.25	1.23	0.29	0.09	0.11	83,097	4.920
4	68.96	34.49	137.94	16.25	1.36	0.16	0.13	0.06	85,662	4.933
5	103.44	34.49	172.41	32.50	1.70	0.32	0.23	0.12	101,146	5.005
6	137.91	34.48	206.88	48.76	2.04	0.48	0.31	0.17	117,164	5.069
7	137.83	68.88	275.59	32.50	2.72	0.32	0.43	0.12	155,073	5.191
8	206.78	68.88	344.53	65.01	3.40	0.64	0.53	0.22	177,357	5.249
9	275.74	68.89	413.52	97.51	4.08	0.96	0.61	0.29	199,939	5.301
10	172.32	103.37	379.05	32.50	3.74	0.32	0.57	0.12	179,301	5.254
11	206.79	103.36	413.51	48.76	4.08	0.48	0.61	0.17	195,477	5.291
12	310.23	103.38	517.00	97.51	5.10	0.96	0.71	0.29	203,150	5.308
13	241.30	137.88	517.06	48.76	5.10	0.48	0.71	0.17	220,800	5.344
14	275.79	137.89	551.56	65.01	5.44	0.64	0.74	0.22	247,138	5.393
15	413.70	137.90	689.50	130.01	6.80	1.28	0.83	0.36	288,898	5.461

Generalized NCHRP 1-28A Model (M-E Design Guide)

k1	k2	k3	R^2
674	0.734	-0.014	0.99

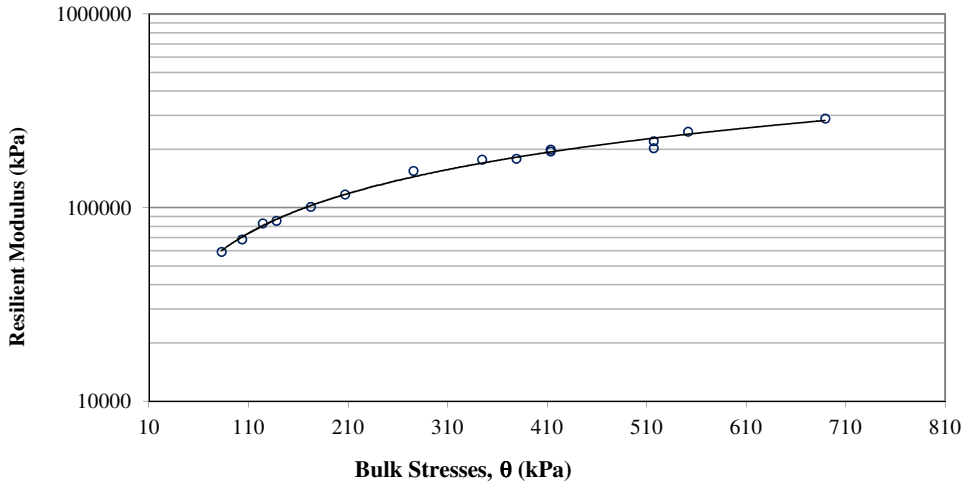

GAB Resilient Modulus Test Results

Georgia Pavement Research Center
Southern Polytechnic State University

		Test Date:	10/16/2012
QPL ID:	108T	Specimen Preparation Date:	10/16/2012
Source Location	Mayo Mine	Specimen Diameter (in):	6
GAB Character:	Limerock	Specimen Height (in.)	12
w_{opt} (%):	13.6	Compaction w_c (%)	13.6
Max. γ_d (pcf):	112.6	w_c after Testing (%):	
		Tested By:	sk

Test Seq.	σ_1 (kPa)	σ_3 (kPa)	θ (kPa)	τ_{oct} (kPa)	I/Pa	τ_{oct}/Pa	Log(I/Pa)	Log(τ_{oct}/Pa+1)	M_R (kPa)	Log M_R
1	41.39	20.70	82.79	9.75	0.82	0.10	-0.09	0.04	51,162	4.709
2	62.07	20.70	103.47	19.50	1.02	0.19	0.01	0.08	80,707	4.907
3	82.76	20.70	124.16	29.25	1.23	0.29	0.09	0.11	111,972	5.049
4	68.98	34.50	137.98	16.25	1.36	0.16	0.13	0.06	121,451	5.084
5	103.45	34.50	172.45	32.50	1.70	0.32	0.23	0.12	148,323	5.171
6	137.93	34.50	206.93	48.76	2.04	0.48	0.31	0.17	169,934	5.230
7	137.85	68.90	275.65	32.50	2.72	0.32	0.43	0.12	205,916	5.314
8	206.80	68.90	344.60	65.01	3.40	0.64	0.53	0.22	247,618	5.394
9	275.75	68.90	413.55	97.51	4.08	0.96	0.61	0.29	285,405	5.455
10	172.35	103.40	379.15	32.50	3.74	0.32	0.57	0.12	255,027	5.407
11	206.83	103.40	413.63	48.76	4.08	0.48	0.61	0.17	268,592	5.429
12	310.25	103.40	517.05	97.51	5.10	0.96	0.71	0.29	311,801	5.494
13	241.33	137.90	517.13	48.76	5.10	0.48	0.71	0.17	326,041	5.513
14	275.80	137.90	551.60	65.01	5.44	0.64	0.74	0.22	342,615	5.535
15	413.70	137.90	689.50	130.01	6.80	1.28	0.83	0.36	404,077	5.606

Generalized NCHRP 1-28A Model (M-E Design Guide)

k1	k2	k3	R^2
803	0.862	-0.012	0.96

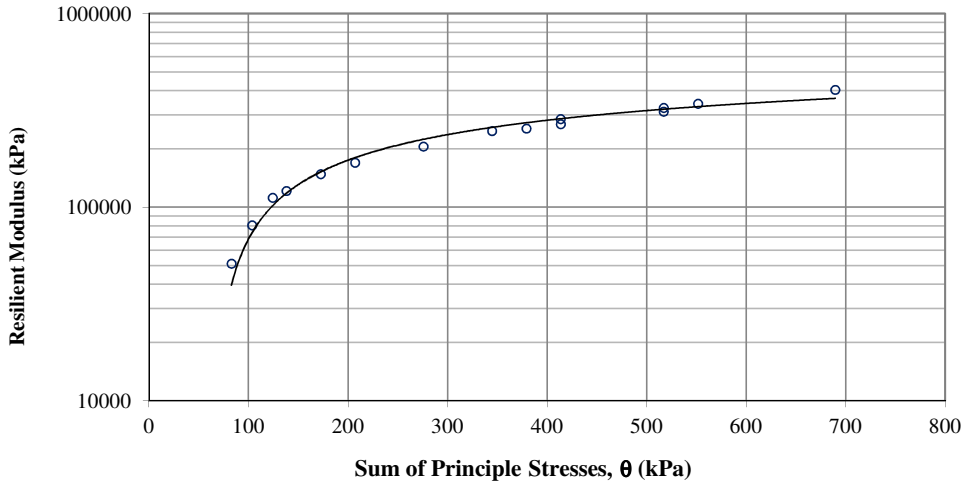

GAB Resilient Modulus Test Results

Georgia Pavement Research Center
Southern Polytechnic State University

		Test Date:	9/25/2012
QPL ID:	118C	Specimen Preparation Date:	9/24/2012
Source Location	Columbus, GA	Specimen Diameter (in):	6
GAB Character:	Granite Gneiss	Specimen Height (in.)	12
w_{opt} (%):	6	Compaction w_c (%)	6
Max. γ_d (pcf):	137.2	w_c after Testing (%):	
		Tested By:	sk

Test Seq.	σ_1 (kPa)	σ_3 (kPa)	θ (kPa)	τ_{oct} (kPa)	I/Pa	τ_{oct}/Pa	Log(I/Pa)	Log(τ_{oct}/Pa+1)	M_R (kPa)	Log M_R
1	41.39	20.70	82.79	9.75	0.82	0.10	-0.09	0.04	60,185	4.779
2	62.07	20.70	103.47	19.50	1.02	0.19	0.01	0.08	80,342	4.905
3	82.76	20.70	124.16	29.25	1.23	0.29	0.09	0.11	100,494	5.002
4	68.98	34.50	137.98	16.25	1.36	0.16	0.13	0.06	107,959	5.033
5	103.45	34.50	172.45	32.50	1.70	0.32	0.23	0.12	125,055	5.097
6	137.93	34.50	206.93	48.76	2.04	0.48	0.31	0.17	139,861	5.146
7	137.85	68.90	275.65	32.50	2.72	0.32	0.43	0.12	172,333	5.236
8	206.80	68.90	344.60	65.01	3.40	0.64	0.53	0.22	209,947	5.322
9	275.75	68.90	413.55	97.51	4.08	0.96	0.61	0.29	238,418	5.377
10	172.35	103.40	379.15	32.50	3.74	0.32	0.57	0.12	229,952	5.362
11	206.83	103.40	413.63	48.76	4.08	0.48	0.61	0.17	243,382	5.386
12	310.25	103.40	517.05	97.51	5.10	0.96	0.71	0.29	274,366	5.438
13	241.33	137.90	517.13	48.76	5.10	0.48	0.71	0.17	282,005	5.450
14	275.80	137.90	551.60	65.01	5.44	0.64	0.74	0.22	298,856	5.475
15	413.70	137.90	689.50	130.01	6.80	1.28	0.83	0.36	343,076	5.535

Generalized NCHRP 1-28A Model (M-E Design Guide)

k1	k2	k3	R^2
782	0.801	-0.084	0.99

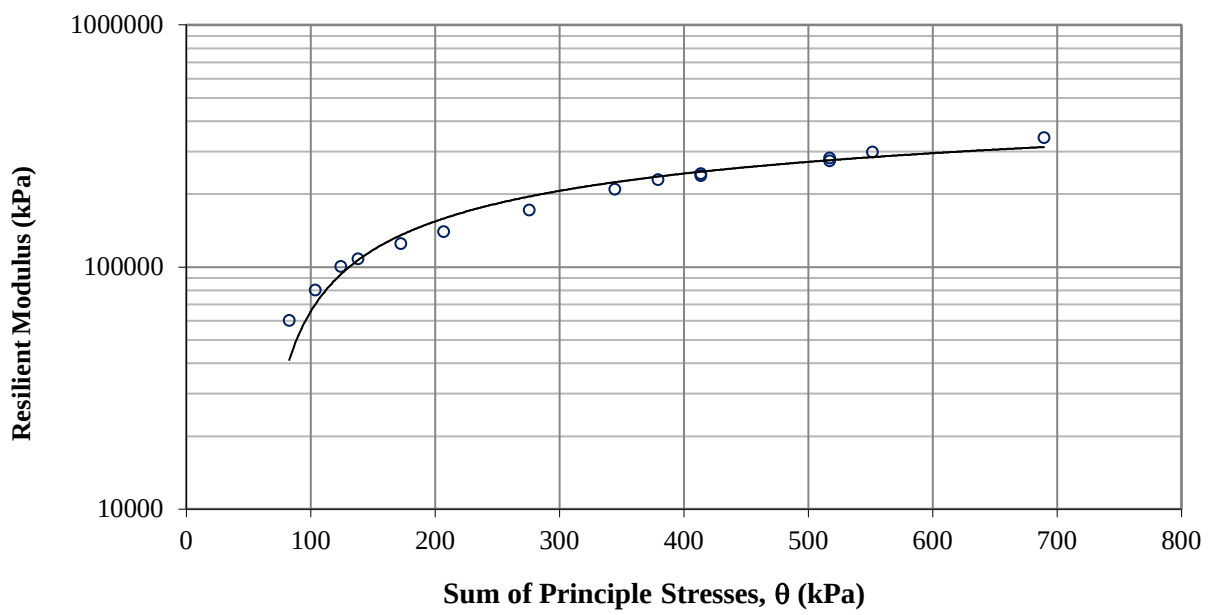

GAB Resilient Modulus Test Results

Georgia Pavement Research Center
Southern Polytechnic State University

		Test Date:	9/12/2012
QPL ID:	141C	Specimen Preparation Date:	9/11/2012
Source Location	Dahlonega, GA	Specimen Diameter (in):	6
GAB Character:	Granite Gneiss	Specimen Height (in.)	12.5
w_{opt} (%):	5.6	Compaction w_c (%)	3.0
Max. γ_d (pcf):	135.2	w_c after Testing (%):	
		Tested By:	sk

Test Seq.	σ_1 (kPa)	σ_3 (kPa)	θ (kPa)	τ_{oct} (kPa)	I/Pa	τ_{oct}/Pa	Log(I/Pa)	Log(τ_{oct}/Pa+1)	M_R (kPa)	Log M_R
1	41.39	20.70	82.79	9.75	0.82	0.10	-0.09	0.04	55,622	4.745
2	62.07	20.70	103.47	19.50	1.02	0.19	0.01	0.08	65,835	4.818
3	82.76	20.70	124.16	29.25	1.23	0.29	0.09	0.11	79,450	4.900
4	68.98	34.50	137.98	16.25	1.36	0.16	0.13	0.06	79,966	4.903
5	103.45	34.50	172.45	32.50	1.70	0.32	0.23	0.12	99,198	4.997
6	137.93	34.50	206.93	48.76	2.04	0.48	0.31	0.17	111,963	5.049
7	137.85	68.90	275.65	32.50	2.72	0.32	0.43	0.12	132,262	5.121
8	206.80	68.90	344.60	65.01	3.40	0.64	0.53	0.22	168,411	5.226
9	275.75	68.90	413.55	97.51	4.08	0.96	0.61	0.29	176,961	5.248
10	172.35	103.40	379.15	32.50	3.74	0.32	0.57	0.12	167,521	5.224
11	206.83	103.40	413.63	48.76	4.08	0.48	0.61	0.17	191,609	5.282
12	310.25	103.40	517.05	97.51	5.10	0.96	0.71	0.29	199,623	5.300
13	241.33	137.90	517.13	48.76	5.10	0.48	0.71	0.17	230,961	5.364
14	275.80	137.90	551.60	65.01	5.44	0.64	0.74	0.22	243,731	5.387
15	413.70	137.90	689.50	130.01	6.80	1.28	0.83	0.36	264,936	5.423

Generalized NCHRP 1-28A Model (M-E Design Guide)

k1	k2	k3	R^2
643	0.767	-0.111	0.99

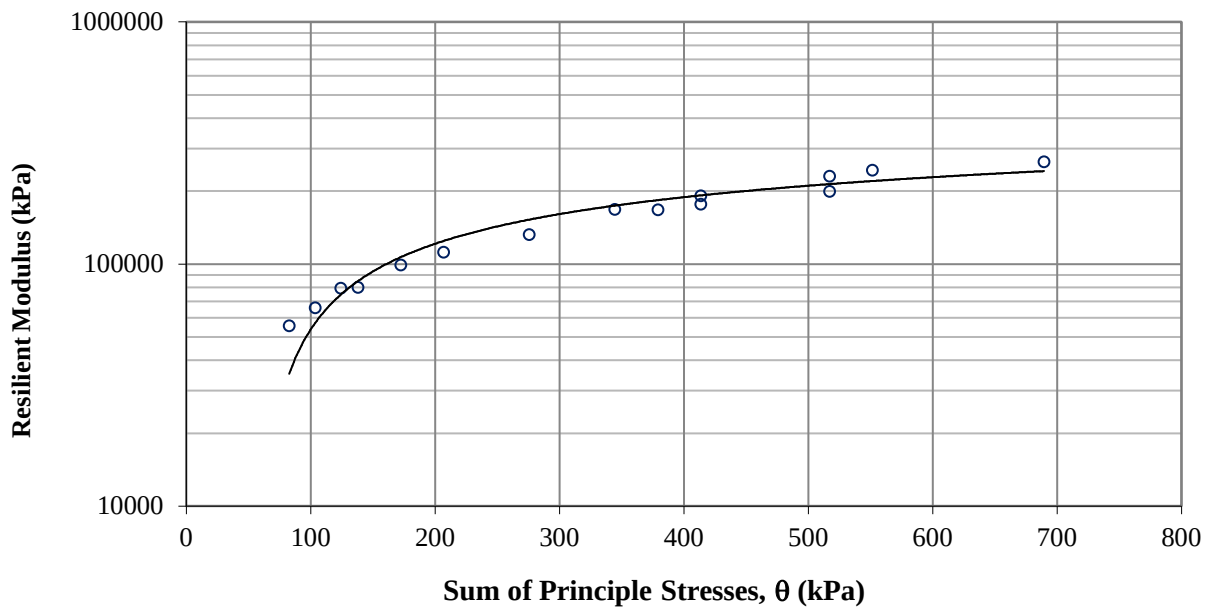

GAB Resilient Modulus Test Results

Georgia Pavement Research Center
Southern Polytechnic State University

		Test Date:	2/14/2013
QPL ID:	158C	Specimen Preparation Date:	2/14/2013
Source Location	Walton County	Specimen Diameter (in):	6
GAB Character:	Biotite Gneiss	Specimen Height (in.)	12
w_{opt} (%):	6.4	Compaction w_c (%)	6.3
Max. γ_d (pcf):	135	w_c after Testing (%):	
		Tested By:	sk

Test Seq.	σ_1 (kPa)	σ_3 (kPa)	θ (kPa)	τ_{oct} (kPa)	I/Pa	τ_{oct}/Pa	Log(I/Pa)	Log(τ_{oct}/Pa+1)	M_R (kPa)	Log M_R
1	41.39	20.70	82.79	9.75	0.82	0.10	-0.09	0.04	83,171	4.920
2	62.07	20.70	103.47	19.50	1.02	0.19	0.01	0.08	95,402	4.980
3	82.76	20.70	124.16	29.25	1.23	0.29	0.09	0.11	117,949	5.072
4	68.98	34.50	137.98	16.25	1.36	0.16	0.13	0.06	120,419	5.081
5	103.45	34.50	172.45	32.50	1.70	0.32	0.23	0.12	140,097	5.146
6	137.93	34.50	206.93	48.76	2.04	0.48	0.31	0.17	152,130	5.182
7	137.85	68.90	275.65	32.50	2.72	0.32	0.43	0.12	178,458	5.252
8	206.80	68.90	344.60	65.01	3.40	0.64	0.53	0.22	203,951	5.310
9	275.75	68.90	413.55	97.51	4.08	0.96	0.61	0.29	221,069	5.345
10	172.35	103.40	379.15	32.50	3.74	0.32	0.57	0.12	200,717	5.303
11	206.83	103.40	413.63	48.76	4.08	0.48	0.61	0.17	219,189	5.341
12	310.25	103.40	517.05	97.51	5.10	0.96	0.71	0.29	255,438	5.407
13	241.33	137.90	517.13	48.76	5.10	0.48	0.71	0.17	248,265	5.395
14	275.80	137.90	551.60	65.01	5.44	0.64	0.74	0.22	259,946	5.415
15	413.70	137.90	689.50	130.01	6.80	1.28	0.83	0.36	270,655	5.432

Generalized NCHRP 1-28A Model (M-E Design Guide)

k1	k2	k3	R^2
965	0.564	-0.010	0.99

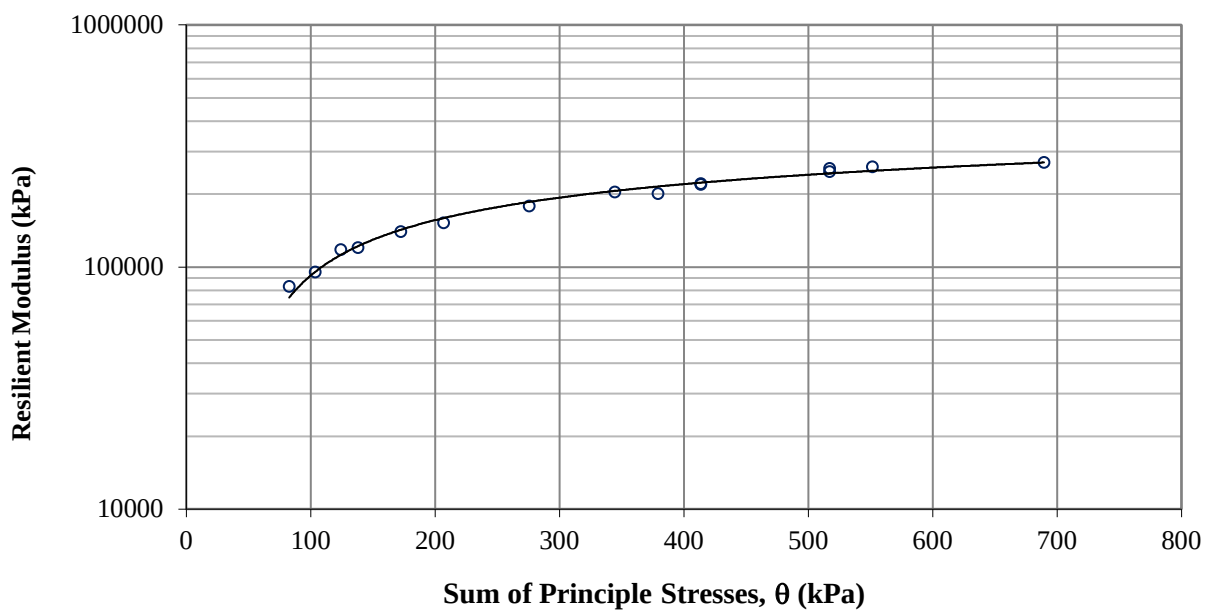

GAB Resilient Modulus Test Results

Georgia Pavement Research Center
Southern Polytechnic State University

		Test Date:	9/5/2012
QPL ID:	165T	Specimen Preparation Date:	9/4/2012
Source Location	I75 Unadilla	Specimen Diameter (in):	6
GAB Character:	Recycled Conc.	Specimen Height (in.)	12.5
w_{opt} (%):	7	Compaction w_c (%)	6.8
Max. γ_d (pcf):	134	w_c after Testing (%):	
		Tested By:	sk

Test Seq.	σ_1 (kPa)	σ_3 (kPa)	θ (kPa)	τ_{oct} (kPa)	I/Pa	τ_{oct}/Pa	Log(I/Pa)	Log(τ_{oct}/Pa+1)	M_R (kPa)	Log M_R
1	41.39	20.70	82.79	9.75	0.82	0.10	-0.09	0.04	109,869	5.041
2	62.07	20.70	103.47	19.50	1.02	0.19	0.01	0.08	119,587	5.078
3	82.76	20.70	124.16	29.25	1.23	0.29	0.09	0.11	140,586	5.148
4	68.98	34.50	137.98	16.25	1.36	0.16	0.13	0.06	151,882	5.182
5	103.45	34.50	172.45	32.50	1.70	0.32	0.23	0.12	167,390	5.224
6	137.93	34.50	206.93	48.76	2.04	0.48	0.31	0.17	182,261	5.261
7	137.85	68.90	275.65	32.50	2.72	0.32	0.43	0.12	208,473	5.319
8	206.80	68.90	344.60	65.01	3.40	0.64	0.53	0.22	258,156	5.412
9	275.75	68.90	413.55	97.51	4.08	0.96	0.61	0.29	287,672	5.459
10	172.35	103.40	379.15	32.50	3.74	0.32	0.57	0.12	277,386	5.443
11	206.83	103.40	413.63	48.76	4.08	0.48	0.61	0.17	289,765	5.462
12	310.25	103.40	517.05	97.51	5.10	0.96	0.71	0.29	311,941	5.494
13	241.33	137.90	517.13	48.76	5.10	0.48	0.71	0.17	341,335	5.533
14	275.80	137.90	551.60	65.01	5.44	0.64	0.74	0.22	360,236	5.557
15	413.70	137.90	689.50	130.01	6.80	1.28	0.83	0.36	417,396	5.621

Generalized NCHRP 1-28A Model (M-E Design Guide)

k1	k2	k3	R^2
1173	0.626	-0.019	0.99